

## **General Disclaimer**

### **One or more of the Following Statements may affect this Document**

- This document has been reproduced from the best copy furnished by the organizational source. It is being released in the interest of making available as much information as possible.
- This document may contain data, which exceeds the sheet parameters. It was furnished in this condition by the organizational source and is the best copy available.
- This document may contain tone-on-tone or color graphs, charts and/or pictures, which have been reproduced in black and white.
- This document is paginated as submitted by the original source.
- Portions of this document are not fully legible due to the historical nature of some of the material. However, it is the best reproduction available from the original submission.



NASA JR- 152587

STANFORD REMOTE SENSING LABORATORY

TECHNICAL REPORT 76-3

Final Report For

The National Aeronautics and Space Administration

Research Grant NASG-5050

(NASA-CR-152587) FIELD MAPPING FOR HEAT CAPACITY MAPPING DETERMINATIONS: GROUND SUPPORT FOR AIRBORNE THERMAL SURVEYS Final Report (Stanford Univ.) 98 p HC A05/MF A01

N77-32568  
Unclassified  
CSCI 08G G3/43 49296

FIELD MAPPING FOR HEAT CAPACITY

MAPPING DETERMINATIONS: Ground Support

For Airborne Thermal Surveys

June 1976



REMOTE SENSING LABORATORY  
SCHOOL OF EARTH SCIENCES

STANFORD UNIVERSITY • STANFORD, CALIFORNIA

STANFORD REMOTE SENSING LABORATORY  
TECHNICAL REPORT 76-3

Final Report For  
The National Aeronautics and Space Administration  
Research Grant NASG-5050.

FIELD MAPPING FOR HEAT CAPACITY  
MAPPING DETERMINATIONS: Ground Support  
For Airborne Thermal Surveys

June 1976

Stuart E. Marsh  
Researcher  
Dept. of Applied Earth Sciences  
Remote Sensing Laboratory  
Stanford University  
Stanford, California 94305

R.J.P. Lyon, Principal Investigator  
Dept. of Applied Earth Sciences  
Remote Sensing Laboratory  
Stanford University  
Stanford, California 94305

R.J.P. Lyon

## TABLE OF CONTENTS

	<u>page</u>
ABSTRACT	1
I. INTRODUCTION	2
II. COMPARISON OF THERMAL MODELS	2
III. PISGAH-LAVIC LAKE STUDY	14
A. Site Description	14
B. Albedo Measurements and Analysis	15
C. Surface Temperature Measurements and Analysis	16
IV. A "SANDBOX" STUDY	19
A. Objectives	19
B. Measurements	19
C. Results	20
V. CONCLUSIONS	20
VI. APPENDICES:	
1. Statistical Compilation Bi-Directional Reflectance Data	
2. ISCO Bi-Directional Reflectance Measurements	
3. Measured Surface and Probe Temperatures	
4. Graphical Representation of Measured Diurnal Surface Temperature v. Thermal Model Runs	
5. Detailed Analysis of Site 1-1 Employing SURTEMP Thermal Model	
6. Tautochrones from Playa Probe Measurements	

KEY TO SYMBOLS EMPLOYED

Symbol	Explanation	Source/Worker	(Page used)
$\gamma$ (or T.I.)	Thermal inertia	Watson	(3) Table 2
$F_n$	Average flux into ground nth interval	Jaeger	(3)
$T_p$	Period of flux $F_n$	Jaeger	(3)
$V_s$	Surface temperature as periodic step function	Jaeger/ Watson	(3)(16)
$FS_n$	Solar heating flux component	Jaeger	
$FA_n$	Atmospheric heating flux component	Jaeger	(3)
$FG_n$	Ground radiation flux component	Jaeger	(3)
$S.$	Solar constant	Watson	(3)
$Z$	Solar zenith angle	Watson	(3)
$m(z)$	Atmospheric transmission factor (air mass)	Watson	(3)
$\Sigma$	Emissivity	standard	(3)
$\lambda$	Latitude	Watson	(4)
$\phi'$	Latitude	Rosema	Table 2
$A$	Albedo	Lyon/Watson	(3)
$\alpha$	Albedo	Jaeger/Watson (3)	Outcalf (7)
$a$	Albedo	Rosema	Table 2
$\sigma$	Stefan-Boltzmann constant	standard	(3)
$\delta$	Solar declination	Lyon/Watson	(4)
DEC	Solar declination	Outcalt	Table 2
$\delta'$	Solar declination	Rosema	Table 2
$d$	Dip	Watson	(4)
$\phi$	Strike azimuth from north	Watson	(4)
$f$ (or $fs$ )	Cloud cover factor (or solar input)	Watson	Table 2;(3)(4)
$w$	Diurnal angular frequency	DeVries/ Watson	(4)
$D$	Damping depth	DeVries	
$t$	Local time from noon	Watson	(4)
$T_N$ , $T_D$ or $T_{AN}$ , $T_{AD}$	Sky temperature (night, day)	Watson	(3)
$T_{sky}$	Sky radiant temperature	Outcalt	(7), Table 2
$R$	Radius vector of sun	Outcalt	(7), Table 2
$D$	Dust content atmosphere	Outcalt	Table 2
$u$	Wind speed	Outcalt	Table 2
$v$	Wind speed	Rosema	Table 2

KEYS TO SYMBOLS EMPLOYED CONTINUED

Symbol	Explanation	Source/Worker	(Page used)
q	Air humidity	Outcalt	Table 2
s	Air humidity	Rosema	Table 2
X <sub>p</sub>	Soil porosity	Rosema	Table 2
w	Precipitable water (atmosphere)	Outcalt	Table 2
p	Station atmospheric pressure	Outcalt	Table 2
C	Volumetric heat capacity	DeVries	
GC	Volumetric heat capacity	Outcalt	Table 2
	Thermal diffusivity	Watson/Lyon	(3)
GD	Thermal diffusivity	Outcalt	Table 2
ρ	Density	standard	
c	Specific heat	standard	
k	Thermal conductivity	standard	
X <sub>m</sub>	Volume fraction minerals in soil	DeVries	Table 2
X <sub>o</sub>	Volume fraction organics in soil	DeVries	Table 2
X <sub>w</sub>	Volume fraction water in soil	DeVries	Table 2
Z <sub>0</sub>	Surface roughness (Aerodynamic roughness)	Outcalt	(7), Table 2
X <sub>w</sub>	Wet fraction soil	Outcalt	(7)
SHDRAT	Shadow fraction	Outcalt	Table 2
T <sub>2</sub>	Air temperature	Outcalt	Table 2
T <sub>a</sub>	Air temperature	Rosema	Table 2
h	Depth subsoil water level	Rosema	Table 2
̄T	Temperature at subsoil water level	Rosema	Table 2
θ	Moisture characteristics	Rosema	Table 2
R	Net radiation balance	standard	(7)
H	Vertical transfer sensible heat to or from air column	standard	(7)
LE	Evaporation	standard	(7)
G	Net flux sensible heat into or out of soil	standard	(7)
ΔT	Change in temperature		
Z <sub>2</sub> , K, r, σ	Fixed constants	Outcalt	(7)
(Q+q)		Outcalt	(7)
U <sub>2</sub>		Outcalt	(7)
Z <sub>s</sub>		Outcalt	(7)
K <sub>s</sub>		Outcalt	(7)

## ABSTRACT

Thermal models from 3 sources (Watson, Outcalt and Rosema) were compared using similar input data and found to yield very different results. Watson-type models are very sensitive to albedo variations and to back-radiation from the sky.

Field data with which to check the validity of models are rare and usually insufficient parameters were measured. Our Pisgah Crater-Lavic Lake data, for March 29-30, 1975, have been re-examined to indicate the serious discrepancy between results for thermal inertia, between JPL calculations (Kahle et al. 1976) and ours, when made using the same original data sets.

Roof-top modelling experiments are underway to explore the practicality of determining thermal parameters of a known standardized material (Ottawa sand), when using remotely sensed data.

## I. INTRODUCTION

The Stanford Remote Sensing Laboratory has maintained a long and close relationship with thermal infrared mapping experiments. The often difficult acquisition of this experience has made us uniquely aware of both the advantages and problems of thermal mapping employing modelling techniques of thermal parameters with repeated diurnal aircraft and/or satellite coverage. This same expertise with field measurement programs has made it painfully apparent to us that great difficulties exist in the determination of thermal parameters at the ground-air interface in an absolute sense.

The work performed under this grant attempts to assess these determinations. This assessment includes a comparison of thermal mapping schemes, and the JPL/Stanford field effort at Pisgah Crater, California which indicated estimates of these "body-parameters" of the surficial materials may be in error as much as 100%. In light of these indications a study of a material with laboratory-determined thermal conductivity and diffusivity was begun to attempt to fix confidence limits on attempts to make absolute measurements of soil/rock thermal inertia.

Adequate technology and reasonable software exists to create thermal inertia images from twice daily aircraft-satellite coverage, however, the accuracy of these determinations in terms of absolute measure remains to be established (Kahle, et.al., 1976).

## II. COMPARISON OF THERMAL MODELS

The prediction of diurnal surface temperatures, given the thermal parameters of a material, is of considerable significance to any thermal study. The contemporary principles of one-dimensional heat flow on the earth's surface can be converted into mathematical models to resolve surface temperatures, and have been programmed by a number of scientists. The mathematical model is an extremely valuable technique, and infrared studies are improved by understanding the modelling results and using them to help recognize variations in thermal properties and anomalous geothermal sites.

In order to study and perhaps analyze the significance of thermal modelling the components of four competitive models that compute the diurnal surface temperature will be analyzed. These models represent advances in our understanding of heat flow over the past five years. All four models were written for digital computations since they are based on rather complicated mathematical solutions. By comparing results of the models the significance of various thermal parameters will be made clear, and the applicability of their results to delineation of surface materials will be apparent.

#### A. Description of Thermal Models

MODEL 1. Watson (1971a and 1971b) developed the first computer program of thermal modelling for interpretation of infrared images. A mathematical model for the diurnal surface temperature variation of the earth's surface was derived from the one-dimensional heat-conduction equation of Jaeger (1953) by applying the Laplace transform;

$$F_n = \frac{\gamma}{\pi T_p} \sum_{s=1}^m v_s \phi_{n-s+1}. \quad (1)$$

where  $F_n$  is the average flux into the ground in the nth interval, ( $\gamma$ ) is thermal inertia,  $T_p$  is the period of the flux,  $v_s$  is the surface temperature as a periodic step function, and  $\phi_{n-s+1}$  is a set of coefficients determined solely by the number of incremental steps  $m$ , in the period  $T_p$ . The flux into the ground,  $F_n$ , is considered to be the result of solar heating,  $FS_n$ ; atmospheric heating,  $FA_n$ ; and radiation from the ground,  $FG_n$ .

$$F_n = FS_n + FA_n - FG_n. \quad (2)$$

where

$$\begin{aligned} FS_n &= fS. (1-A)M(Z) \cos Z + \sigma T_{AD}^{-4} = \Sigma v_n^4 \cdot day \\ &= \sigma T_{AN}^{-4} - \Sigma v_n^4 = 0. \quad night \end{aligned} \quad (3)$$

and  $f$  is cloud cover,  $S.$  is the solar constant,  $A$  is albedo,  $M(Z)$  is air mass or an atmospheric transmission ( $M(Z) = 1-0.2 \sec Z$ ),  $Z$  is the zenith angle.  $\sigma$  is the Stefan-Boltzmann constant,  $T_{AN}$  is the effective nighttime sky temperature,  $T_{AD}$  is the effective day time sky temperature, and  $\Sigma$  is the mean emissivity.

TABLE I

## THERMAL PARAMETERS

Typical Values of Thermal Conductivity (cal cm <sup>-1</sup> sec <sup>-1</sup> °C <sup>-1</sup> )			Typical Values of Thermal Diffusivity (cm <sup>2</sup> sec <sup>-1</sup> )			Typical Values of Emisivity (%)		
Material	Value	Source	Material	Value	Source	Material	Value	Source
Quartz	0.021	Sellers	Quartz	0.044	Sellers	Water	92-99	Sellers
Clay Minerals	0.007	Sellers	Clay Minerals	0.015	Sellers	Fresh Snow	82-99.3	Sellers
Organic Matter	0.006	Sellers	Organic Matter	0.0010	Sellers	Ice	96	Sellers
Water	0.00137	Sellers	Air	0.0114	Sellers	Sand, dry light	89-90	Sellers
Ice	0.0012	Sellers	Water	0.0014	Sellers	Sand, wet	93	Sellers
Air	0.00006	Sellers	Granite	0.0127	Ingersoll et al.	Gravel, coarse	91-92	Sellers
Granite	0.0065	Sellers	Limestone	0.0001	Ingersoll et al.	Limestone, light gray	91-92	Sellers
Limestone	0.0048	Ingersoll et al.	Sandstone	0.0113	Ingersoll et al.	Ground, moist here	95-98	Sellers
Sandstone	0.0062	Ingersoll et al.	Quartz sand, dry, medium-fine	0.0020	Ingersoll et al.	Desert	90-91	Sellers
Quartz sand, dry, medium-fine	0.0063	Ingersoll et al.	Quartz sand, 0.32 moisture medium-fine	0.0033	Ingersoll et al.	Grass, high dry	90	Sellers
Soil, very dry	0.0004-0.0008	Ingersoll et al.	Soil, very dry	0.002-0.003	Ingersoll et al.	Oak Woodland	90	Sellers
Soil, wet	0.003-0.008	Ingersoll et al.	Soil, wet	0.004-0.010	Ingersoll et al.	Pine Forest	90	Sellers
Typical Values of Volumetric Heat Capacity (cal cm <sup>-3</sup> °C <sup>-1</sup> )			Typical Values of Thermal Inertia (cal cm <sup>-2</sup> °C <sup>-1</sup> sec <sup>-1</sup> )			Typical Values of Albedo (% wavelength varies)		
Quartz	0.46	Van Wijk & De Vries	Quartz	0.098	Sellers	Water	6-21	Sellers
Organic Matter	0.60	Van Wijk & De Vries	Organic Matter	0.019	Sellers	Fresh Snow	75-95	Sellers
Water	1.00	Van Wijk & De Vries	Water	0.037	Sellers	Sand dune, dry	35-45	Sellers
Air	0.00029	Van Wijk & De Vries	Air	0.0001	Sellers	Sand dune, wet	20-30	Sellers
Granite	0.513	Ingersoll et al.	Granite	0.058	Ingersoll et al.	Soil, dark	5-15	Sellers
Limestone	0.394	Ingersoll et al.	Limestone	0.053	Ingersoll et al.	Soil, moist gray	10-20	Sellers
Sandstone	0.346	Ingersoll et al.	Sandstone	0.058	Ingersoll et al.	Soil, dry light sand	25-45	Sellers
Quartz sand, dry, medium-fine	0.314	Ingersoll et al.	Quartz sand dry, medium-fine	0.014	Ingersoll et al.	Desert	25-30	Sellers
Quartz sand, 0.32 moisture, medium fine	0.428	Ingersoll et al.	Silts	0.020	Friedman	Chaparral	15-20	Sellers
			Pumice sand	0.009	Friedman	Meadow, green	10-20	Sellers
			Tuff	0.040	Friedman	Forest, deciduous	10-20	Sellers
			Quartz monzonite	0.060	Friedman	Forest, coniferous	5-15	Sellers
			Carbonates	0.011-0.038	Friedman	Silts	40	Friedman
						Pumice Sand	80	Friedman
						Tuff	40	Friedman
						Quartz monzonite	40	Friedman

The model to this point assumes the ground is flat, therefore, to improve the model a topographic correction was introduced. Assuming that a change in surface slope will only alter significantly the incident solar flux.

$$FS_n = fS \cdot (1-A)M(Z) \cos Z'. \quad (4)$$

where  $\cos Z'$  is the zenith angle modified for local slope of dip angle  $d$  and strike azimuth from north  $\phi$ .

$$\cos Z' = \cos(\lambda - ds\sin\phi) \cos\delta (\cos(wt + dc\cos\phi) + \tan(\lambda - ds\sin\phi)\tan\delta).$$

And  $\lambda$  is  $\Sigma h$  local latitude,  $\delta$  is sun's declination,  $t$  is local time from noon,  $w$  the diurnal angular frequency. Significant topographic variation would therefore produce, for a single site, a large variation in surface temperature that would be at a maximum near noon and at a minimum near dawn.\*\*

Atmospheric effects are treated in terms of the cloud cover factors and transmission as a function of zenith angle. The model accounts for variations in convection, evaporation, and condensation in the night and day sky temperature terms.

$$FA_n = \sum_{AD}^4 \text{day} \quad (5)$$
$$= \sum_{AN}^4 \text{night}$$

---

\*\* Recent work by Watson (1975) has uncovered an error in the equation for zenith angle modified for local slope variations. Watson now expresses the relation:

$$\cos Z' = \cos d \cos Z - \sin d (\sin \phi \cos \delta \sin wt - \cos \phi \sin \delta \cos \lambda - \sin \delta \sin \lambda \cos wt).$$

However, because we have taken strike and dip in the model comparisons that follow to be zero the results are completely unaffected. Either the relation for  $\cos Z'$  originally contained in Watson's model or the correct relation will reduce (when strike and dip are both zero) to the normal zenith angle relation,

$$\cos Z - \cos \lambda \cos \delta \cos wt + \sin \lambda \sin \delta$$

which is correctly formulated in the model.

From analysis of computer runs Watson (1971a) concluded that daytime variations of the sky temperature have a small effect on the ground temperature changes because insulation is the major source of surface heating; while at night, however, it has a marked effect on surface temperature because it is the major source of heating.

The radiation from the ground,  $FG_n$  is affected by a number of surface state effects.

$$FG_n = \Sigma \sigma V_s^4 \quad (6)$$

Equation (1) is solved subject to equations (2) through (6) by making an initial estimate of  $V_s$  and iteratively improving the solution. The surface parameters of thermal inertia, albedo, and emissivity help formulate the initial guess. The properties of thermal inertia and albedo also strongly affect the amplitude of diurnal temperature variations and therefore significantly affect the accuracies of the model calculations.

Watson et al. (1971b), has employed the WATEMP model in the study of an area near Mill Creek, Oklahoma. Model results agreed with thermal contrasts exhibited by thermal infrared images from altitudes of 150m to 17 km.

MODEL 2. Subsequent to the development of the Watson thermal model a similar program was developed, also based on a sinusoidal input for solar flux, at the Stanford Remote Sensing Lab. The Stanford temperature model program, SURTEMP, was independently written early in 1972 by Andrew Green for fully interactive use on IBM 360/67 and subsequently adapted for use on the PDP-10 computer by Frank Honey. The program is intentionally similar to that of Watson in that input consists of cloud cover factor, albedo, emissivity, thermal inertia, latitude and sun's declination, orientation, and inclination of the surface, and the day and night sky temperatures. However, differences exist in the computations using thermal inertia and emissivity, and in establishing the initial estimate of surface temperature. The Watson program iteratively solves the equation for  $\phi$  values until  $\Delta T$  between the last two iterations is  $0.1^\circ\text{K}$ . SURTEMP solves the equation employing a

maximum of 20 iterations ( $\phi$  values). From the work of Jaeger (1953) this should yield an error in amplitude of the approximate results of about 2%.

MODEL 3. A digital surface-climate simulator was developed by Outcalt (1972) following an analog solution for the diurnal surface thermal, and energy transfer, regimes based upon equilibrium temperature solutions by Myrup (1969). Though the model was developed for climatological studies, it is nevertheless applicable to surface thermal infrared studies in that it computes the diurnal variation of temperature from the surface to a depth of 25 cm. The basic equation of energy transfer or radiation balance,

$$R = H + LE + G. \quad (7)$$

set equal to zero, is the basis of the Myrup solution. Where  $H$  is the vertical transfer of sensible heat to or from the air column,  $Le$  is the evaporation, and  $G$  is the net rate or flux of sensible heat into or out of the soil. By characterizing these terms by measurable parameters the Outcalt model takes the form:

$$(1-\alpha)(Q+q) + \Sigma \sigma T_{sky}^4 - \Sigma \sigma T_o^4 + \frac{\rho k^2 U_2}{(ln Z_2/Z_o)^2} x \\ C(T_2 - rZ_2 - T_o) + L q_2 - (X_w/L) f(T_o) + \\ \frac{K_s}{(Z_s/2)} (T_n - T_o) = 0. \quad (8)$$

where  $Z_2$ ,  $k$ ,  $r$ ,  $\rho$ , are fixed constants;  $(Q+q)$ ,  $T_{sky}$ ,  $U_2$ ,  $q_2$ ,  $T_2$ , are meteorological variables; and  $\alpha$ ,  $\Sigma$ ,  $Z_o$ ,  $X_w$ ,  $Z_s$ ,  $K_s$ , are terrain variables.

The number of boundary conditions of the Outcalt model greatly exceed the Watson or SURTEMP models. However, the model results contain estimates of climatological and soil conditions useful to the climatologist (see Table 2).

MODEL 4. A most recent thermal model was developed by Rosema (1974) to calculate the diurnal variation of surface temperature. The program solves the heat transport equations numerically using parabolic differential equations. It initially calculates soil conductivities and heat capacities, followed by calculations of matrix potential and temperatures, and heat and water balance. Input of the Rosema model like that of Outcalt is of greater relevance to the climatologist or soil scientists.

B. Comparison of Thermal Models

In an attempt to understand the implications of the differences in input parameters and mathematical solutions between these four models, data sets and output temperatures were compared. The SURTEMP program was already established on the Stanford PDP-10 system and therefore available. Watson's (1971a) program had been published, and after modifications to achieve compatibility with the Stanford IBM 360/67 system by this author, it too became available. (Cost of the Watson thermal model (WATEMP) program on the Stanford IBM 360/67 far exceeded SURTEMP runs; each input set required approximately 0.75 minute CPU Time or roughly \$6.00). Although the Outcalt and Rosema modeling programs themselves were not available at that time, test run results had been published and these results could therefore be compared to either program available at Stanford.

R.J.P. Lyon (1974) over the past several years has run comparisons of the Friedman (1968) field data to the SURTEMP model.

Carefully documented and measured field data relating the model input parameters to surface temperatures are quite rare. The only significant, geologically relevant, study to date is that of Friedman (1968), but though this study did relate surface temperatures to albedo, emissivity and thermal inertia, sky temperatures were not measured, and no calculations of thermal models appear. By assuming the soil parameters are correct and knowing that the cloud cover factor for those days was zero, the SURTEMP program was run, varying slope orientation and inclination and sky temperatures until model temperatures matched observed temperatures.

By comparing  $\Delta T$  between maximum and minimum temperatures Lyon was able to conclude that surface dip slope changes of 15 to 50% and surface strike changes of 10 to 33%, will produce a  $1^{\circ}\text{C}$  change in maximum or minimum target temperature. Watson (1974a) compared the differential change in property values which produced a  $1^{\circ}\text{C}$  change in predawn temperature and arrived at similar results. Other parametric variations, which will produce a  $1^{\circ}\text{C}$  change in target temperature are listed below:

TABLE 2

INPUT PARAMETERS OF THE THERMAL MODELS

<u>WATSON-SURTEMP</u>	<u>OUTCALT</u>	<u>ROSEMA</u>
Cloud Cover (f)	Solar Declination (DEC)	Albedo (a)
Albedo (A)	Radius Vector of Sun (R)	Emissivity ( $\Sigma$ )
Emissivity ( $\Sigma$ )	Sky Radiant Temperature ( $T_{sky}$ )	Porosity ( $X_p$ )
Thermal Inertia ( $\gamma$ )	Dust Content (D)	Vol. Qtz. Content ( $X_m$ )
Latitude ( $\lambda$ )	Air Temperature ( $T_2$ )	Vol. Clay + Feldspar Content ( $X_m$ )
Suns Declination ( $\delta$ )	Wind Velocity (u)	Vol. Organics Content (Xo)
Strike ( $\phi$ )	Air Humidity (q)	Latitude ( $\phi'$ )
Dip (d)	Precipitable Water (w)	Day (Suns Declination) ( $\delta'$ )
Day and Night Sky Temperature	Station Pressure (p)	Aerodynamic Roughness (Zo)
( $T_N$ )      ( $T_D$ )	Soil Vol. Heat Capacity (GC)	Windspeed (v)
	Soil Thermal Diffusivity (GD)	Air Temperature (Ta)
	Surface Roughness (Zo)	Air Humidity (s)
	Albedo ( $\alpha$ )	Depth of Subsoil Water Level (h)
	Wet Fraction ( $X_w$ )	Temp at Subsoil Water Level ( $\bar{T}$ )
	Shadow Fraction (SHDRAT)	Moisture Characteristics ( $\theta$ )

Percent Variability for 1° Change

<u>Parameter</u>	<u>Lyon</u>	<u>Watson</u>
Albedo (A)	1.5-3	17
Emissivity ( $\Sigma$ )	25	2
Thermal Inertia (Y)	12-15	10
Sky Temperature $T_N$ or $T_D$	1-2	--

It is apparent that a considerable discrepancy exists between the calculated results of Watson and Lyon, for albedo and emissivity while the thermal inertia values are quite similar. Watson (1974a) did not calculate a percent change for sky temperature variation. In an attempt to resolve these discrepancies, the Watson model was run using the same Mono Lake data (Friedman 1968) used by Lyon to form his conclusions. These comparisons are plotted on the following figures, input parameters and comparison of maximum, minimum, and temperature differences appear on each graph.

Initial comparison involved using two different rock types. Figures 1 and 2 compare the programs for olivine basalt lapilli (Qvb) and silty playa and deltaic deposits (Qal). Inspection of the variations indicates that the nature of the diurnal surface temperature curves are quite similar. Maximum and minimum temperatures depart from one another by only one degree for Qvb, and the  $\Delta T$  for both runs are within 1°C. Comparison runs of sky temperatures, (Figures 3-4), using the same input data for lacustrine carbonate (Qm), were made. The shape of the curves are again similar and variations in  $\Delta T$  are less than 1°C.

Variation between the two programs appears to be unrelated to the sky temperature chosen.

Comparison runs of albedo and emissivity are compared on Figures 5-6. The curves are again quite similar in shape, and  $\Delta T$  is again within 1°C.

A number of preliminary conclusions can be made concerning these two models. As one would expect the programs are quite similar, and the

Figure 1

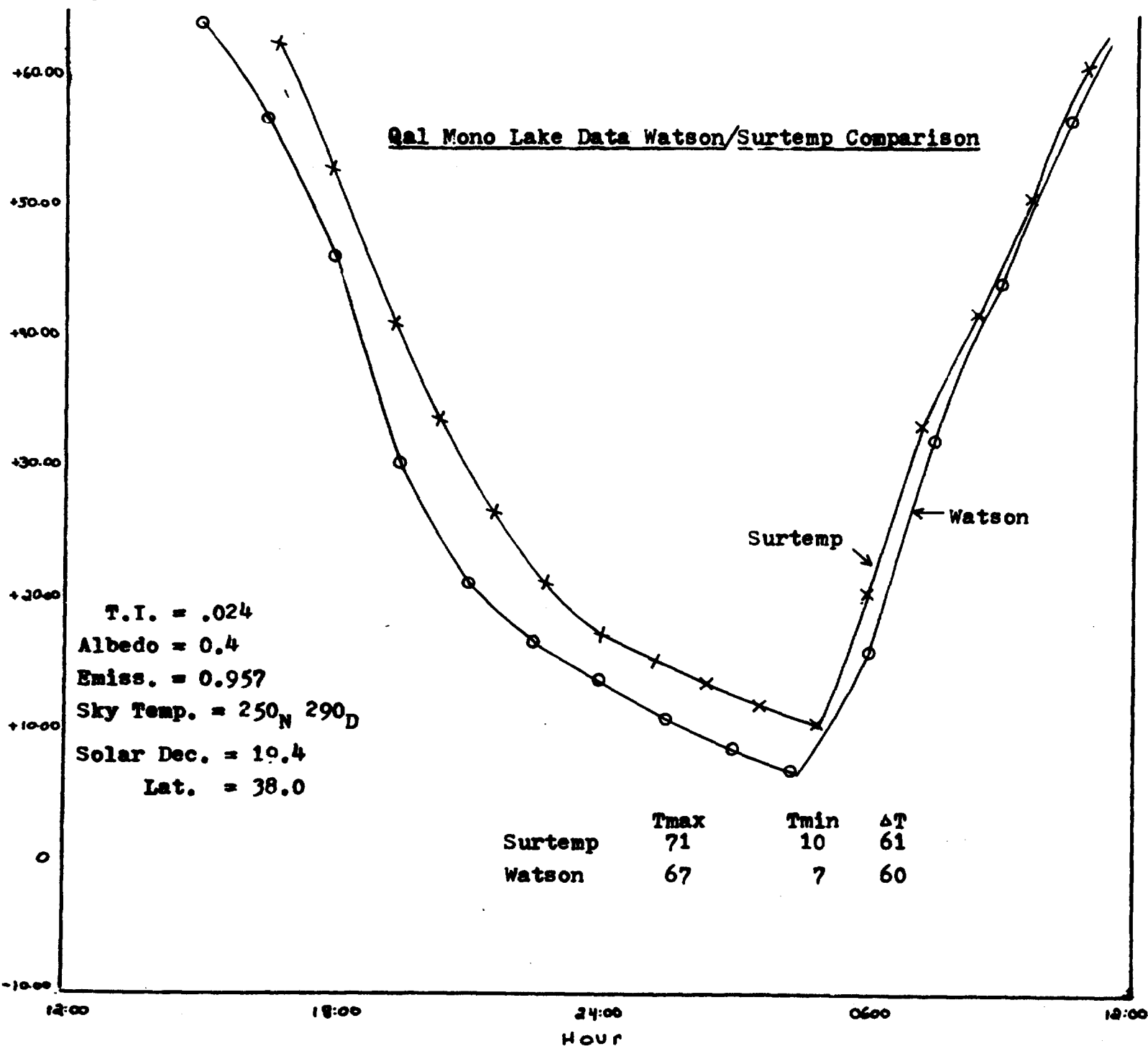
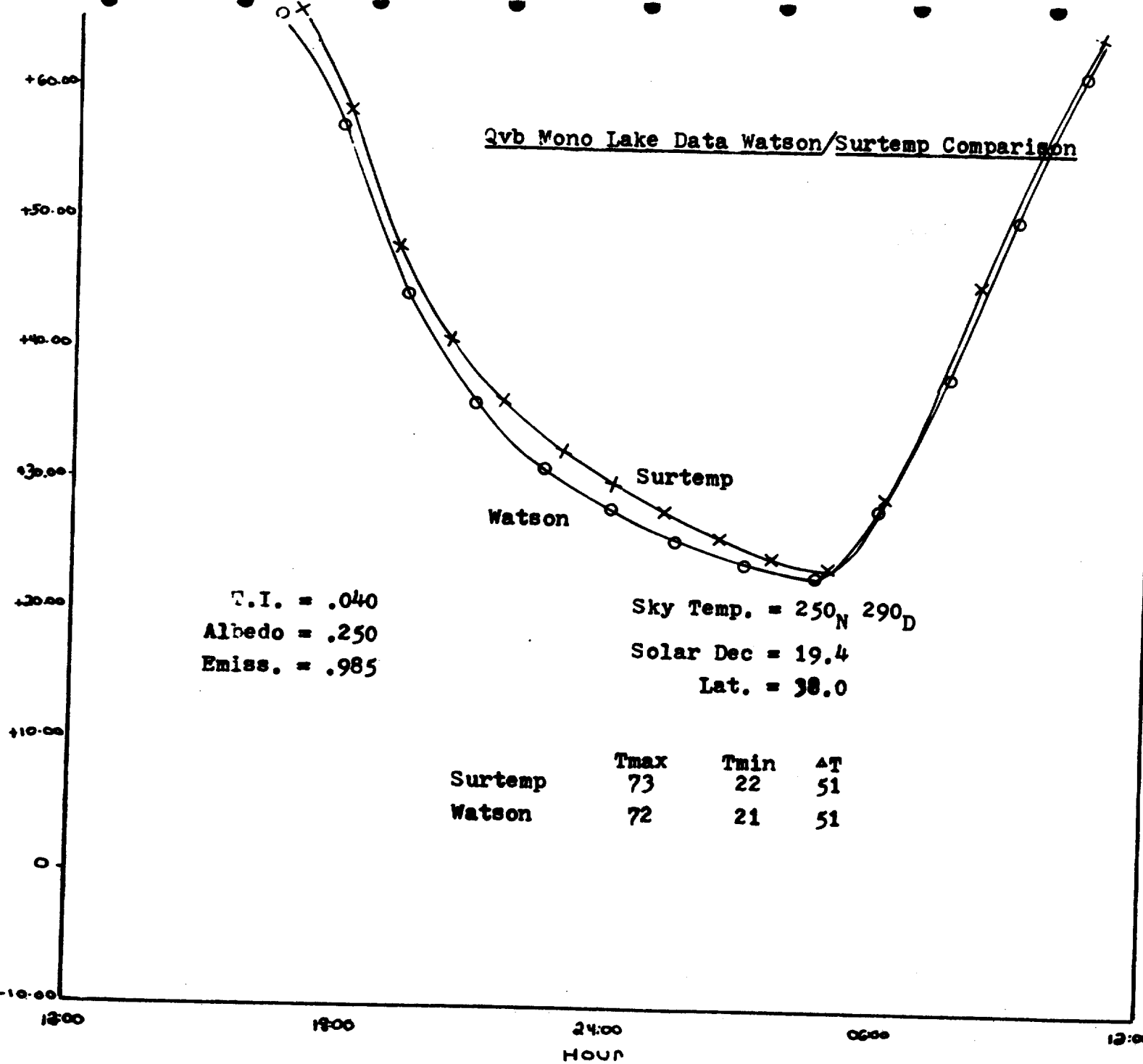


Figure 2

SURFACE TEMP. DEGREES C



3m Mono Lake Data Sky Temperature Test  
Watson/Surtemp Comparison 280/310

T.I. = 0.11  
 Albedo = 0.80  
 Emiss. = 0.974

Sky Temp. = 280<sub>N</sub> 310<sub>D</sub>  
 Solar Dec = 19.4  
 Lat. = 38.0

Surtemp  
 Watson

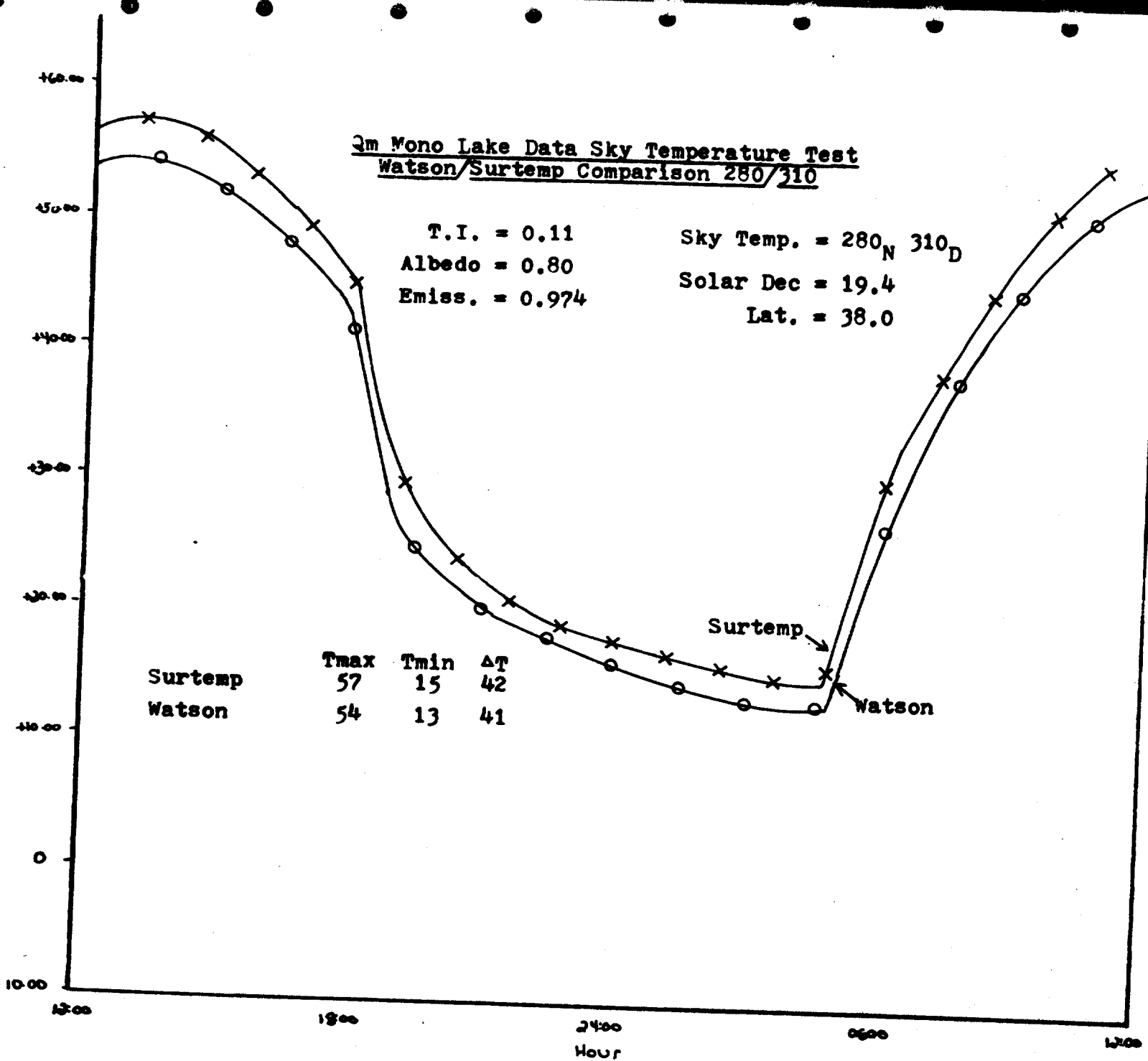
Tmax	Tmin	ΔT
57	15	42
54	13	41

Surtemp

Watson

SURFACE TEMP DEGREES C

Figure 3



Qm Mono Lake Data Sky Temperature Test  
Watson/Surtemp Comparison 270/280

T.I. = .011

Albedo = 0.8

Emiss. = 0.974

Sky Temp. = 270<sub>N</sub> 280<sub>D</sub>

Solar Dec = 19.4

Lat. = 38.0

	Tmax	Tmin	ΔT
Surtemp	34	3	31
Watson	32	1	31

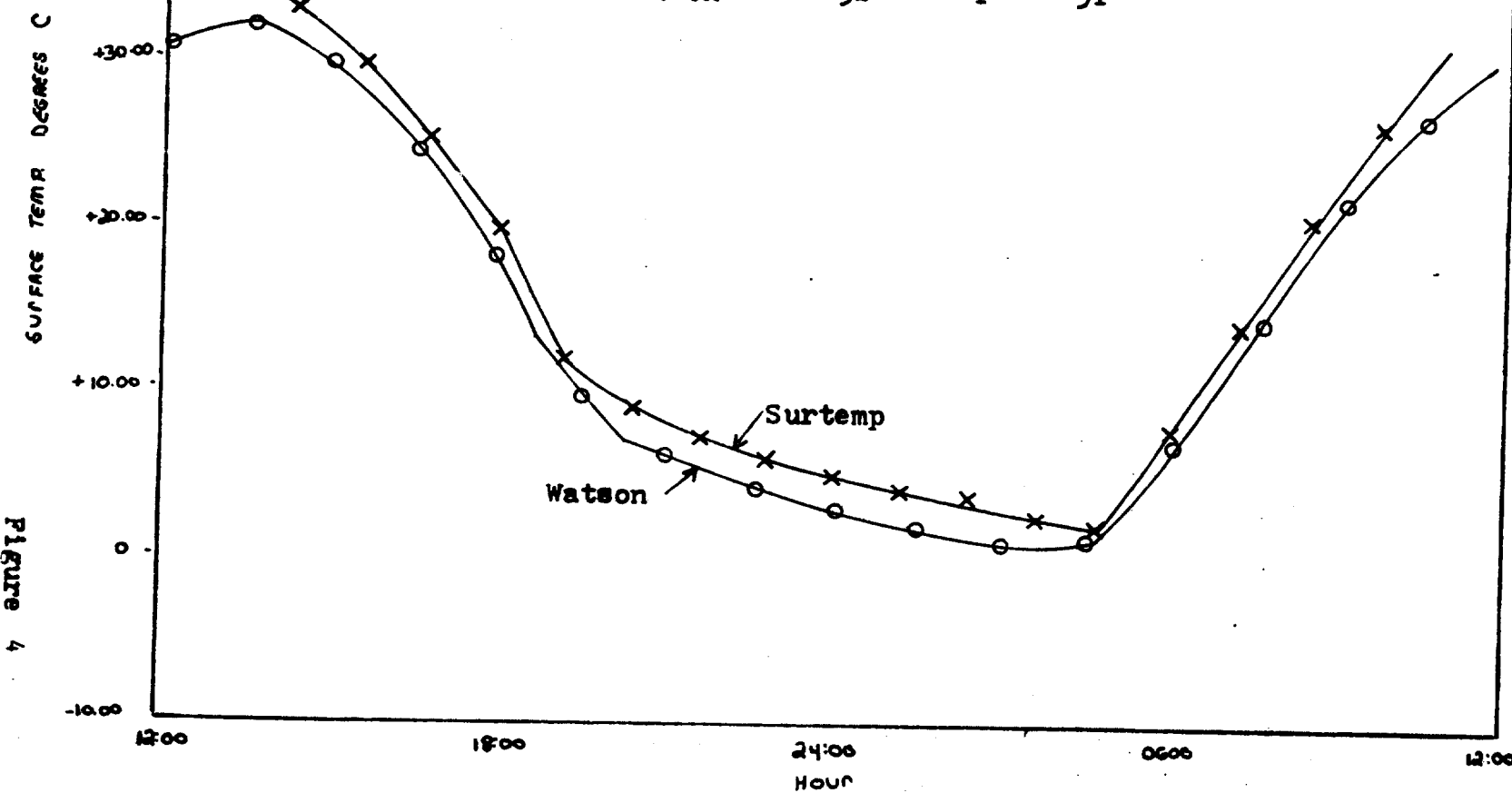
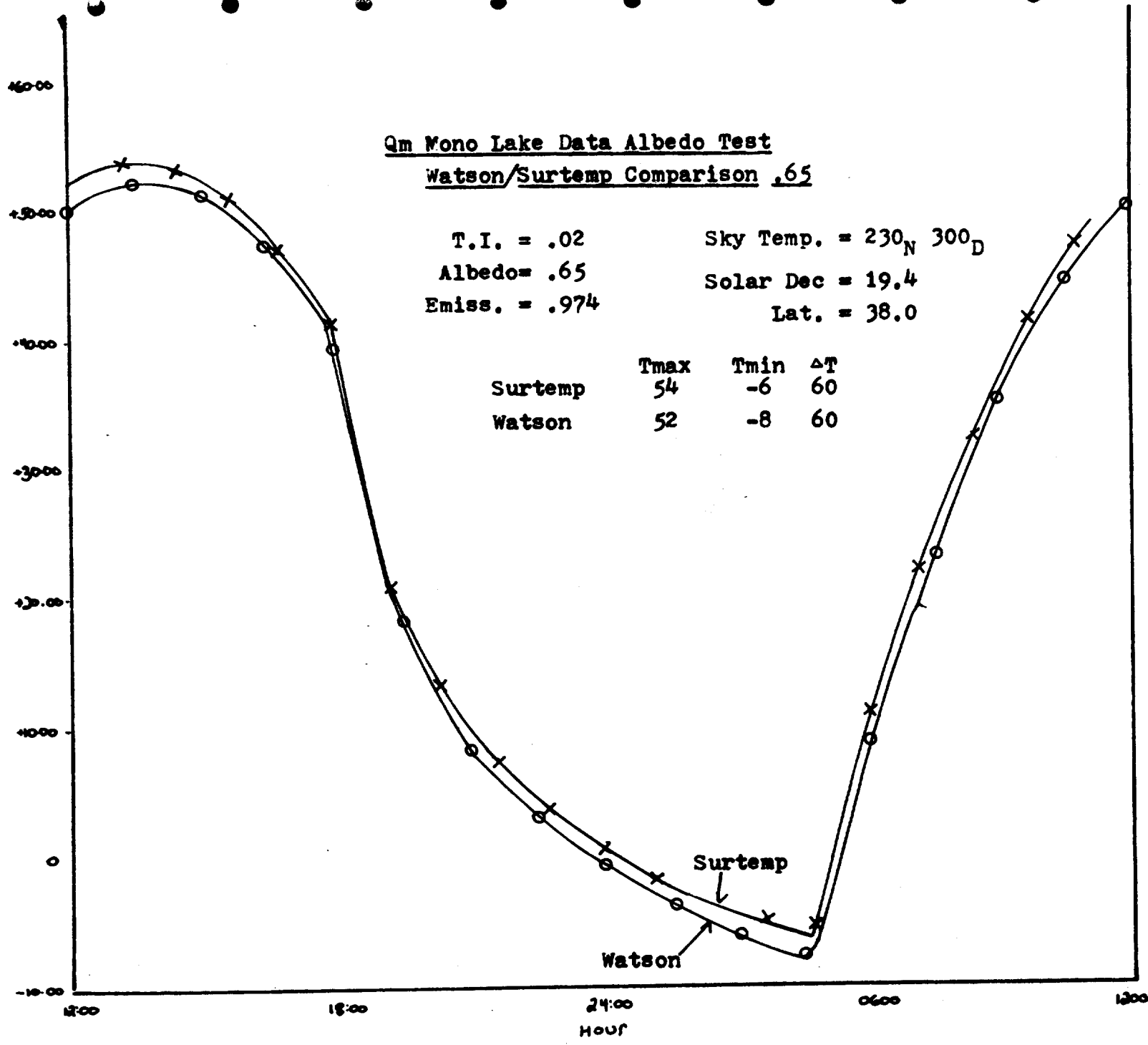


Figure 5

SURFACE TEMPERATURE



Qbt Mono Lake Emissivity Test  
Watson/Surtemp Comparison .947

T.I. = .04  
Albedo = 0.4  
EMiss. = 0.947

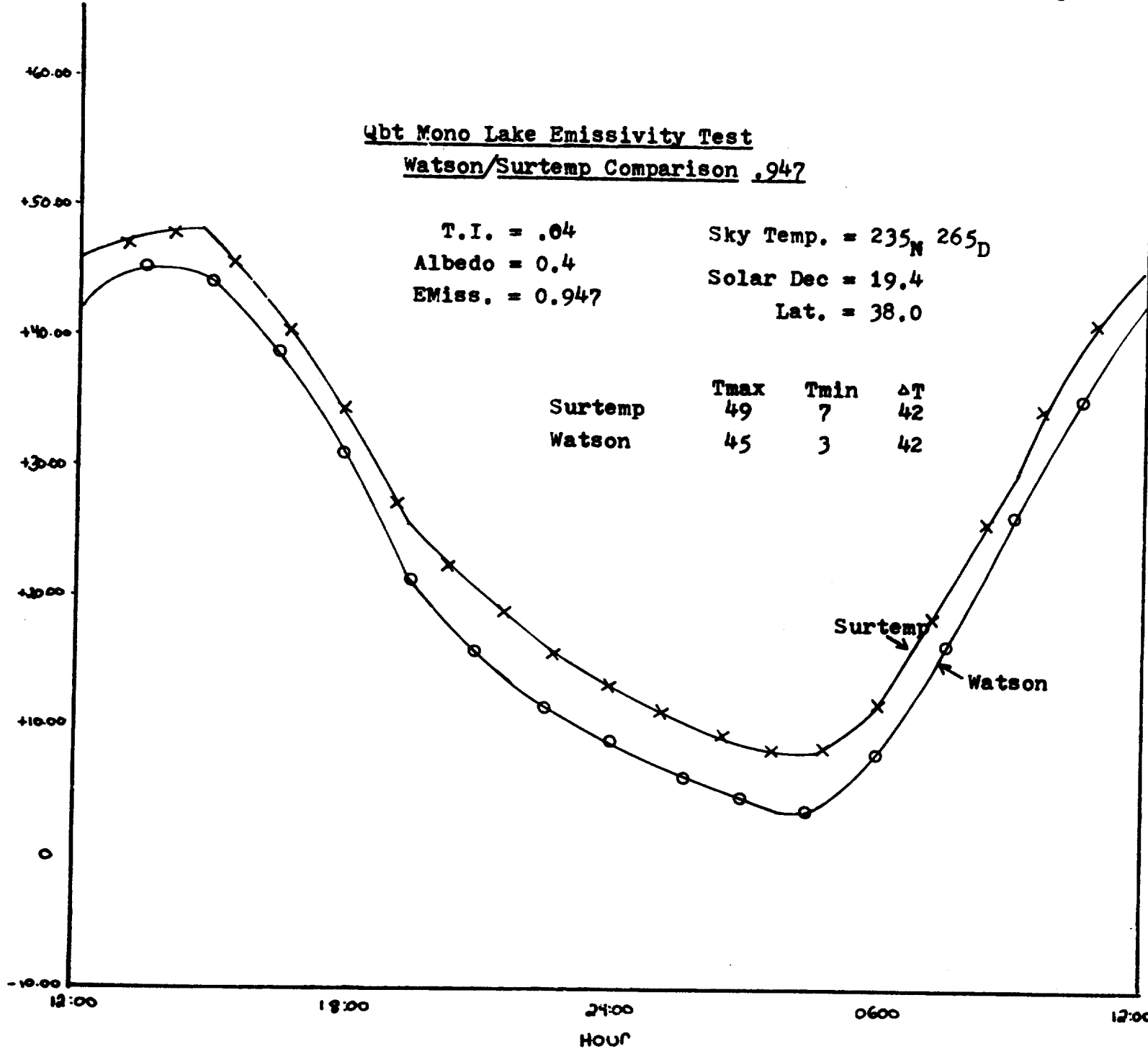
Sky Temp. = 235<sub>N</sub> 265<sub>D</sub>  
Solar Dec = 19.4  
Lat. = 38.0

Surtemp  
Watson

	Tmax	Tmin	ΔT
Surtemp	49	7	42
Watson	45	3	42

Surtemp  
Watson

SURFACE TEMP. DEGREES C



similarity in the shape of the diurnal variation curves would tend to confirm this. Inspection of the sky temperature change comparisons would indicate that within both models a  $1^{\circ}\text{C}$  change in target would arise from a small change in sky temperature, (<5%). Inspection of all the graphs indicates the largest discrepancy between the two programs occurs between the post sunset (2000 hours) and predawn (0400 hours). Differences in maximum and minimum temperatures however are only between one and four degrees ( $\text{C}$ ). The fact that the largest variations occur in the predawn hours and that Watson's (1974a) estimate of differential change in property values is taken at the predawn temperature does not necessarily provide an explanation for the discrepancies, because the shape of the curves appear similar for varying input parameter values. It is unclear what number of runs were made by Watson; to reach this conclusion, however, from the amount of data published by Watson it may be assumed his data base exceeded the two to six runs made by Lyon for each of his parameter change comparisons. This may have induced the discrepancies, nevertheless there is no strong evidence for this conclusion and could only be resolved through further runs of WATEMP and SURTEMP. An additional factor that undoubtably would vary the program results concerns the site location. The percent change discrepancies may in fact be due to the range of input variables used. Changes in emissivity, for example, that would produce a  $1^{\circ}\text{C}$  change in surface temperature in the 0.94 to 0.95 range may be different in a lower or high range of values (i.e. 0.91 to 0.93 or 0.96 to 0.98). There is no explanation of the ranges used in Watson's (1974a) analysis, so a definitive conclusion concerning this effect can not be made; Lyon's data however are for real rock materials and parametric variations measured in the field (using Friedman, 1968, values).

It is surprising that estimates of percent change by the two researchers should vary considerably for albedo and emissivity and not for thermal inertia, and particularly so, after noting in the previous discussion of thermal parameters the significance of thermal inertia to target temperature variations. To resolve this, further comparisons would have to be made. It is concluded that the difference between the two program results are probably caused by variations in the initial temperature approximation and the number of iterations for each solution. The Watson program consistently

gives lower temperature estimates for any particular hour. The shape of the curves are quite similar and temperature differences are minor except during the late evening to predawn hours.

A comparison of the Outcalt (1972) thermal model to the Watson (1971a) and SURTEMP models was made using published input and model results of a test run inserted both into the Stanford IBM 360 WATEMP program, and the PDP-10 SURTEMP program. Input parameters given by Outcalt (and corresponding to the WATEMP-SURTEMP model) are:

Latitude =  $49.3^{\circ}$   
Solar decl. =  $-14.9^{\circ}$   
Albedo = 0.15  
Sky radiant T. =  $235^{\circ}\text{K}$   
Soil thermal diffus. = .0056 (cgs)  
Soil vol. heat capac. = 0.500 (cgs)  
Shadow ratio = 0.0

From the diffusivity ( $\alpha$ ) and volumetric heat capacity ( $C$ ) it is possible to compute conductivity ( $k$ ) and thermal inertia ( $\gamma$ ) from the relation:

$$\alpha = \frac{k}{\rho c}$$

$$\gamma = (kC)^{1/2}$$

$$0.0056 = k/0.500$$

$$\gamma = (0.0028 \times 0.500)^{1/2}$$

$$k = 0.0028 \text{ cal cm}^{-2} \text{ sec}^{-1} \text{ }^{\circ}\text{C}^{-1}$$

$$\gamma = 3.74 \times 10^{-2} \text{ cal cm}^{-2} \text{ sec}^{-1} \text{ }^{\circ}\text{C}^{-1}$$

An emissivity of 0.98 was assumed from the description of the site—"Needle-Ice Event", and the slope orientation and inclination are assumed to be zero from the shadow ratio. Additional input for the Outcalt model included values for air column and soil conditions.

Results of the comparison run are illustrated on Figures 7 and 8. The shape of both curves are similar, and maximum temperature varies by only  $1^{\circ}\text{C}$ , minimum by  $4^{\circ}\text{C}$ , and  $\Delta T$  by  $3^{\circ}\text{C}$ . Interestingly, again the largest discrepancy

000000000

TIMES, FINAL SURFACE TEMPERATURES, AND INPUT TEMPERATURES

12.0	12.2	14.6	13.2	14.1	14.7	14.4	13.1	12.0	15.6	9.0	8.5	16.8	3.9	4.6
18.0	1.3	0.6	19.2	-0.4	-0.4	20.4	-1.7	-1.3	21.6	-2.7	-1.9	22.8	-3.4	-2.6
24.0	-4.1	-3.0	1.2	-4.7	-3.2	2.4	-5.2	-3.8	3.6	-5.6	-3.9	4.8	-6.0	-4.0
6.0	-6.4	-4.1	7.2	-6.7	-2.0	8.4	-3.5	1.0	9.6	2.1	4.1	10.8	7.9	8.4

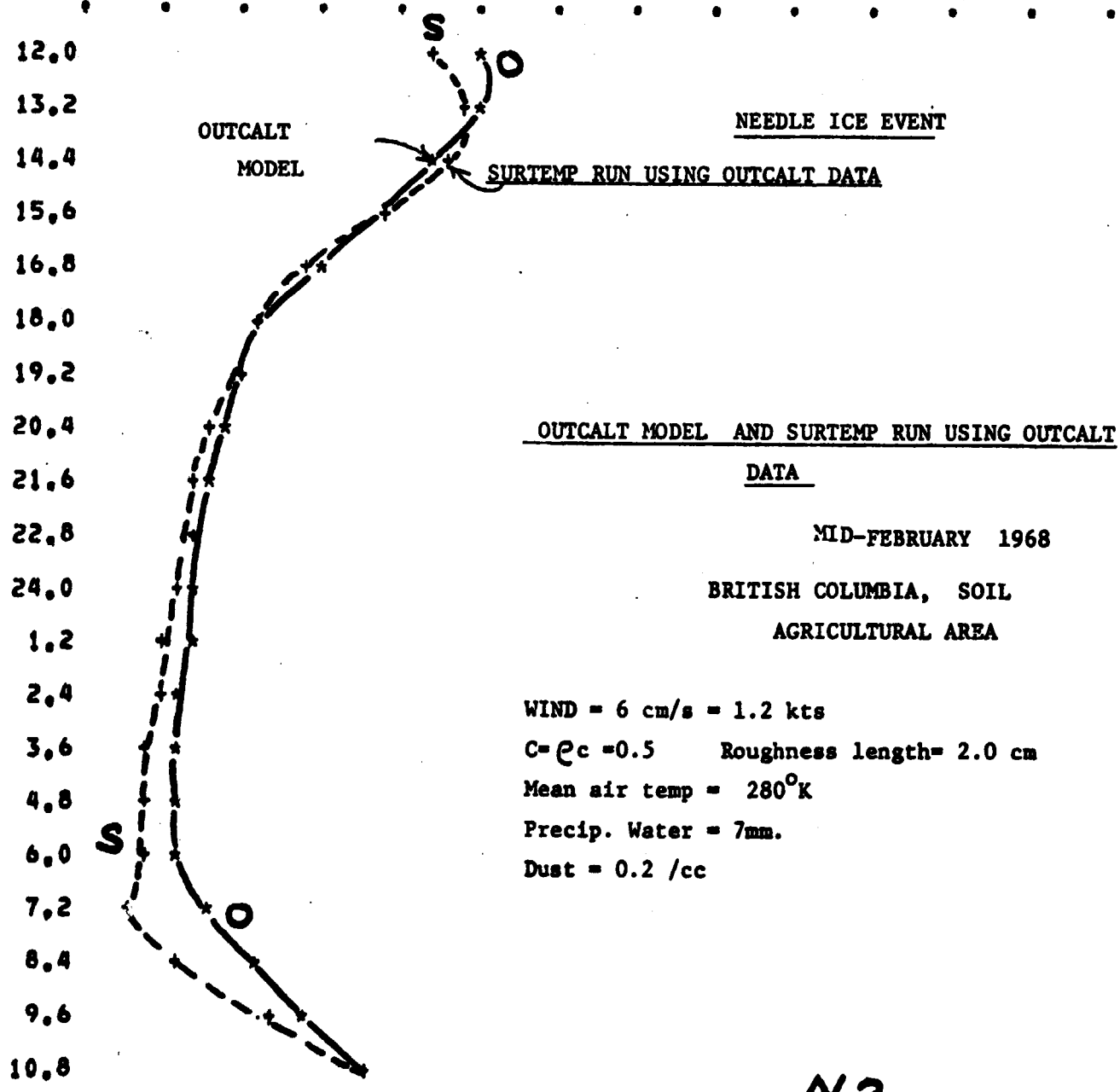
T MAX 14.1 T MIN -6.7 AVERAGE TEMP 0.67

PROGRAM PARAMETERS CURRENT VALUES

(5) CLOUD 0.0 (6) ALB 0.150 (7) EMS 0.9800 (8) T IN 0.037 (9) LAT 49.3  
(10) DEC -15.0 (11) DIP 0.0 (12) STR 0.0 (13) TN 253.0 (14) TD 253.0

PLOT OF FINAL TEMP (+) AND INPUT TEMP (\*) AGAINST TIME

-10 -5 0 5 10 15 20 25 30 35 40 45 50 55 60



N2

Figure 7

000000000

TIMES, FINAL SURFACE TEMPERATURES, AND INPUT TEMPERATURES

12.0	12.2	11.5	13.2	14.1	13.0	14.4	13.1	14.4	15.6	9.0	5.7	16.8	3.9	2.0
18.0	1.3	-1.0	19.2	-0.4	-2.2	20.4	-1.7	-3.5	21.6	-2.7	-4.4	22.8	-3.4	-5.3
24.0	-4.1	-6.0	1.2	-4.7	-6.8	2.4	-5.2	-7.2	3.6	-5.6	-7.8	4.8	-6.0	-8.0
6.0	-6.4	-8.1	7.2	-6.7	-6.9	8.4	-3.5	-4.4	9.6	2.1	-0.9	10.8	7.9	5.0

T MAX 14.1 T MIN -6.7 AVERAGE TEMP 0.67

PROGRAM PARAMETERS CURRENT VALUES

(5) CLOUD 0.0 (6) ALB 0.150 (7) EMS 0.9800 (8) T IN 0.037 (9) LAT 49.3  
(10) DEC -15.0 (11) DIP 0.0 (12) STR 0.0 (13) TN 253.0 (14) TD 253.0

PLOT OF FINAL TEMP (+) AND INPUT TEMP (\*) AGAINST TIME

-10 -5 0 5 10 15 20 25 30 35 40 45 50 55 60

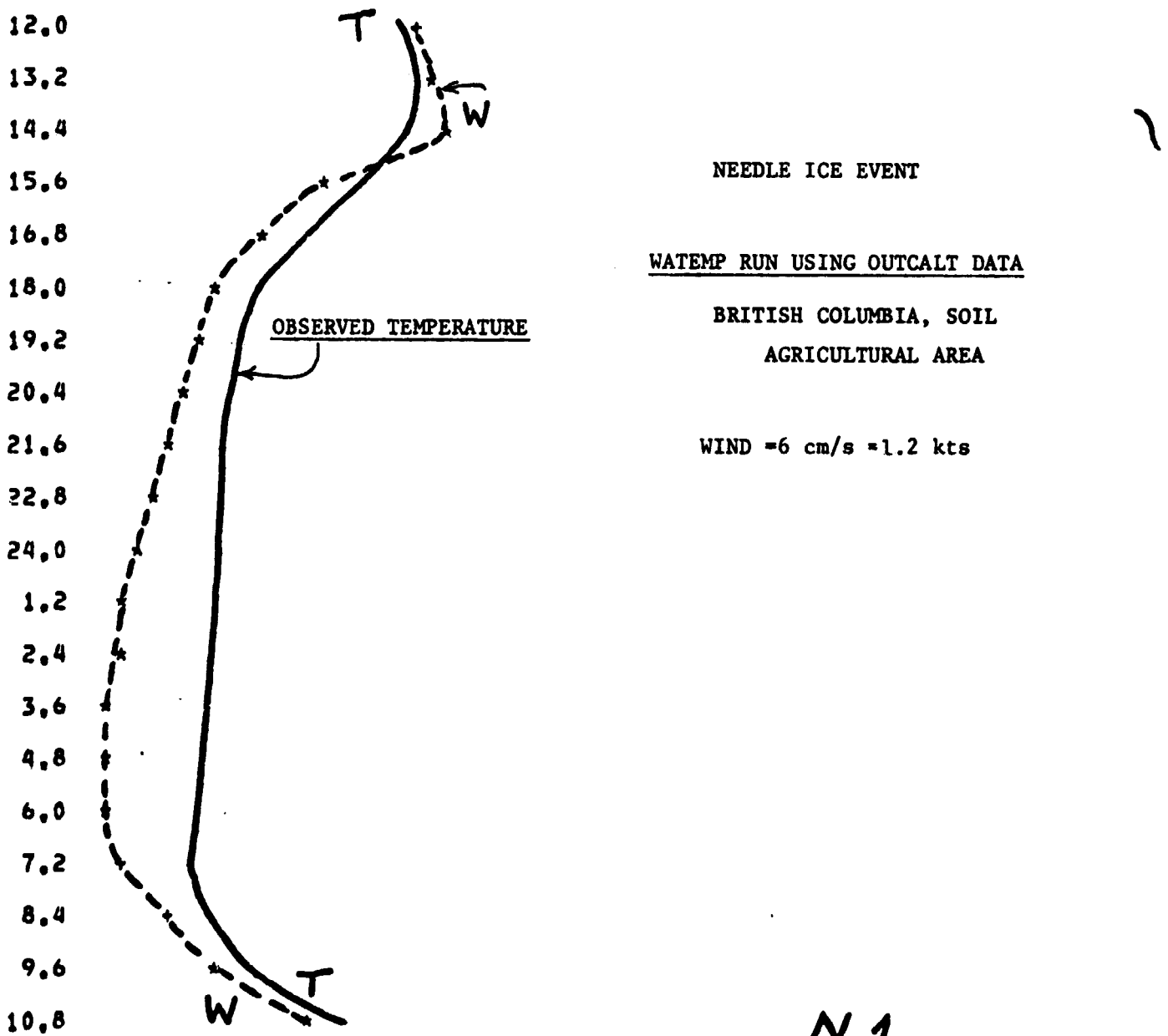


Figure 8

between the two models exists in the predawn hours. From the comparison it appears we can tentatively conclude that both programs yield similar temperature estimates ( $\pm 4^{\circ}\text{C}$ ). The additional complexity of Outcalt's program however does not necessarily make its results more accurate. Uncertainty of parameters must still exist and added parameters may increase total uncertainties. To ensure the usefulness of a model the additional parameters that are of value only to the climatologist should be disregarded by the geologist or geophysicist. This would make the job of collecting field data simpler and the model less cumbersome to use.

Two comparisons of the ROSEMA/WATEMP/SURTEMP models were made using the input parameters published by Rosema (1974) for coarse sand and Basin clay at sites in Holland ( $52^{\circ}\text{N}$ ), that he does not describe in detail. Input values given by Rosema applicable to the Watson program are:

	<u>Coarse Sand</u>	<u>Basin Clay</u>
Albedo	0.30	0.15
Emissivity	0.92	0.94
Vol. Qtz. Content } X	0.60	0.00
Vol. Clay + Feldspar } m	0.00	0.46
Vol. organics (X <sub>o</sub> )	0.00	0.00
Latitude	52.0°	52.0°
Day	April 12	April 12

Values of sky temperature and thermal inertia had to be estimated. The selection of sky temperature for the location and season of the test, at a ground temperature of  $280^{\circ}\text{K}$  was fixed somewhat arbitrarily at  $260^{\circ}\text{K}$  night and  $270^{\circ}\text{K}$  day. \*\*\* Selection of thermal inertia was somewhat less arbitrary. Employing the De Vries (1933) equation for soil heat capacity:

$$C = 0.46X_m + 0.60X_o + X_w \text{ cal cm}^{-3} \text{ }^{\circ}\text{C}^{-1} \quad (9)$$

the coarse sand with a moisture content of 0.20, would have a heat capacity of:

$$C = 0.46(0.60) + 0.60(0.0) + (0.20) = 0.476 \quad (10)$$

---

\*\*\* Humidity at the site should produce close night and day temperatures (Lyon, personal communication 1975).

with a moisture content of 0.20; the Basin clay would have a heat capacity of:

$$C = 0.46 (0.46) + 0.60 (0.0) + (0.30) = 0.512 \quad (11)$$

Estimates of conductivities given by Sellers (1965) and De Vries (1963) at moisture contents of 0.20 are  $4.2 \times 10^{-3}$  and  $5.3 \times 10^{-3} \text{ cal cm}^{-1} \text{ sec}^{-1} {}^{\circ}\text{C}^{-1}$  for coarse sand; and  $3.5 \times 10^{-3}$  and  $2.8 \times 10^{-3} \text{ cal cm}^{-1} \text{ sec}^{-1} {}^{\circ}\text{C}^{-1}$  for Basin clay. Taking the mean of these values with the calculation of estimated volumetric heat capacities calculated, values of thermal inertia ( $\gamma$ ) can be estimated:

$$\begin{aligned} \gamma &= \rho (kC)^{1/2} \\ \text{Coarse sand} &= (4.8 \times 10^{-3} \times 0.48)^{1/2} \quad (12) \\ &= 0.048. \\ \text{Basin clay} &= (3.2 \times 10^{-3} \times 0.51)^{1/2} \\ &= 0.040. \quad (13) \end{aligned}$$

Results from the comparisons (figure 9) indicate a large discrepancy of surface temperature. The comparison, nevertheless, was a useful exercise in showing the difficulty of obtaining thermal parameters for any given test. The large uncertainty in our estimation of appropriate sky temperature and thermal inertia illustrate their significant effects on modeling of the diurnal temperature variation.

Certain added ambiguities exist in the Watson-Rosema Comparison: Within the description of the parameters of the sample materials, by Rosema (1974), it is difficult to imagine an absolute zero quartz content in the Basin clay. Also somewhat surprising are the results given by WATEMP. It is unusual that surface temperatures in early April at a north latitude of  $52^{\circ}$  could reach  $50^{\circ}\text{C}$ .

#### C. Discussion

The value of thermal models seems apparent from the previous discussion. The thermal models of Watson and SURTEMP appear quite similar, and hold an advantage over those of Outcalt and Rosema in their simplicity of input parameters. When used to differentiate rock and soil types as on infrared

0000000000  
 TIMES, FINAL SURFACE TEMPERATURES, AND INPUT TEMPERATURES  
 12.0 53.5 0.0 13.2 56.1 0.0 14.4 55.8 20.2 15.6 52.7 18.1 16.8 47.0 14.0  
 18.0 39.6 10.9 19.2 33.1 8.4 20.4 29.3 6.3 21.6 26.6 4.9 22.8 24.5 4.1  
 24.0 22.9 3.3 1.2 21.5 2.9 2.4 20.3 2.4 3.6 19.3 2.0 4.8 18.3 1.8  
 6.0 20.3 2.4 7.2 26.6 5.8 8.4 33.5 9.2 9.6 41.4 13.0 10.8 48.4 17.0

T MAX 56.1 T MIN 18.3 AVERAGE TEMP 34.50

HOLLAND  
BASIN CLAY

PROGRAM PARAMETERS CURRENT VALUES

(5) CLOUD 0.0 (6) ALB 0.150 (7) EMS 0.9400 (8) T IN 0.040 (9) LAT 52.0  
 (10) DEC 8.3 (11) DIP 0.0 (12) STR 0.0 (13) TN 260.0 (14) TD 270.0

PLOT OF FINAL TEMP (+) AND INPUT TEMP (\*) AGAINST TIME

-10 -5 0 5 10 15 20 25 30 35 40 45 50 55 60

12.0

13.2

14.4

15.6

16.8

18.0

19.2

20.4

21.6

22.8

24.0

1.2

2.4

3.6

4.8

6.0

7.2

8.4

9.6

10.8

ROSEMA INPUT DATA

SURTEMP, USING ROSEMA INPUT

Minerals..  $\rho$  c  
 $K = 3.2 \times 10^{-3}$  assumed.

WIND = 5m/s = 10 kts.

$T_N = 260$   $T_D = 270^{\circ}$  K

T.I. = 0.04 calc

Figure 9

BC1

-10 -5 0 5 10 15 20 25 30 35 40 45 50 55 60

imagery, the model indicates that thermal inertia is a good discriminator of materials, and the effects of thermal inertia on surface temperatures are maximized near dawn. Thus dawn represents the optimum time to observe thermal contrasts due to thermal property differences.

### III. PISGAH-LAVIC LAKE STUDY (March 29-30, 1975)

#### A. Site Description

The Pisgah Crater-Lavic Lake area is located in the Mohave Desert, San Bernardino County, California. It is approximately 38 miles east-southeast of the town of Barstow. Pisgah Crater and its associated flow is nearly 14 miles long and 4 miles across. At the southeastward end of the flow is Lavic Dry Lake approximately 2 miles in diameter. Other details of the area appear in Kahle, et.al., 1976.

The Pisgah Crater flow is composed of numerous thin olivine basalt flows. The top of this flow sequence is made up of both pahoehoe (ropy) and aa (jagged-clinkery) lava. The aa lava is dark gray, or more usually, black in color and has an extremely rough surface. The pahoehoe lava is a "medium" dark gray in color and has a smoother undulatory surface. Both types of surface can accumulate windblown sand or silt. Pisga.. Crater is made of cinders (that range in color from black to grayish red), and small bombs. The crater floor is pahoehoe basalt.

Lavic Dry Lake is a very flat playa composed of a very pale, yellowish-brown silty clay. Neal (1965) determined the playa is made up of 79% clay (essentially montmorillonite and illite) 20.7% granular components, and 0.2% accessories with a bulk density of 1.67. The playa had an approximate maximum relief of 2 1/2 feet. Numerous areas on the playa are mantled by pebbles or cobbles of basalt or alluvial fan material. These mantling materials are somewhat anomalous as they are found some distance from their obvious source. Gawarecki (1964) reports they are believed to be ice rafted to their current position when sufficient lake levels existed.

Alluvial fan material is found along the borders of Lavic Lake. This material is a heterogeneous conglomerate derived from present topographic highs. It is a yellowish gray color with a sparse vegetation cover.

Measurement sites at the crater, designated, "Crater outeredge" and "Crater station" consisted of cinders, clinkers and bombs; site "Crater outside Basalt" consisted of aa and pahoehoe basalt east of the cone viewed from a distance. Site "Crater center" was measured from a distance and consisted of solidified pahoehoe lava; Site "Crater Red Cinder" consisted of an area of predominantly Red cinder on the inner lip of the crater; and site "Crater Road" consisted of compacted cinders and dirt.

Lavic Lake sites 1-1, 1-2, 1-3, 1-4, 2-2, 2-3, consist of the pale yellowish-brown silty clay. Site 2-1 was on alluvium (Figure Map 1).

#### B. Albedo Measurements and Analysis

Measurements of albedo were made at the test sites on Lavic Lake and at the crater employing an ISCO spectral radiometer and an EXOTECH radiometer by Stanford Remote Sensing Lab personnel. These measurements were necessary to better understand the site locations and to provide the necessary input data for our thermal model. The procedure involved making a number (5-25) of readings at each site attempting to include the greatest diversity in surficial conditions, with concurrent readings of white reflectance standards of BaSO<sub>4</sub> and Fiberfrax. ISCO readings (see Appendix 2) were made from 0.400 to 1.55 micrometers with a bandpass interval of .025 micrometers in the visible and a bandpass interval of .050 micrometers in the near-IR. Exotech readings were collected in detail at the Lavic Lake sites. The instrument sensed in the same channels as the LANDSAT MSS sensor (0.5-.6, .6-.7, .7-.8, .8-1.1 micrometers). Twenty-five readings at Stations 2-1 (alluvium), 1-1 and Base camp (playa) were made, and five readings at Stations 1-2, 1-3, 2-2A, 2-2B, 2-2A (playa) were made (Figure Map 1). Appendix 1 catalogues these measurements and yields values of bandpass, reflectance, and "pseudo-CIE" color coordinates for each channel and calculates an albedo for each site.

The albedo values from the Exotech measurement sites are compiled in Table 3 along with means and standard deviations for each location. The 75 playa measurements yielded a mean of 0.375 and a standard deviation of 0.027 (7% variation) while the 25 alluvium sites (2-1) yielded a mean of .295 and a standard deviation of .018 (6% variations). These statistical checks indicate

indicate that complete discrimination is possible between playa and alluvium within ( $1\sigma$ ) one standard deviation interval. However, a slight overlap exists at the two standard ( $2\sigma$ ) deviation interval. The seven distinct playa stations (1-1, 1-2, 1-3, 2-2A, 2-2B, 2-2, BC) cannot be separately delineated by the albedo values except for station 2-2 which can be discriminated by albedo within a two standard deviation interval. A contour map of the site albedos (figure 10) visually expresses this discriminatory ability of albedo.

To determine the most favorable spectral information for discrimination of the playa sites the complete data set (Appendix 1) was input to the BMD07M (stepwise discriminant analysis) program developed by the UCLA Health Sciences Computing Facility (April 10, 1972). The results showed that the simple bandpass of channel BP5\* (.6-.7  $\mu\text{m}$ ) had the greatest success (55%) at discrimination by itself. This was followed by R5 reflectance .6-.7  $\mu\text{m}$  (82%), R4 reflectance .5-.6  $\mu\text{m}$  (83%), BP4 bandpass .5-.6  $\mu\text{m}$  (85%), and R74 ratio of reflectances .8-1.1 by .5-.6  $\mu\text{m}$ ), for the pair, trio, quartet, quintet as used, respectively. This is graphically displayed in Figure 11. Of the 25 sites measured at station 1-1, 17 were correctly classified and of the 25 at station base camp 18 were correctly classified, using the quintet, with 84% success level. At this level, the program employing the input quintet, all measured sites were correctly classified at stations 1-2, 1-3, 2-2, 2-2A, 2-2B. Station 2-1 within alluvium is readily distinguishable from the playa and of the 25 sites measured 24 were correctly classified.

It seems reasonable to conclude then that though total albedo is a necessary measurement for thermal modelling it is not entirely successful at spectral discrimination. Greater spectral discriminatory ability is available employing individual spectral bands and ratios of bands using a simple ratiometer of the EXOTECH type. Thus LANDSAT satellite data could have been used to discriminate between sites of this degree of spectral albedo differences.

#### C. Surface Temperature Measurements and Analysis - Pisgah Crater and Lavic Lake

Stanford Remote Sensing Lab personnel were able to provide much needed expertise in the collection of field thermal measurements. We made use of several Barnes (PRT) Radiation thermometers and thermistor probes. Appendix 3 catalogues these measurements and Appendix 6 graphically display the probe

\* BP 4, 5, and 7 are bandpass radiances and R4, 5, 6, and 7 are bi-directional reflectances using LANDSAT type bandpass filters (EXOTECH).

SITE LOCATIONS LAVIC LAKE

N

To Crater

1-4  
1-5  
1-6  
BC

2-1  
2-2b

2-2a

2-2

1-3

1-2

1-1

•2 miles  
1056 ft

Figure Map 1

TABLE 3

Albedo Determinations:

## PLAYA

Site:	<u>1-1</u>	<u>1-1N</u>	<u>1-1E</u>	<u>1-1S</u>	<u>1-1W</u>
	.352	.378	.340	.364	.367
	.359	.378	.348	.344	.387
	.348	.377	.349	.398	.372
	.354	.401	.354	.369	.368
	.363	.367	.355	.377	.363
$\bar{x}$ =	.355	.380	.349	.370	.371
s=	.006	.013	.006	.020	.009

$$\bar{x}_{\text{total}} = .365 \quad n=25$$

$$s_{\text{total}} = .016$$

Site:	<u>1-2</u>	<u>1-3</u>	<u>2-2A</u>	<u>2-2B</u>	<u>2-2</u>
	.368	.404	.365	.385	.461
	.365	.369	.347	.386	.469
	.373	.375	.348	.388	.457
	.391	.372	.377	.375	.450
	.392	.370	.353	.384	.448
$\bar{x}$ =	.378	.378	.358	.384	.457
s=	.013	.015	.013	.005	.009

Site:	<u>BC</u>	<u>BCN</u>	<u>BCS</u>	<u>BCE</u>	<u>BCW</u>
	.364	.370	.355	.353	.368
	.366	.416	.388	.360	.368
	.377	.393	.360	.362	.365
	.410	.353	.359	.360	.365
	.372	.366	.369	.364	.370
$\bar{x}$ =	.378	.380	.366	.360	.367
s=	.019	.025	.013	.004	.002

$$\bar{x}_{\text{total}} = .370 \quad n=25$$

$$s_{\text{total}} = .016$$

-----

$$\bar{x}_{\text{playa}} = .375 \quad n=75$$

$$s_{\text{playa}} = .027$$

Table 3 continued

## ALLUVIUM

Site:	<u>2-1</u>	<u>2-1N</u>	<u>2-1E</u>	<u>2-1S</u>	<u>2-1W</u>
	.293	.299	.288	.305	.298
	.287	.273	.358	.290	.298
	.293	.282	.278	.300	.272
	.290	.291	.311	.303	.271
	.286	.288	.298	.311	.312
$\bar{x}$ =	.290	.287	.307	.302	.290
s=	.003	.010	.031	.008	.018

$$\bar{x}_{\text{total}} = .295$$

n=25

$$s_{\text{total}} = .018$$

Emissivity for the playa was assumed, at each site, to be .985.

CONTOUR OF SITE ALBEDO VALUES

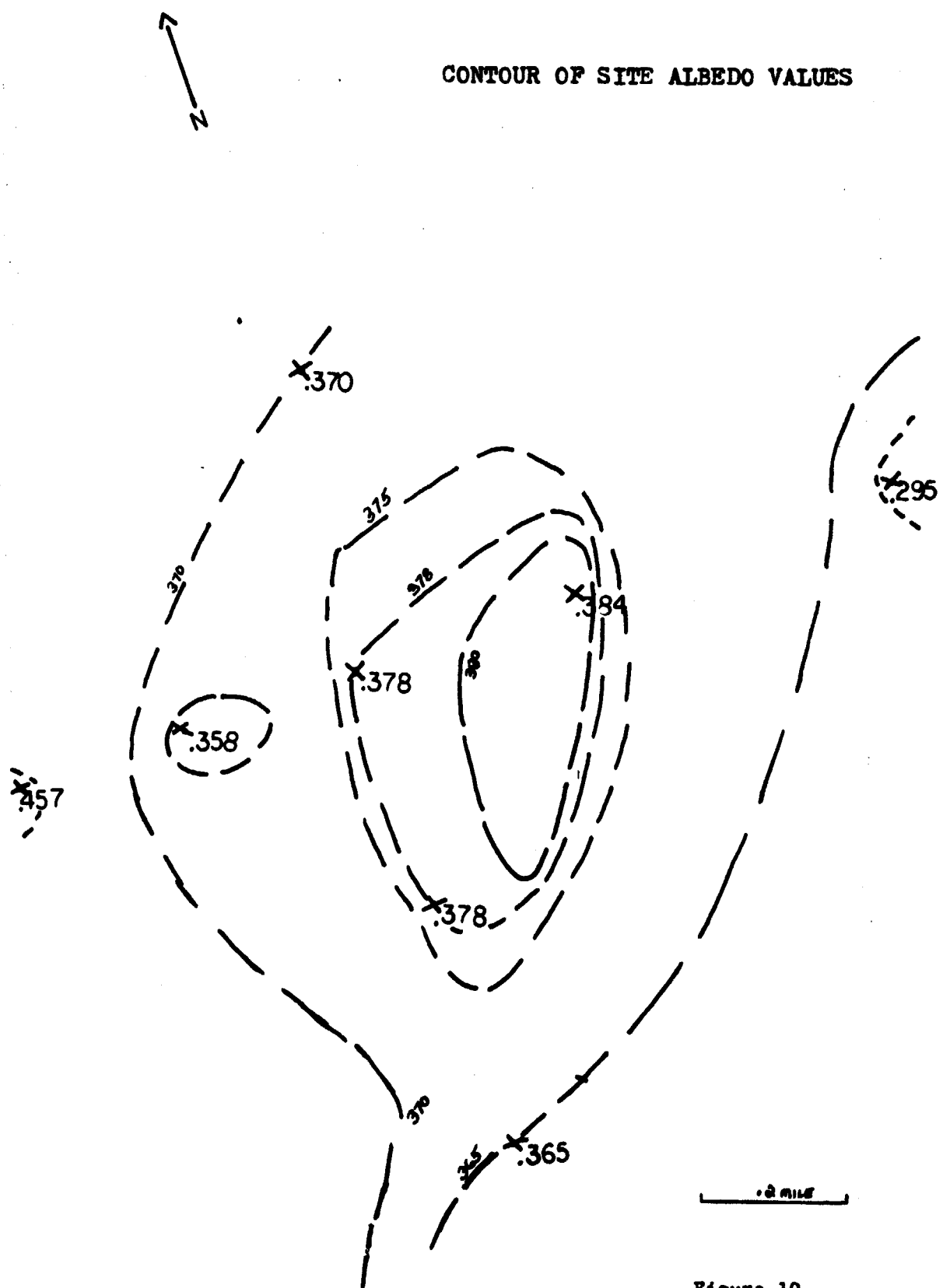
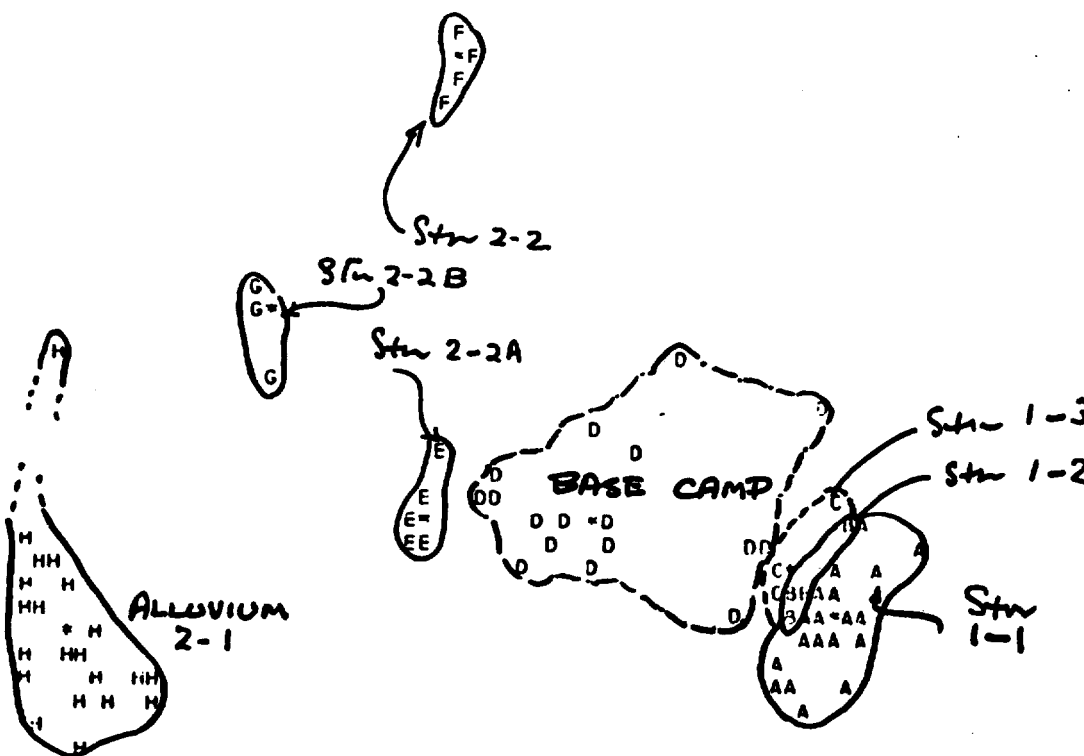


Figure 10

FIGURE 11

-10.456	-5.621	-3.204	-0.797	1.630	4.048	6.465	8.882	11.299
11.299	10.896	10.494	10.091	9.688	9.285	8.882	8.479	8.076
9.076	8.682	8.285	7.882	7.479	7.076	6.688	6.285	5.882
7.673	7.271	6.868	6.465	6.062	5.659	5.256	4.853	4.450
6.450	6.062	5.659	5.256	4.853	4.450	4.048	3.645	3.242
4.048	3.645	3.242	2.839	2.436	2.033	1.630	1.227	0.825
3.645	3.242	2.839	2.436	2.033	1.630	1.227	0.825	0.422
3.242	2.839	2.436	2.033	1.630	1.227	0.825	0.422	0.019
2.839	2.436	2.033	1.630	1.227	0.825	0.422	0.019	-0.384
2.436	2.033	1.630	1.227	0.825	0.422	0.019	-0.384	-0.787
2.033	1.630	1.227	0.825	0.422	0.019	-0.384	-0.787	-1.190
1.630	1.227	0.825	0.422	0.019	-0.384	-0.787	-1.190	-1.593
1.227	0.825	0.422	0.019	-0.384	-0.787	-1.190	-1.593	-1.996
0.825	0.422	0.019	-0.384	-0.787	-1.190	-1.593	-1.996	-2.398
0.422	0.019	-0.384	-0.787	-1.190	-1.593	-1.996	-2.398	-2.801
0.019	-0.384	-0.787	-1.190	-1.593	-1.996	-2.398	-2.801	-3.204
-0.384	-0.787	-1.190	-1.593	-1.996	-2.398	-2.801	-3.204	-3.607
-0.787	-1.190	-1.593	-1.996	-2.398	-2.801	-3.204	-3.607	-4.010
-1.190	-1.593	-1.996	-2.398	-2.801	-3.204	-3.607	-4.010	-4.413
-1.593	-1.996	-2.398	-2.801	-3.204	-3.607	-4.010	-4.413	-4.816
-1.996	-2.398	-2.801	-3.204	-3.607	-4.010	-4.413	-4.816	-5.219
-2.398	-2.801	-3.204	-3.607	-4.010	-4.413	-4.816	-5.219	-5.621
-2.801	-3.204	-3.607	-4.010	-4.413	-4.816	-5.219	-5.621	-6.024
-3.204	-3.607	-4.010	-4.413	-4.816	-5.219	-5.621	-6.024	-6.427
-3.607	-4.010	-4.413	-4.816	-5.219	-5.621	-6.024	-6.427	-6.830
-4.010	-4.413	-4.816	-5.219	-5.621	-6.024	-6.427	-6.830	-7.233
-4.413	-4.816	-5.219	-5.621	-6.024	-6.427	-6.830	-7.233	-7.636
-4.816	-5.219	-5.621	-6.024	-6.427	-6.830	-7.233	-7.636	-8.039
-5.219	-5.621	-6.024	-6.427	-6.830	-7.233	-7.636	-8.039	-8.442
-5.621	-6.024	-6.427	-6.830	-7.233	-7.636	-8.039	-8.442	-8.844
Var:	Success along							-9.247
-6.024	4: BP 5	55% alme						-9.650
-6.427	8: R 5	82 Fair						-10.053
-5.830	7: R 4	93 Trio						-10.456
-7.233	3: BP 4	88 Quartet						
-7.636	13: R 7/4	84 Quintet.						
-8.039								
-8.442								
-8.844								
-9.247								
-9.650								
-10.053								
-10.456								

LAVIC LAKE

PLAYA + ALLUVIUM

8 classes.

N=100

5 Step

11.299

-8.039

-3.204

1.630

6.465

D-19 CPU

measurements for the playa sites, as tautochrones, or depth-temperature plots. The scale of the tautochrones permit positioning to within .5°C and .5 cm depth, and therefore should be considered accurate representations. Appendix 4 shows the measured (average of the 5 readings) surface temperatures (solid line) compared with runs of the SURTEMP and WATEMP programs.

The major concern in the determination of input parameters entails the selection of a thermal inertia value ( $\gamma$ ) to accurately match the measured surface temperatures. Various methods were employed to arrive at a value that can be considered reliable. Input parameters that are evident for the dry lake sites, are;

Latitude: 34.66°  
Dip : 0.0  
Strike : 0.0  
Sun's Declination: 03°02.9'.

The work of Neal (1965) provided pertinent data on the bulk density and composition of the Lavic Lake playa; soil moisture samples were taken during the mission and provided data yielding weight % water at .09% (vol. fraction .20%). With this data it is possible to apply the DeVries (1963) formula for volumetric heat capacity (C) of the playa material,

$$C = 0.46 X_m + 0.60 X_o + X_w, \quad (14)$$

where  $X_m$  = vol. fract. minerals  $X_o$  = vol. fract. organic, and  $X_w$  = vol. fract. water. DeVries also determined a formula for the damping depth of a soil related to thermal diffusivity ( $\alpha$ ),

$$(2 \alpha/w)^{1/2} = D \quad (15)$$

where D = Damping depth, and w = angular period of the diurnal wave ( $7.276 \times 10^{-5}$  rad sec<sup>-1</sup>). The damping depth is that depth where the surface temperature considered at a sinusoidal wave, is reduced by 1/e (.37). From inspection of the tautochrones at the playa sites the damping depth occurs at 10 cm.

Employing this knowledge we can solve for thermal diffusivity and arrive at a value of  $3.64 \times 10^{-3}$  cm<sup>2</sup> sec<sup>-1</sup>. If we consider this value and that for volumetric heat capacity (C=.568) to be valid then the thermal inertia of the playa can be calculated after first determining thermal conductivity (K).

Now,

$$\alpha = k/C \quad 3.64 \times 10^{-3} = k/.568 \\ k = 2.07 \times 10^{-3} \text{ cal cm}^{-1} \text{ sec}^{-1} {}^{\circ}\text{C}^{-1} \quad (16)$$

$$\gamma = (kC)^{1/2} = (2.07 \times 10^{-3} \times .568)^{1/2} \\ = .034 \text{ cal cm}^{-2} {}^{\circ}\text{C}^{-1} \text{ sec}^{-1}. \quad (17)$$

Additional information needed for the SURTEMP thermal model included a cloud cover factor assumed initially to be zero, a hemispherical net sky radiation term (sky temperature) for the day and night, and the emissivity of the surface approximated from measurements of similar surfaces at 0.985. From previous work (see Section II) of Lyon (1975) we note that an inaccuracy in the emissivity of 25% will produce only a  ${}^{\circ}\text{C}$  change in surface temperature, employing the SURTEMP program. However, as we have noted, the thermal model is quite sensitive to sky temperature. Unfortunately a net radiometer, necessary for these measurements, was not available and thus sky temperature could be only approximated from the known meteorological conditions. These calculations and approximations along with the albedo measurements were performed for each of the playa sites and closestfits to the observed data were plotted (Appendix 4). As can be seen, fairly close fits can be achieved with day and night sky temperatures of  $240^{\circ}$ ,  $230^{\circ}\text{K}$  respectively and employing the calculate thermal inertia ( $\gamma$ ) of  $.034 \text{ cal cm}^{-2} {}^{\circ}\text{C}^{-1} \text{ sec}^{-1}$ .

Discussion of these results with the JPL investigators, whom we were assisting, indicated that they believed a more accurate thermal inertia value for the playa fell between  $.01\text{--}.03 \text{ cal cm}^{-2} {}^{\circ}\text{C}^{-1}$ . The thermal model developed by Kahle (1976) compensates for wind at the site and they felt this meteorological variable (not directly included in the SURTEMP model) invalidated our results. To further explore this discussion additional SURTEMP runs were made analyzing station 1-1, (Appendix 5). It was determined by using the cloud cover factor to simulate a moderate wind speed (i.e. loss of input heating) and by altering the sky temperature the results could be made to approximately conform to a thermal inertia of  $.02 \text{ cal cm}^{-2} {}^{\circ}\text{C}^{-1} \text{ sec}^{-1}$ .

Unfortunately, we have not convincingly proven, even in the simple case of the playa material, what is the true value for the thermal inertia! Though admittedly the SURTEMP program does not include a compensating factor for strong windspeeds, it must also be pointed out that the JPL results were based on an assumption that the playa moisture content was zero! It can be shown

that this assumption can reduce a final thermal inertia value by more than 30%. Scientific integrity would therefore force us to conclude that an exact measure of thermal inertia was not determined by either group. If it is to be accurately estimated, precise measures of net sky radiation, emissivity, soil moisture, and wind speed must be made and included in thermal modeling.

It is abundantly clear that solution of thermal models using real data is not a simple problem, and much remains to be done. The problem is especially complex if the measurements are made from a remote vehicle.

#### IV. SANDBOX STUDY

##### A. Objectives

In an attempt to determine the accuracy of thermal inertia determinations by remote sensing techniques a study was begun at the Remote Sensing Lab. Though many workers are now reporting thermal inertia values using various computer model deviations of the heat conduction equation, it is difficult to fix confidence limits to these determinations. Therefore, after a considerable search, a standard material was found for which both thermal conductivity and diffusivity had been determined by direct laboratory techniques at varying moisture contents. A heat transfer study by Moench (1969) had determined these parameters for 20/30 mesh Ottawa sand (quartz, 0.5 to 0.8 mm size).

The sand could thus be placed under simulated natural conditions and attempts made to correctly determine its thermal properties. If successful further impetus would be gained for heat capacity mapping. If, however, a thorough experiment proved completely unsuccessful, we would be forced to examine the total validity of thermal inertia determinations and their discrimination by remote sensing techniques.

We have only begun preliminary experimentations, but these results and tentative assessments will be reported.

##### B. Measurements

In order to simulate natural soil conditions the sand was placed within a square box, constructed of Douglas Fir and sealed with water-safe glue, nails, and screws. The thickness of the walls is uniformly 6.3 cm, and it is 30.5 cm deep and 45.7 cm long and wide. The sand and thermistor probes placed within the sand were allowed to equilibrate for over one week.

For this preliminary work the same information was collected as was collected during the Pisgah-Lavic Lake mission. This procedure was adopted in order to assess the importance of accurate, in situ, net sky radiation and emissivity measurements. All other parameters were accurately measured, including albedo (.5-1.1 $\mu$ m) which was determined to be 0.54. The thermal measurements are compiled in Table 4 and the tautochrone of the data is depicted in figure 12. The emissivity of the sand was considered to be about 0.95, and the sky temperature (day and night) were both estimated at 263°K. Partly cloudy conditions existed sporadically during the day and evening and seemed to indicate a slight cloud cover factor.

#### C. Results

The water content of the sand was kept as close to zero as possible, yielding, from Moench's work, an expected thermal inertia of  $0.0166 \text{ cal cm}^{-2} \text{ }^{\circ}\text{C}^{-1} \text{ sec}^{-1}$ . Figure 13 represents the best fit for the observed data with these input parameters. The 5° $\text{C}$  discrepancy between the measured and modeled final temperatures, when the thermal inertia is known, succinctly states the need for more accurate measurements of net sky radiation, emissivity, and cloud cover-windspeed:

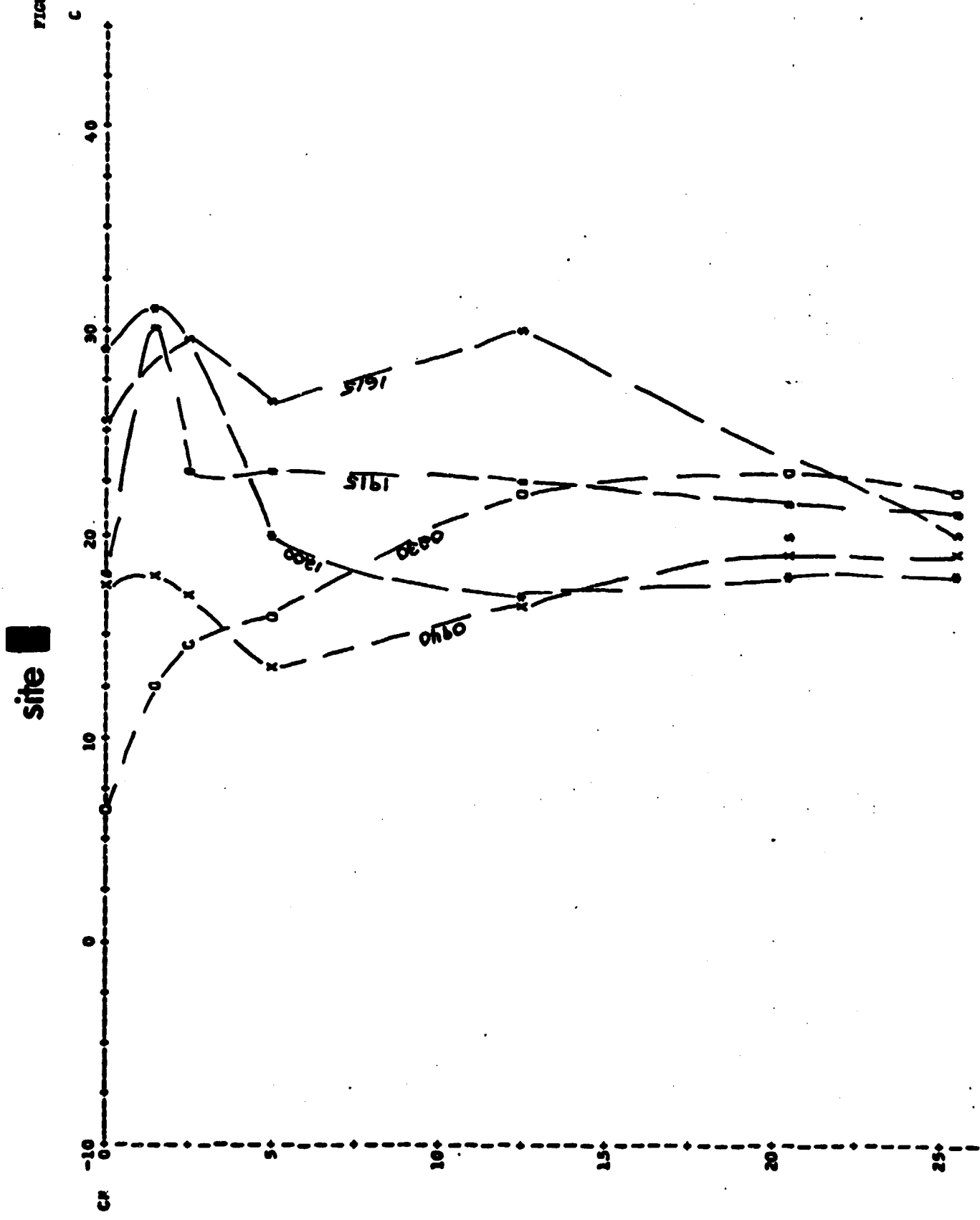
During this NASA grant a "look-up table" program for thermal inertia, based upon SURTEMP, was developed. The program allows for the construction of a 3-dimensional matrix, developed from the standard (or fixed) input data sets and with variable albedo and day and night temperature as the sand ordinates. Thus for any particular time of day and or night, a similar table, as seen in figure 14, can be generated. In this instance, the program yields a thermal inertia value of  $0.0195 \text{ cal cm}^{-2} \text{ }^{\circ}\text{C}^{-1} \text{ sec}^{-1}$ . The input is identical to that of figure 13. Comparison of these techniques allows us therefore to conclude the inaccuracies in our input parameters has produced a discrepancy of .003 in the thermal inertia.

These efforts are continuing and will be expanded with renewed funding for the HCMM program.

#### V. CONCLUSIONS

- A. Little agreement exists today between results from several thermal models using the same input data sets.
- B. Each model has a varying degree of sensitivity to any specified parameter,

FIGURE 12



12:35 SAT 4 OCT 75

<FBUDI>SEM,;1

UNNNNNNNNN

TIMES, FINAL SURFACE TEMPERATURES, AND INPUT TEMPERATURES

12.0	35.7	29.2	13.2	37.4	31.0	14.4	35.8	30.4	15.4	31.0	100.0	16.8	23.4	25.7
18.0	14.3	21.5	19.2	10.1	17.8	20.4	7.6	100.0	21.6	5.8	100.0	22.8	4.5	100.0
24.0	3.4	100.0	1.2	2.6	100.0	2.4	1.9	7.0	3.6	1.3	100.0	4.8	0.8	100.0
6.0	0.3	6.0	7.2	6.2	100.0	8.4	14.8	100.0	9.6	23.6	17.7	10.8	30.9	25.4

T MAX 37.4 T MIN 0.3 AVERAGE TEMP 14.57

PROGRAM PARAMETERS CURRENT VALUES

(5) CLOUD	0.1	(6) ALP	0.540	(7) EMS	0.9500	(8) T IN	0.017	(9) LAT	37.5
(10) DFC	3.8	(11) DTP	0.0	(12) STR	0.0	(13) TN	263.0	(14) TD	263.0

PLOT OF FINAL TEMP (+) AND INPUT TEMP (\*) AGAINST TIME

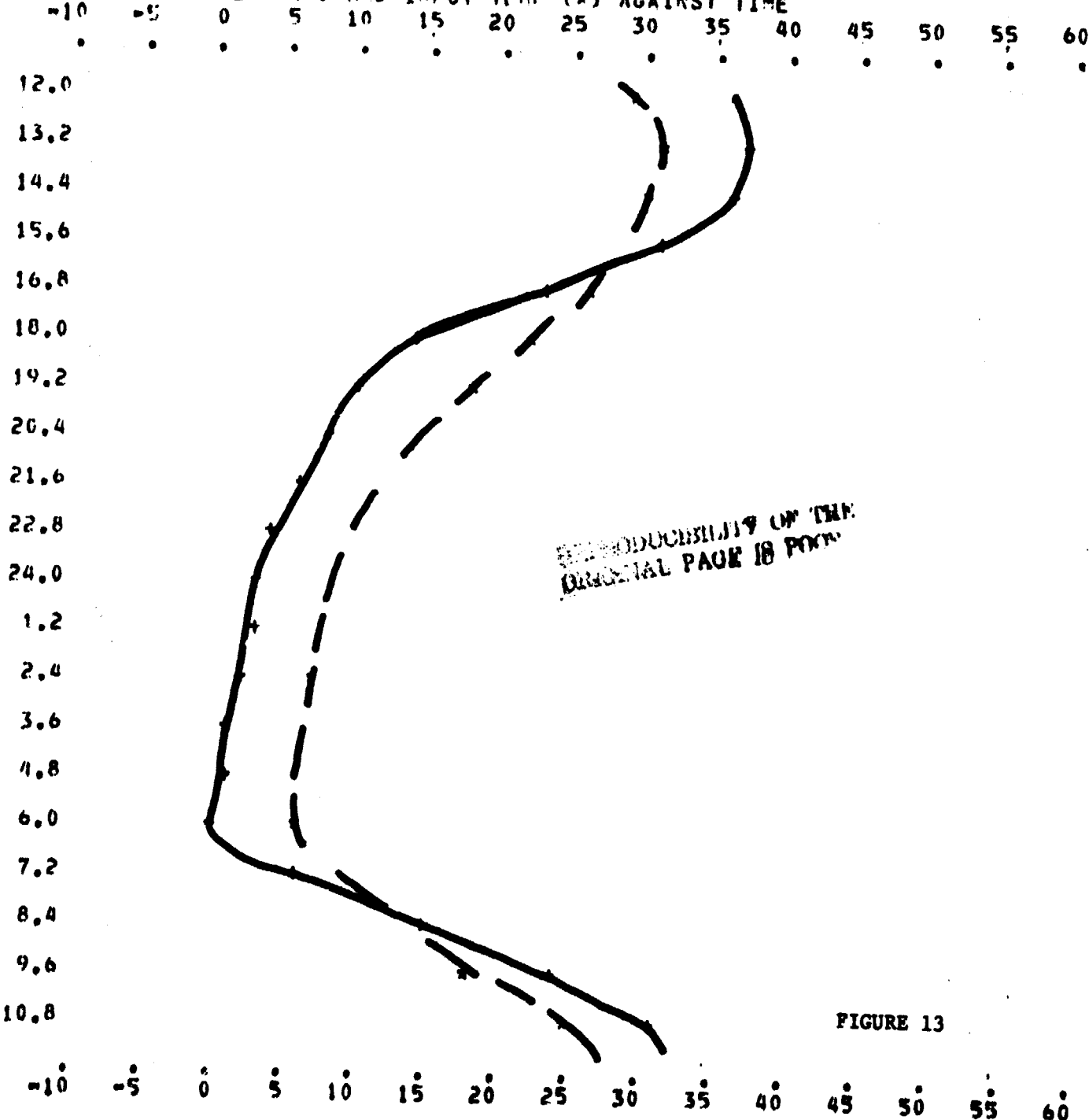


FIGURE 13

TABLE 4

"SANDBOX" EXPERIMENT TEMPERATURES

Date/Time	DEPTH PROBE (cm)						AIR SURFACE	AIR(10cm) ABOVE SURFACE	WIND mph	PRT-5 SURFACE						MEAN
	1.27	2.54	5.08	12.70	20.32	25.40										
10/3/75	(°C)						(°C)	(°C)		(°C)						
0936	17.8	17.2	13.7	16.7	18.9	18.8	23.5	21.2	2	18.0	17.5	18.2	17.5	17.5	17.7	
1048	24.6	23.4	16.5	16.5	18.4	18.4	28.8	25.5	0	26.0	25.0	25.5	25.2	25.5	25.4	
1205	30.8	29.4	20.2	16.9	18.1	18.2	29.5	29.5	0	29.2	29.1	28.9	29.4	29.6	29.2	
1312	30.5	29.4	22.0	17.4	18.1	18.3	26.8	23.6	0-5	28.0	28.4	28.5	27.9	28.1	28.2	
1425	32.8	31.3	24.2	18.6	18.5	18.7	32.7	26.6	3-5	29.8	30.4	30.4	30.9	30.4	30.4	
1650	30.0	29.4	26.5	20.9	19.9	19.8	29.7	26.2	0-3	25.5	25.6	25.9	25.9	25.4	25.7	
1800	25.4	26.3	25.3	21.9	20.7	20.4	29.1	23.2	0-2	21.0	21.5	22.5	21.9	20.4	21.5	
1830	23.8	25.2	24.7	22.1	21.0	20.6	22.7	22.4	0	19.5	19.4	19.9	20.5	19.4	19.7	
1915	20.9	22.8	23.2	22.7	21.5	21.0	19.0	19.3	0-1	17.4	17.5	18.5	17.8	17.9	17.8	
0224	12.4	14.7	15.8	22.0	22.8	22.2	17.0	12.2	0	6.0	6.5	6.5	7.0	7.5	6.7	
0600	11.0	12.8	13.4	19.9	21.5	21.4	11.5	12.1	0	5.8	6.2	6.2	6.0	6.1	6.0	

PLANE OF THERMAL INERTIA TABLE FOR ALBEDO INDEX 3 (ALBEDO=.5333)

DAY TEMPERATURE

NIGHT:	10.0	13.0	16.0	19.0	22.0	25.0	28.0	31.0	34.0	37.0	40.0
0	.0195	.0195	.0195	.0195	.0195	.0195	.0195	.0195	.0190	.0185	.0185
3.0	.0195	.0195	.0195	.0195	.0195	.0195	.0195	.0195	.0195	.0195	.0195
6.0	.0195	.0195	.0195	.0195	.0195	.0195	.0195	.0195	.0195	.0195	.0195
9.0	.0195	.0195	.0195	.0195	.0195	.0195	.0195	.0195	.0195	.0195	.0195
12.0	.0195	.0195	.0195	.0195	.0195	.0195	.0195	.0195	.0195	.0195	.0195
15.0	.0195	.0195	.0195	.0195	.0195	.0195	.0195	.0195	.0195	.0195	.0195
18.0	.0195	.0195	.0195	.0195	.0195	.0195	.0195	.0195	.0195	.0195	.0195
21.0	.0195	.0195	.0195	.0195	.0195	.0195	.0195	.0195	.0195	.0195	.0195
24.0	.0195	.0195	.0195	.0195	.0195	.0195	.0195	.0195	.0195	.0195	.0195
27.0	.0195	.0195	.0195	.0195	.0195	.0195	.0195	.0195	.0195	.0195	.0195
30.0	.0195	.0195	.0195	.0195	.0195	.0195	.0195	.0195	.0195	.0195	.0195

FIGURE 14

mostly to sky temperature.

- C. A net radiometer appears to be a vital part of any ground installation, and the net-radiation balances as a function of time of day and weather, are necessary.
- D. Fitting remotely-sensed data to spot locations around weather station sites, on flat ground, may be possible, but extrapolation to outlying areas is unlikely.
- E. Relative determinations of thermal properties may be possible using remote sensing, but absolute value determinations appear most unlikely.

## VII. REFERENCES

- CARSLAW, H.S. and JAEGER, J.C., 1959, Conduction of Heat in Solids, Clarendon Press, Oxford, pp. 386.
- DIBBLEE, T.W., Jr., 1965, Preliminary geologic map - Pisgah Crater and Vicinity, Calif., U.S.G.S. Technical Letter: NASA-4, 3pp.
- DEIRMENDJIAN, D., 1960, Atmospheric Extinction of Infrared Radiation, Quart. J.R. Meteor. Soc., V. 86, p. 371-381.
- DE VRIES, D.A., 1963, Thermal Properties of Soils: W.R. Van Wijk (ed.), Physics of Plant Environment, Amsterdam North Holland Publishing Co., p. 210-235.
- FISCHER, W.A., 1965, FRIEDMAN, J.D., SOUSA, T.M., Preliminary Results of Aerial Infrared Surveys at Pisgah Crater, California, U.S.G.S. Technical Letter: NASA-5, 12 pp.
- FLEAGLE, R.G., 1950, Radiation Theory of Local Temperature Differences, Journ. of Meteorology, Vol. 7, p. 114-120.
- FRIEDMAN, J.D., 1968, Thermal Anomalies and Geologic Features of Mono Lake Area, California, as Revealed by Infrared Imagery, Tech. Letter NASA 82.
- Gawarecki, S.J., 1964, Geologic Reconnaissance Report of the Pisgah Crater, California Area, U.S.G.S. Technical Letter: NASA-2, 11 pp.
- GEIGER, R., 1966, The Climate Near the Ground, Harvard University Press, Boston, 611 pp.
- HACKFORTH, H.L., 1960, Infrared Radiation, McGraw-Hill Book Co., Inc., New York.
- HASE, H., 1971, Surface Heat Flow Studies for Remote Sensing of Geothermal Resources: Proc. 7th International Symposium on Remote Sensing of the Environment, Univ. of Michigan, Vol. 1, p. 237-245.
- JAEGER, J.C., 1953, Conduction of Heat in a Solid with Periodic Boundary Conditions, with an Application to the Surface Temperature of the Moon: Cambridge Philos. Soc. Proc., Vol. 49, p. 355-359.
- KUNDE, V.G., 1965, Theoretical Relationship between equivalent Blackbody Temperatures and Surface Temperatures Measured by the NIMBUS HRIR: Observations from the NIMBUS I Meteorological Satellite, NTIS N66-12130-136, p. 23-36.
- KAHLE, A.B., et. al., 1976, Thermal Inertia Mapping, Geophysical Research Letters, vol. 3, no. 1, p. 26-28.

- LEE, W.H.K., and UYEDA, S., 1965, Review of Heat Flow Data: Terrestrial Heat Flow, American Geophys. Union, Geophysical Monograph, No. 8, p. 87-190.
- LYON, R.J.P., 1974, Field Mapping Determinations: Ground Support for Airborne Thermal Surveys with Application to Search for Geothermal Resources; Stanford Remote Sensing Lab Technical Report 74-8, 50 pp.
- MAUL, G.A., and SIDRAN, M., 1973, Atmospheric Effects on Ocean Surface Temperature Sensing from the NOAA Satellite Scanning Radiometer, Jour. Geophy. Research, Vol. 78, p. 1909-1916.
- MOENCH, A.F., 1969, An Evaluation of Heat Transfer Coefficients in Moist Porous Media; Ph.D. Dissertation unpublished, U. of Arizona.
- NEAL, J. Ted., 1965, Geology, Mineralogy, and Hydrology of U.S. Playas, Air Force Cambridge Research Laboratories-65-266, Environmental Research Papers, No. 96.
- OUTCALT, S.I., 1972, The Development and Application of a Simple Digital Surface-Climate Simulator: Journ. of Applied Meteorology, Vol. 11, p. 629-636.
- ROSEMA, A., 1974, Simulation of the Thermal Behavior of Bare Soils for Remote Sensing Purposes; NIWARS Study Report 16, 13 pp.
- SCHWALB, A., 1972, Modified Version of the Improved TIROS Operational Satellite (ITOS D-G), NOAA Tech. Memorandum NESS 35, U.S. Dept. of Commerce, 48 pp.
- SELLERS, W.D., 1965, Physical Climatology, Univ. of Chicago Press, Chicago, 272 pp.
- SMITH, R.W., 1969, Thermal Dynamics at the Earth-Air Interface: the Implications for Remote Sensing of the Geologic Environment, Stanford Univ. Remote Sensing Lab Tech. Report 69-4, 56 pp.
- SMITH, W.L., RAO, P.K., LOFFLER, R., CURTIS, W.R., 1970, The Determination of Sea-Surface Temperatures from Satellite High Resolution Infrared Window Radiation Measurements, Monthly Weather Review, Vol. 98, p. 604-611.
- SPENCER, J.W., 1971, Surface-Temperature Sensing Programs for Subsurface Conditions and Geothermal Sources; Unpublished M.S. Thesis, Cornell Univ. 54 pp.
- VAN WIJK, W.R. and DE VRIES, D.A., 1963, The Atmosphere and the Soil: Physics of Plant Environment, Amsterdam North Holland Publishing Co., 382 pp.
- WARK, D.G., YAMAMOTO, G., LIENESCH, J.H., 1962, Methods of Estimating Infrared Flux and Surface-Temperature from Meteorological Satellites; Jour. of Atmosph. Sciences, Vol. 19, p. 369-384.

- WATSON, K., 1971a, A Computer Program of Thermal Modeling for Interpretation of Infrared Images; U.S.G.S. Report NTIS PB-203578, 33 pp.
- WATSON, K., ROWAN, L.C. OFFIELD, T.W., 1971b, Application of Thermal Modeling in the Geologic Interpretation of Infrared Images: Proc. 7th International Symposium on Remote Sensing of the Environment, Univ. of Michigan, Vol. 3, p. 2017-2041.
- WATSON, K., 1974a, Geothermal Reconnaissance from Quantitative Thermal Infrared Images: Summaries 9th International Symposium on Remote Sensing of the Environment, Univ. of Michigan, p. 209-210.
- WATSON, K., 1974b, Geothermal Reconnaissance from Quantitative Thermal Images: 9th International Symposium on Remote Sensing of the Environment, Univ. of Michigan, p. 1919-1928.
- WISE, W.S., 1966, Geologic Map of the Pisgah and Sunshine Cone Lava Fields, U.S.G.S. Technical Letter: NASA-11, 5 pp.

APPENDIX I

STATISTICAL COMPIRATION BI-DIRECTIONAL

SUMMARY SHEETS

REFLECTANCE DATA - PISGAH MISSION #2

OUTPUT KEY

901	121000	1.0	1.190	1.720	1.0	1.640	1.870	0.000	15	LL	1-1
CODE	TIME	GAIN	VOLTS	VOLTS	GAIN	VOLTS	VOLTS	SOLRMIR	FIELD	SITE	
			CH 4	CH 5		CH 6	CH 7		OF		

0.336        0.393

Pseudo-CIE color coordinates, a measure of "color" of the target

2.447	3.713	3.225	4.378	0.283	0.339	0.386	0.400	0.352
BP 4	BP 5	BP 6	BP 7	R 4	R 5	R 6	R 7	Albedo
(Radiances w.	cm <sup>-2</sup> )		)					(averaged)

1.036	1.181	1.413	1.139	1.364	1.197
R 76	R 75	R 74	R 65	R 64	R 54
					(reflectance ratios)

1.	STATISTICAL DATA FROM PLATE TAPE # 2. ALBECNU CALLULATL ALBUM
2.	901 121000 1.0 1.150 1.720 1.0 1.640 1.870 0.000 15. LL 1-1
3.	2.136 0.363
4.	2.447 3.713 3.243 4.376 0.283 0.339 0.386 0.400 0.352
5.	1.036 1.161 1.413 1.139 1.364 1.197
6.	902 121100 1.0 1.150 1.740 1.0 1.700 1.950 0.000 15. LL 1-1
7.	0.323 0.396
8.	2.360 3.756 3.346 4.562 0.274 0.343 0.401 0.417 0.359
9.	1.041 1.216 1.523 1.169 1.403 1.252
10.	903 121200 1.0 1.130 1.670 1.0 1.620 1.930 0.000 15. LL 1-1
11.	0.326 0.390
12.	2.325 3.697 3.134 4.516 0.265 0.329 0.382 0.413 0.348
13.	1.083 1.254 1.534 1.158 1.417 1.223
14.	904 121300 1.0 1.150 1.763 1.0 1.650 1.900 0.000 15. LL 1-1
15.	0.324 0.402
16.	2.365 3.753 3.245 4.447 0.274 0.347 0.389 0.407 0.354
17.	1.046 1.173 1.404 1.121 1.419 1.256
18.	905 121400 1.0 1.240 1.820 1.0 1.670 1.680 0.000 15. LL 1-1
19.	0.337 0.401
20.	2.540 3.926 3.285 4.401 0.295 0.359 0.394 0.403 0.363
21.	1.022 1.123 1.364 1.098 1.334 1.215
22.	906 123010 1.0 1.270 1.780 1.0 1.770 2.040 0.000 15. LL 1-1N
23.	0.338 0.384
24.	2.636 3.641 3.486 4.769 0.301 0.352 0.420 0.438 0.378
25.	1.094 1.243 1.455 1.190 1.393 1.171
26.	907 123100 1.0 1.250 1.850 1.0 1.760 2.020 0.000 15. LL 1-1N
27.	0.331 0.390
28.	2.507 3.889 3.158 4.723 0.295 0.366 0.417 0.434 0.378
29.	1.040 1.185 1.434 1.139 1.407 1.235
30.	908 123200 1.0 1.220 1.770 1.0 1.810 2.040 0.000 15. LL 1-1N
31.	0.330 0.384
32.	2.597 3.020 3.569 4.765 0.289 0.351 0.429 0.438 0.377
33.	1.021 1.250 1.514 1.225 1.003 1.211
34.	909 123300 1.0 1.320 1.880 1.0 1.940 2.130 0.000 15. LL 1-1N
35.	0.336 0.387
36.	2.709 4.053 3.833 4.977 0.313 0.372 0.461 0.457 0.401
37.	0.992 1.223 1.402 1.239 1.474 1.189
38.	910 123400 1.0 1.200 1.900 1.0 1.670 1.940 0.000 15. LL 1-1N
39.	0.323 0.409
40.	2.407 4.053 3.205 4.539 0.285 0.372 0.395 0.417 0.367
41.	1.055 1.121 1.464 1.062 1.388 1.306
42.	911 124000 1.0 1.130 1.700 1.0 1.570 1.800 0.000 15. LL 1-1N
43.	0.333 0.401
44.	2.225 3.871 3.083 4.216 0.273 0.333 0.372 0.384 0.340
45.	1.026 1.146 1.397 1.117 1.302 1.219
46.	912 124100 1.0 1.180 1.570 1.0 1.650 1.840 0.000 15. LL 1-1N
47.	0.340 0.389
48.	2.426 3.607 3.245 4.308 0.285 0.327 0.391 0.390 0.348

REPRODUCTION OF THE  
ORIGINAL PAGE IS POOR

60.	0.970	1.192	1.368	1.197	1.374	1.148					
61.											
62.	913	124233	1..J	1.140	1.760	1.0	1.610	1.870	0.000	15.	LL 1-1E
63.	0..324	0..404									
64.	2.346	3.798	3.164	4.378	0.275	0.344	0.381	0.396	0.349		
65.	1..035	1..150	1..436	1..103	1..386	1..251					
66.											
67.	914	124330	1..J	1.170	1.750	1.0	1.670	1.870	0.000	15.	LL 1-1E
68.	0..330	0..400									
69.	2.405	3.777	3.235	4.378	0.282	0.342	0.396	0.396	0.354		
70.	0..999	1..156	1..462	1..157	1..403	1..212					
71.											
72.	915	124400	1..J	1.190	1.780	1..J	1.62J	1.890	0.000	15.	LL 1-1E
73.	0..331	0..400									
74.	2.447	3.841	3.134	4.424	0.287	0.348	0.384	0.400	0.355		
75.	1..042	1..149	1..393	1..103	1..337	1..213					
76.											
77.	916	124500	1..0	1.230	1.860	1..0	1.660	1.990	0.000	15.	LL 1-1S
78.	0..328	0..401									
79.	2..527	3..011	3..265	4..654	0..288	0..362	0..385	0..419	0..363		
80.	1..048	1..157	1..457	1..064	1..339	1..259					
81.											
82.	917	124600	1..0	1.140	1.710	1..0	1.640	1.880	0.000	15.	LL 1-1S
83.	0..327	0..377									
84.	2..346	3..652	3..225	4..401	0..267	0..333	0..380	0..396	0..344		
85.	1..042	1..169	1..334	1..141	1..425	1..249					
86.											
87.	918	124700	1..0	1.330	2.010	1..0	1.850	2.120	0.000	15.	LL 1-1S
88.	0..339	0..347									
89.	2..551	3..325	3..552	4..954	0..325	0..391	0..431	0..446	0..398		
90.	1..036	1..141	1..375	1..102	1..327	1..204					
91.											
92.	919	124800	1..0	1.293	1.830	1..0	1.750	1.960	0.000	15.	LL 1-1S
93.	0..342	0..392									
94.	2..649	3..947	3..448	4..585	0..301	0..356	0..407	0..413	0..369		
95.	1..015	1..159	1..365	1..141	1..344	1..1d2					
96.											
97.	920	124900	1..0	1.250	1..850	1..0	1.830	2..040	0.000	15.	LL 1-1S
98.	0..333	0..395									
99.	2..509	3..959	3..610	4..769	0..292	0..360	0..426	0..429	0..377		
100.	1..009	1..192	1..469	1..182	1..457	1..232					
101.											
102.	921	125000	1..0	1.193	1..820	1..0	1..690	1..970	0.000	15.	LL 1-1S
103.	0..324	0..401									
104.	2..447	3..926	3..326	4..608	0..285	0..360	0..400	0..423	0..367		
105.	1..057	1..177	1..433	1..114	1..403	1..260					
106.											
107.	922	125100	1..0	1.293	1..920	1..0	1..770	2..050	0.000	15.	LL 1-1W
108.	0..331	0..399									
109.	2..649	4..138	3..488	4..792	0..309	0..379	0..420	0..440	0..387		
110.	1..048	1..161	1..425	1..108	1..359	1..227					
111.											
112.	923	125200	1..0	1.220	1..810	1..0	1..720	1..990	0.000	15.	LL 1-1W
113.	0..329	0..396									
114.	2..507	3..504	3..387	4..054	0..292	0..358	0..408	0..428	0..371		
115.	1..048	1..195	1..432	1..140	1..394	1..223					
116.											
117.	924	125300	1..0	1.200	1..840	1..0	1..660	1..970	0.000	15.	LL 1-1W
118.	0..325	0..403									
119.	2..467	3..968	3..06	4..608	0..288	0..363	0..398	0..423	0..368		

120. 1.063 1.165 1.471 1.335 1.383 1.253  
 121.  
 122. 925 125400 1.0 1.160 1.770 1.0 1.690 1.970 0.000 15. LL 1-1W  
 123. 0.322 0.393  
 124. 2.446 3.620 3.328 4.508 0.278 0.350 0.400 0.423 0.363  
 125. 1.057 1.210 1.521 1.145 1.439 1.257  
 126.  
 127. 926 133500 1.0 1.170 1.770 1.0 1.720 1.960 0.000 15. LL 1-2  
 128. 0.325 0.397  
 129. 2.405 3.820 3.337 4.585 0.283 0.356 0.410 0.423 0.368  
 130. 1.032 1.189 1.496 1.152 1.450 1.259  
 131.  
 132. 927 135800 1.0 1.180 1.810 1.0 1.660 1.940 0.000 15. LL 1-2  
 133. 0.321 0.405  
 134. 2.386 3.904 3.265 4.539 0.280 0.364 0.395 0.419 0.364  
 135. 1.060 1.151 1.474 1.087 1.410 1.297  
 136.  
 137. 928 134000 1.0 1.160 1.790 1.0 1.740 2.020 0.000 15. LL 1-2  
 138. 0.319 0.390  
 139. 2.336 3.862 3.427 4.723 0.280 0.360 0.415 0.426 0.373  
 140. 1.051 1.211 1.555 1.153 1.480 1.283  
 141.  
 142. 929 134200 1.0 1.240 1.900 1.0 1.810 2.090 0.000 15. LL 1-2  
 143. 0.322 0.400  
 144. 2.248 4.095 3.569 4.884 0.299 0.381 0.432 0.451 0.391  
 145. 1.043 1.181 1.506 1.132 1.443 1.274  
 146.  
 147. 930 134300 1.0 1.240 1.890 1.0 1.830 2.100 0.000 15. LL 1-2  
 148. 0.323 0.390  
 149. 2.546 4.074 3.610 4.908 0.299 0.379 0.437 0.453 0.392  
 150. 1.036 1.193 1.513 1.151 1.459 1.268  
 151.  
 152. 932 135300 1.0 1.220 1.770 1.0 1.680 1.920 0.000 15. LL 1-3  
 153. 0.323 0.394  
 154. 2.307 3.820 3.306 4.493 0.300 0.359 0.403 0.414 0.369  
 155. 1.021 1.155 1.382 1.124 1.345 1.197  
 156.  
 157. 933 135400 1.0 1.240 1.820 1.0 1.700 1.950 0.000 15. LL 1-3  
 158. 0.324 0.397  
 159. 2.543 3.946 3.346 4.562 0.304 0.369 0.408 0.420 0.375  
 160. 1.031 1.161 1.381 1.107 1.340 1.211  
 161.  
 162. 934 135500 1.0 1.220 1.830 1.0 1.690 1.910 0.000 15. LL 1-3  
 163. 0.332 0.403  
 164. 2.557 3.947 3.326 4.470 0.300 0.371 0.405 0.412 0.372  
 165. 1.016 1.112 1.375 1.094 1.354 1.237  
 166.  
 167. 935 135500 1.0 1.210 1.790 1.0 1.700 1.900 0.000 15. LL 1-3  
 168. 0.333 0.399  
 169. 2.487 3.862 3.346 4.447 0.297 0.363 0.408 0.410 0.369  
 170. 1.005 1.130 1.379 1.125 1.373 1.220  
 171.  
 172. 936 140800 1.0 1.100 1.550 1.0 1.710 1.910 0.000 15. LL BC  
 173. 0.322 0.391  
 174. 2.265 3.565 3.306 4.470 0.275 0.341 0.419 0.421 0.364  
 175. 1.005 1.236 1.533 1.230 1.525 1.240  
 176.  
 177. 937 140900 1.0 1.070 1.730 1.0 1.670 1.950 0.000 15. LL BC  
 178. 0.309 0.404  
 179. 2.204 3.735 3.285 4.562 0.267 0.357 0.409 0.430 0.366

180.	1.351	1.034	1.637	1.146	1.529	1.335
181.	-	-	-	-	-	-
182.	933	141000	1.0	1.210	1.810	1.0
183.	J.352	J.402	-	-	-	-
184.	2.447	3.604	3.346	4.124	0.302	0.373
185.	1.001	1.117	1.341	1.116	1.380	1.230
186.	-	-	-	-	-	-
187.	939	141100	1.0	1.220	1.840	1.0
188.	0.313	0.402	-	-	-	-
189.	2.507	4.180	3.671	5.069	0.304	0.400
190.	1.045	1.130	1.570	1.144	1.502	1.313
191.	-	-	-	-	-	-
192.	940	141200	1.0	1.140	1.750	1.0
193.	J.321	J.395	-	-	-	-
194.	2.346	3.777	3.326	4.539	0.285	0.361
195.	1.033	1.185	1.503	1.147	1.455	1.268
196.	-	-	-	-	-	-
197.	941	143400	1.0	1.010	1.600	1.0
198.	0.314	0.402	-	-	-	-
199.	2.363	3.559	3.123	4.193	0.273	0.360
200.	1.012	1.182	1.552	1.169	1.540	1.317
201.	-	-	-	-	-	-
202.	942	143500	1.0	1.160	1.830	1.0
203.	0.315	0.402	-	-	-	-
204.	2.360	3.547	3.387	4.769	0.313	0.411
205.	1.061	1.175	1.547	1.111	1.458	1.312
206.	-	-	-	-	-	-
207.	943	143700	1.0	1.120	1.700	1.0
208.	J.353	J.356	-	-	-	-
209.	2.305	3.671	3.225	4.470	C.302	0.456
210.	1.045	1.128	1.501	1.138	1.437	1.263
211.	-	-	-	-	-	-
212.	944	143700	1.0	0.970	1.560	1.0
213.	0.312	J.405	-	-	-	-
214.	2.302	3.374	2.856	4.032	0.263	0.434
215.	1.055	1.166	1.555	1.105	1.477	1.337
216.	-	-	-	-	-	-
217.	945	143800	1.0	1.000	1.620	1.0
218.	0.310	J.406	-	-	-	-
219.	2.402	3.501	2.931	4.193	0.271	0.364
220.	1.060	1.169	1.574	1.103	1.484	1.346
221.	-	-	-	-	-	-
222.	946	144500	1.0	0.920	1.550	1.0
223.	0.305	0.414	-	-	-	-
224.	1.921	2.353	2.880	3.494	0.256	0.358
225.	1.021	1.137	1.542	1.113	1.559	1.401
226.	-	-	-	-	-	-
227.	947	144600	1.0	1.090	1.630	1.0
228.	0.324	0.393	-	-	-	-
229.	2.244	3.523	3.022	4.355	0.302	0.376
230.	1.086	1.110	1.558	1.112	1.326	1.246
231.	-	-	-	-	-	-
232.	948	144700	1.0	0.930	1.530	1.0
233.	0.316	J.402	-	-	-	-
234.	2.022	3.310	2.900	3.940	0.272	0.354
235.	1.021	1.165	1.514	1.136	1.476	1.309
236.	-	-	-	-	-	-
237.	949	144800	1.0	0.960	1.550	1.0
238.	0.318	0.407	-	-	-	-
239.	2.022	3.353	2.880	3.671	0.272	0.358

240.		1.015	1.150	1.486	1.113	1.465	1.317				
241.	950	1.44500	1.0	1.010	1.0580	1.0	1.510	1.710	0.000	15.	LL BCE
242.	0.317	J. 404									
243.	2.082	3.416	2.951	4.009	0.280	0.365	0.410	0.419	0.368		
244.	1.022	1.143	1.475	1.123	1.463	1.303					
245.											
246.	951	1.45000	1.0	0.950	1.170	1.0	1.420	1.620	0.000	15.	LL BCE
247.	0.320	0.401									
248.	0.342	0.394									
249.	2.022	3.204	2.773	3.002	0.299	0.345	0.342	0.405	0.353		
250.	1.034	1.176	1.365	1.137	1.455	1.260					
251.											
252.	952	1.45100	1.0	0.980	1.480	1.0	1.420	1.690	0.000	15.	LL BCE
253.	0.322	0.394									
254.	2.022	3.204	2.778	3.063	0.278	0.347	0.352	0.423	0.360		
255.	1.036	1.177	1.321	1.129	1.411	1.250					
256.											
257.	953	1.45200	1.0	0.970	1.480	1.0	1.470	1.680	0.000	15.	LL BCE
258.	0.321	0.390									
259.	2.022	3.204	2.830	3.040	0.275	0.347	0.400	0.420	0.362		
260.	1.034	1.170	1.528	1.170	1.477	1.262					
261.											
262.	954	1.45300	1.0	0.920	1.500	1.0	1.460	1.690	0.000	15.	LL BCE
263.	0.327	0.405									
264.	1.031	3.247	2.859	3.063	0.261	0.352	0.403	0.423	0.360		
265.	1.045	1.202	1.618	1.147	1.545	1.347					
266.											
267.	955	1.45400	1.0	0.940	1.460	1.0	1.510	1.710	0.000	15.	LL BCE
268.	0.314	0.354									
269.	1.034	3.102	2.901	4.009	0.267	0.343	0.418	0.428	0.364		
270.	1.023	1.248	1.603	1.220	1.577	1.234					
271.											
272.	956	1.45500	1.0	0.950	1.500	1.0	1.440	1.670	0.000	15.	LL BCE
273.	0.314	0.354									
274.	1.030	3.247	2.819	3.917	0.278	0.362	0.406	0.426	0.368		
275.	1.046	1.178	1.233	1.129	1.462	1.301					
276.											
277.	957	1.45600	1.0	0.950	1.470	1.0	1.490	1.630	0.000	15.	LL BCM
278.	0.322	0.400									
279.	1.031	3.193	2.920	3.025	0.276	0.355	0.421	0.416	0.367		
280.	0.988	1.173	1.497	1.187	1.515	1.276					
281.											
282.	958	1.45700	1.0	0.940	1.460	1.0	1.440	1.670	0.000	15.	LL BCM
283.	0.316	0.397									
284.	1.031	3.162	2.619	3.917	0.275	0.352	0.406	0.426	0.365		
285.	1.043	1.213	1.345	1.154	1.479	1.231					
286.											
287.	959	1.45800	1.0	0.930	1.490	1.0	1.450	1.640	0.000	15.	LL BCM
288.	0.313	0.405									
289.	1.031	3.225	2.839	3.848	0.272	0.359	0.409	0.419	0.365		
290.	1.042	1.165	1.538	1.139	1.504	1.320					
291.											
292.	960	1.45900	1.0	0.960	1.470	1.0	1.490	1.650	0.000	15.	LL BCM
293.	0.321	0.397									
294.	1.022	3.113	2.920	3.871	0.281	0.355	0.421	0.421	0.369		
295.	1.000	1.187	1.493	1.187	1.499	1.263					
296.											
297.	961	1.46000	1.0	0.930	1.450	1.0	1.390	1.560	0.000	15.	LL 2-2A
298.	0.320	0.403									
299.	1.021	3.141	2.716	3.705	0.281	0.365	0.402	0.412	0.365		

1.	1.023	1.130	1.453	1.104	1.430	1.295
2.	962	1.1600	1.0	0.870	1.370	1.0
3.		0.314	0.400	0.370	1.300	1.550
4.		1.300	2.971	2.555	2.640	0.345
5.		1.077	1.172	1.252	1.089	1.423
6.		1.160			1.318	
7.	963	1.1710	1.0	0.870	1.350	1.0
8.		0.324	0.397		1.350	1.500
9.		1.343	2.928	2.630	3.525	0.270
10.		1.002	1.151	1.451	1.149	1.468
11.		1.261			1.261	
12.	964	1.1650	1.0	0.870	1.450	1.0
13.		0.324	0.397		1.450	1.640
14.		1.302	2.141	2.819	3.044	0.246
15.		1.016	1.172	1.441	1.153	1.419
16.		1.230			1.230	
17.	965	1.2030	1.0	0.910	1.370	1.0
18.		0.325	0.396		1.350	1.520
19.		1.630	2.974	2.650	3.594	0.276
20.		1.022	1.157	1.448	1.132	1.417
21.		1.251			1.251	
22.	966	1.2060	1.0	0.910	1.493	1.0
23.		0.331	0.397		1.450	1.910
24.		1.647	3.754	3.245	4.470	0.345
25.		1.033	1.137	1.381	1.101	1.337
26.		1.215			1.215	
27.	967	1.2090	1.0	0.910	1.720	1.0
28.		0.331	0.397		1.730	2.010
29.		1.655	3.620	3.407	4.700	0.352
30.		1.035	1.149	1.542	1.145	1.499
31.		1.236			1.236	
32.	968	1.2030	1.0	0.910	1.720	1.0
33.		0.331	0.397		1.730	2.010
34.		1.650	3.750	3.245	4.424	0.368
35.		1.023	1.136	1.380	1.113	1.359
36.		1.221			1.221	
37.	969	1.2030	1.0	0.910	1.740	1.0
38.		0.326	0.397		1.730	2.010
39.		1.646	3.713	3.164	4.401	0.359
40.		1.043	1.145	1.419	1.096	1.360
41.		1.219			1.219	
42.	970	1.2020	1.0	0.910	1.710	1.0
43.		0.331	0.397		1.730	2.010
44.		1.646	3.650	3.204	4.262	0.368
45.		0.998	1.129	1.359	1.131	1.342
46.		1.187			1.187	
47.	971	1.2000	1.0	0.900	1.330	1.0
48.		0.326	0.397		1.330	1.460
49.		1.640	2.686	2.552	3.432	0.307
50.		1.013	1.142	1.401	1.127	1.383
51.		1.227			1.227	
52.	972	1.2010	1.0	0.900	1.330	1.0
53.		0.326	0.397		1.330	1.450
54.		1.620	2.633	2.526	3.525	0.304
55.		0.996	1.134	1.376	1.156	1.379
56.		1.214			1.214	
57.	973	1.2020	1.0	0.880	1.305	1.0
58.		0.326	0.397		1.330	1.500
59.		1.620	2.633	2.526	3.525	0.304
60.		0.996	1.134	1.376	1.156	1.379
61.		1.214			1.214	

360.	1.018	1.194	1.454	1.176	1.432	1.218					
361.											
362.	974	154300	1.0	0.859	1.300	1.0	1.260	1.440	0.000	15.	LL 2-2B
363.		0.317	0.402								
364.		1.719	2.622	2.494	3.387	0.287	0.369	0.418	0.425	0.375	
365.		1.018	1.152	1.479	1.134	1.457	1.235				
366.											
367.	975	154400	1.0	0.690	1.320	1.0	1.300	1.450	0.000	15.	LL 2-2B
368.		0.330	0.396								
369.		1.340	2.8e5	2.535	3.410	0.307	0.374	0.425	0.428	0.393	
370.		1.006	1.147	1.391	1.135	1.383	1.218				
371.											
372.	976	155500	5.0	3.020	4.040	5.0	4.410	5.240	0.000	15.	LL 2-1
373.		0.319	0.397								
374.		1.228	1.980	1.945	2.424	0.222	0.278	0.347	0.324	0.293	
375.		0.932	1.166	1.400	1.251	1.567	1.253				
376.											
377.	977	155600	5.0	2.970	4.570	5.0	4.290	5.170	0.000	15.	LL 2-1
378.		0.319	0.397								
379.		1.208	1.950	1.891	2.392	0.218	0.274	0.338	0.319	0.287	
380.		0.948	1.168	1.465	1.235	1.550	1.255				
381.											
382.	978	155700	5.0	3.050	4.780	5.0	4.380	5.150	0.000	15.	LL 2-1
383.		0.319	0.405								
384.		1.240	2.039	1.931	2.363	0.224	0.286	0.345	0.318	0.293	
385.		0.922	1.112	1.421	1.206	1.541	1.278				
386.											
387.	979	155800	5.0	2.990	4.620	5.0	4.310	5.220	0.000	15.	LL 2-1
388.		0.318	0.398								
389.		1.216	1.972	1.930	2.415	0.219	0.277	0.339	0.323	0.289	
390.		0.950	1.166	1.469	1.228	1.547	1.260				
391.											
392.	980	155900	5.0	2.960	4.540	5.0	4.320	5.100	0.000	15.	LL 2-1
393.		0.320	0.397								
394.		1.204	1.938	1.894	2.360	0.217	0.272	0.340	0.315	0.286	
395.		0.920	1.100	1.450	1.252	1.560	1.251				
396.											
397.	981	160400	5.0	2.910	4.450	5.0	4.290	5.020	0.000	15.	LL 2-1N
398.		0.320	0.397								
399.		1.184	1.900	1.891	2.323	0.227	0.282	0.357	0.328	0.298	
400.		0.919	1.163	1.447	1.265	1.575	1.244				
401.											
402.	982	160500	5.0	2.710	4.070	5.0	3.920	4.510	0.000	15.	LL 2-1N
403.		0.326	0.396								
404.		1.103	1.756	1.726	2.088	0.211	0.258	0.326	0.295	0.272	
405.		0.905	1.142	1.397	1.202	1.542	1.222				
406.											
407.	983	160600	5.0	2.740	4.140	5.0	4.020	4.840	0.000	15.	LL 2-1N
408.		0.320	0.391								
409.		1.115	1.708	1.771	2.240	0.214	0.263	0.335	0.317	0.282	
410.		0.947	1.205	1.482	1.273	1.565	1.230				
411.											
412.	984	160700	5.0	2.900	4.340	5.0	4.160	4.820	0.000	15.	LL 2-1N
413.		0.327	0.396								
414.		1.180	1.853	1.833	2.231	0.226	0.275	0.346	0.315	0.290	
415.		0.911	1.145	1.395	1.257	1.531	1.218				
416.											
417.	985	160700	5.0	2.810	4.350	5.0	4.100	4.800	0.000	15.	LL 2-1N
418.		0.320	0.401								
419.		1.143	1.857	1.806	2.222	0.219	0.276	0.341	0.314	0.287	

420. 0.920 1.138 1.433 1.236 1.557 1.260  
 421. -----  
 422. 986 160600 5.0 2.800 4.210 5.0 4.060 4.700 0.000 15. LL 2-1E  
 423. 0.325 0.396  
 424. 1.139 1.798 1.788 2.176 0.224 0.274 0.338 0.315 0.288  
 425. 0.932 1.148 1.402 1.232 1.505 1.221  
 426. -----  
 427. 987 160900 5.0 3.500 5.430 5.0 4.750 5.990 0.000 15. LL 2-1E  
 428. 0.319 0.401  
 429. 1.472 2.315 2.096 2.769 0.280 0.353 0.396 0.401 0.357  
 430. 1.012 1.135 1.430 1.122 1.413 1.260  
 431. -----  
 432. 988 161000 5.0 2.590 4.060 5.0 3.910 4.710 0.000 15. LL 2-1E  
 433. 0.313 0.397  
 434. 1.054 1.734 1.722 2.180 0.208 0.264 0.325 0.315 0.278  
 435. 0.970 1.193 1.518 1.230 1.565 1.273  
 436. -----  
 437. 989 161100 5.0 3.040 4.010 5.0 4.340 5.060 0.000 15. LL 2-1E  
 438. 0.325 0.399  
 439. 1.236 1.967 1.913 2.341 0.244 0.300 0.361 0.339 0.311  
 440. 0.937 1.129 1.391 1.205 1.484 1.232  
 441. -----  
 442. 990 161200 5.0 2.940 4.400 5.0 4.110 4.900 0.000 15. LL 2-1E  
 443. 0.326 0.395  
 444. 1.196 1.878 1.811 2.268 0.236 0.286 0.342 0.328 0.298  
 445. 0.959 1.145 1.392 1.194 1.452 1.216  
 446. -----  
 447. 991 161300 5.0 2.850 4.340 5.0 4.130 4.710 0.000 15. LL 2-1S  
 448. 0.325 0.400  
 449. 1.159 1.823 1.820 2.180 0.236 0.293 0.365 0.326 0.305  
 450. 0.895 1.114 1.393 1.245 1.546 1.242  
 451. -----  
 452. 992 161300 5.0 2.710 4.160 5.0 3.840 4.530 0.000 15. LL 2-1S  
 453. 0.323 0.401  
 454. 1.103 1.777 1.690 2.098 0.224 0.281 0.339 0.314 0.289  
 455. 0.927 1.117 1.399 1.206 1.509 1.252  
 456. -----  
 457. 993 161400 5.0 2.760 4.180 5.0 4.070 4.730 0.000 15. LL 2-1S  
 458. 0.322 0.395  
 459. 1.123 1.765 1.793 2.190 0.224 0.282 0.359 0.328 0.299  
 460. 0.912 1.161 1.434 1.273 1.572 1.235  
 461. -----  
 462. 994 161400 5.0 2.750 4.280 5.0 4.050 4.850 0.000 15. LL 2-1S  
 463. 0.316 0.398  
 464. 1.119 1.827 1.784 2.245 0.228 0.289 0.358 0.336 0.303  
 465. 0.940 1.163 1.475 1.237 1.570 1.269  
 466. -----  
 467. 995 161400 5.0 2.650 4.400 5.0 4.180 4.950 0.000 15. LL 2-1S  
 468. 0.319 0.398  
 469. 1.159 1.878 1.822 2.291 0.236 0.297 0.369 0.343 0.311  
 470. 0.929 1.154 1.453 1.243 1.565 1.259  
 471. -----  
 472. 1 161500 5.0 2.710 4.120 5.0 3.940 4.710 0.000 15. LL 2-1W  
 473. 0.321 0.394  
 474. 1.103 1.760 1.735 2.180 0.228 0.282 0.352 0.331 0.298  
 475. 0.940 1.173 1.450 1.248 1.543 1.236  
 476. -----  
 477. 2 161600 5.0 2.690 4.150 5.0 3.970 4.620 0.000 15. LL 2-1W  
 478. 0.320 0.399  
 479. 1.095 1.772 1.746 2.139 0.227 0.284 0.355 0.325 0.298



**APPENDIX 2**

**ISCO Bi-DIRECTIONAL REFLECTANCE MEASUREMENTS**

DATE: March 28, 1975 TIME: 1205 LOCATION: Lavic Lake

STANDARD: BaSO<sub>4</sub> OBSERVER: Gary Ballew/ Stuart Marsh

TARGETS: #1 - 1-1B #2 - Base Camp #3 - Alluvium

Time: 1131-1210 1416-1431 1433-1459 1555- 1635-

Wavelength ( $\mu\text{m}$ )	STD	#1	STD	#2	STD	#3
.400	3.25	1.52	3.5	1.25	1.75	0.62
.425	5.61	4.10	18.0	3.5	10.0	1.25
.450	60.0	13.2	57.0	11.0	38	6.0
.475	87.0	21.2	85	17.5	55	9.4
.500	90.0	23.3	87	18.9	57	10.0
.525	88.0	24.0	86	19.4	56	10.5
.550	88.0	24.7	81	19.8	52	10.0
.575	74.0	24.0	70	19.5	47	9.5
.600	99.0	36.5	97	31.0	66	15.0
.625	100	38.0	98	33.0	66	16.5
.650	100	39.0	98	33.5	67	17.0
.675	94.0	35.7	90	31.0	60.5	15.8
.700	81.5	34.0	82	29.0	55.5	15.0
.725	76.5	31.5	74	28.0	49.5	13.8
.750	64.5	27.5	61	23.5	41	11.6
.75	77.0	34.0	74	30.0	53	16
.80	77.0	33.0	73	30	52	16.5
.85	66.0	30.0	63	26	45	13.3
.90	48.0	22.0	45	19.5	33	10.0
.95	37.0	18.2	35	13	23.5	77.7
1.00	40.0	19.6	31.5	15.7	27.0	88.8
1.05	36.5	18.0	34.0	15.0	24.5	8.33
1.10	31.0	16.0	30	13.0	21.0	7.5
1.15	15.0	7.6	13.3	6.2	9.5	3.2
1.20	14.0	7.3	12.4	5.8	9.2	3.5
1.25	26.0	13.0	23.5	12.5	16.5	5.6
1.30	29.0	14.7	27	12.0	18.5	6.5
1.35	14.8	8.15	16	7.0	9.5	3.1
1.40	34.0	5.30	3.4	1.20	2.5	0.6
1.45	7.3	4.50	2.3	0.94	1.4	0.44
1.50	6.2	3.33	5.7	2.70	3.8	1.35
1.55	9.3	15.0	8.6	4.00	6.0	2.2

DATE: March 29, 1975 LOCATION: Pisgah Crater

ISCO HEAD: Probe OBSERVER: G. Ballew

TARGETS: #1 - Cinders Near W. Cone

#2 - Red Cinders, 20' West of #1

Wavelength (μm)	TIME: 1036-1054	BaSo4	Fiberfrax SA = 51°	118-1133	1347-1400	1310-1335
.400	1.80	4.90	0.24	0.30	1.55	
.425	8.0	10.5	0.67	0.80	8.10	
.450	29.0	34.0	2.45	2.65	27.5	
.475	42.0	50.0	3.50	3.80	38.0	
.500	43.0	50.0	3.60	4.10	40.0	
.525	41.0	48.0	3.90	4.30	39.0	
.550	40.0	45.0	3.95	4.25	31.5	
.575	34.0	38.0	3.80	4.20	33.0	
.600	51.0	56.0	5.95	7.00	47.0	
.625	52.0	56.0	6.10	7.50	48.0	
.650	51.0	55.0	6.10	7.85	47.5	
.675	45.0	49.5	5.65	7.40	42.5	
.700	42.0	45.5	5.40	7.25	39.0	
.725	37.5	40.5	4.85	6.70	35.0	
.750	31.5	34.0	4.10	5.90	29.0	
.75	51.0	55.0	6.30	8.20	43.0	
.80	50.0	52.0	6.10	8.50	37.0	
.85	41.0	46.0	5.30	2.25	21.0	
.90	32.0	35.0	4.00	5.70	21.5	
.95	24.5	26.5	2.95	4.30	23.5	
1.00	26.5	29.5	3.10	4.90	22.0	
1.05	24.5	27.0	2.90	4.75	20.0	
1.10	22.5	23.5	2.65	4.50	17.3	
1.15	9.0	10.5	1.20	2.00	7.2	
1.20	9.0	9.5	1.15	2.15	7.6	
1.25	16.5	18.5	2.15	4.20	14.0	
1.30	18.5	21.5	2.45	4.90	15.5	
1.35	10.5	12.0	1.25	2.35	8.0	
1.40	2.25	2.50	0.29	0.30	1.70	
1.45	1.50	1.80	0.21	0.40	1.15	
1.50	4.10	4.70	0.55	1.20	3.4	
1.55	6.00	7.10	0.83	1.75	5.0	

### APPENDIX 3

#### MEASURED SURFACE AND PROBE TEMPERATURES

##### Output Key

###### -- PROBE

OCC	29	2400	1.0	2.0	3.0	4.0	5.0	6.0	
CODE	DAY	TIME	DEPTH	1/2"	2"	5"	10"	15"	20"

###### -- SURFACE

1-1	29	2400	L.	.100	.200	.300	.400	.500	1.0	2.0	3.0	4.0	5.0	05NW	S-5
CODE	DAY	TIME	SETTING	DIGITAL OUTPUT				TEMP. OUTPUT °C				WIND	RADIOMETER		

				PALDE
1.	CCC29 0520	1.4	5.4	5.2 12.5
2.	CCC29 0514	0.5	5.4	9.2 12.3
3.	CCC29 0514	0.5	5.4	9.2 12.3
4.	CCC29 0527	0.5	5.4	9.0 12.1
5.	CCC29 0810	4.0	5.5	8.7 12.0
6.	CCC29 1029	18.4	5.1	9.4 11.8
7.	CCC29 1213	25.6	4.5	10.7 11.7
8.	CCC29 1406	28.0	16.0	13.0 42.0
9.	CCC29 1426	27.3	15.6	13.4 42.0
10.	CCC29 1453	26.7	15.1	13.9 12.1
11.	CCC29 1714	16.8	15.2	15.9 13.1
12.	CCC29 1910	11.5	16.1	15.8 13.7
13.	CCC29 2110	8.2	13.1	14.8 14.2
14.	CCC29 2312	6.5	11.0	13.6 14.3
15.	CCC30 0123	5.4	5.7	12.4 14.1
16.	CCC30 0521	4.2	5.7	11.7 13.8
17.	CCC30 0524	3.6	7.6	11.0 13.5
18.	CCC30 1435	25.9	23.1	16.5 13.2
19.	C C R A T E R C E N T E R			
20.	CC29 0528L	722	715	728 699 -0.4 -0.3 -0.5 -0.1 -1.0 35.0 29.0 14.5W
21.	CC29 0630L	708	708	692 -710 -0.9 -0.9 -0.9 -1.6 -37.0 28.5 10.5W
22.	CC29 0813W	265	326	244 -470 -0.212 9.0 56.0 67.0 72.0 73.0 75.0 46.0 33.0 10N +4
23.	CC29 1013			
24.	CC29 1206			
25.	CC29 1401			
26.	CC29 1420			
27.	CC29 1448			
28.	CC29 1708			
29.	CC29 1903			
30.	CC29 2104			
31.	CC29 2307			
32.	CC30 0119			
33.	CC30 0116			
34.	CC30 0513			
35.	CC30 1429			
36.	C C R A T E R F E C C I N C E F			
37.	RC29 0531L	730	751	757 771 738 3.4 1.0 1.0 1.5 0.5
38.	RC29 0631L	726	737	739 733 -0.3 0.4 0.4 0.5 0.2
39.	RC29 0815W	146	055	-127 .075 .100 4.0 1.6 4.0 2.3 3.0
40.	RC29 1015			
41.	RC29 1207			
42.	RC29 1402			
43.	RC29 1421			
44.	RC29 1449			
45.	RC29 1713			
46.	RC29 1805			
47.	RC29 2106			
48.	RC29 2308			
49.	RC30 0115			
50.	RC30 0317			
51.	RC30 0520			
52.	RC30 1439			
53.	C C R A T E R S C A C			
54.	RR29 0524L	714	721	718 725 720 -0.5 -0.5 -0.5 -0.5 0.0 -0.2
55.	RR29 0632L	720	716	-717 -722 -739 -0.1 -0.1 -0.4 0.2 0.5
56.	RR29 0816W	226	205	-220 -215 .165 7.4 6.9 7.3 7.1 5.5
57.	RR29 1016			
58.	RR29 1205			
59.	RR29 1404			
60.	RR29 1423			

61.	PR29	1450		88.0	92.0	91.0	89.0	95.0
62.	PR29	1711		77.0	77.0	77.0	73.0	79.0
63.	RR29	1908		50.0	51.0	50.0	49.0	48.0
64.	RR29	2108		44.0	43.0	44.0	43.0	45.0
65.	RR29	2309		42.0	42.0	43.0	43.0	42.0
66.	RR30	C120		38.0	36.0	37.0	38.0	38.0
67.	FR30	0318		36.0	35.0	36.0	37.0	38.0
68.	RR30	0521		32.0	32.0	33.0	34.0	35.0
69.	RF30	1431		105.0	109.	104.	104.	103.
70.	C CRATER CUTTEREGEE							
71.	CE29	0535L	.742	.747	.746	.752	.753	0.5
72.	CE29	0634L	.732	.745	.732	.735	.740	0.4
73.	CE29	0815W	.311	.344	.286	.264	.243	10.5
74.	CE29	1018						68.0
75.	CE29	1210						78.0
76.	CE29	1408						78.0
77.	CE29	1424						78.0
78.	CE29	1451						77.0
79.	CE29	1712						59.0
80.	CE29	1908						44.0
81.	CE29	2110						42.0
82.	CE29	2310						42.0
83.	CE30	0121						39.0
84.	CE30	0219						36.0
85.	CE30	0522						34.0
86.	CE30	1432						95.0
87.	C CRATER OUTSIDE BASALT							
88.	E29	0536L	.737	.733	.732	.734	.730	0.2
89.	E29	0635L	.722	.724	.725	.738	.730	-0.1
90.	E29	0820W	.156	.134	.112	.150	.125	5.2
91.	E29	1019						60.0
92.	E29	1211						74.0
93.	E29	1407						82.0
94.	E29	1425						77.0
95.	E29	1452						67.0
96.	E29	1713						63.0
97.	E29	1909						48.0
98.	E29	2112						44.0
99.	E29	2311						43.0
100.	E20	0122						40.0
101.	E20	0320						35.0
102.	E20	0523						32.0
103.	E20	1433						98.0
104.	CC LAVIC LAKE 1-1		PROBLE					
105.	1-129	0442	-3.2	1.0	8.0	11.0		
106.	1-129	0610	2.3	0.0	7.2	10.9		
107.	1-129	0728	0.0	0.5	7.5	10.5		
108.	1-129	0955	12.0	5.7	6.9	10.2		
109.	1-129	1207	20.0	15.4	7.5	10.0		
110.	1-129	1415	24.0	16.1	9.2	10.0		
111.	1-129	1557	21.2	19.1	11.0	10.0		
112.	1-129	1605	15.0	16.4	12.2	10.1		
113.	1-129	2050	3.9	10.0	12.5	11.0		
114.	1-129	2238	0.3	7.0	11.5	11.0		
115.	1-130	0100	-2.0	3.4	10.6	11.8		
116.	1-130	0315	-4.0	1.5	9.0	11.0		
117.	1-130	0610	-6.2	-1.0	7.9	11.0		
118.	1-130	0912	12.7	9.0	7.2	11.0		
119.	1-130	1058	26.1	14.1	7.8	10.8		
120.	1-130	1316	32.0	22.0	9.0	9.6		
121.	1-130	1425	33.5	24.0	10.5	10.0		

122.	C LAVIC LAKE 1-2	PROBE
123.	1-229 0430 -2.0	1.5 9.0 12.9
124.	1-229 0615 -1.5	1.5 6.8 11.0
125.	1-229 0730 -1.5	1.5 6.0 10.9
126.	1-229 1000 10.0	5.1 6.1 11.0
127.	1-229 1215 1% 1	11.7 7.0 10.5
128.	1-229 1220 15.9	12.5 9.4 10.1
129.	1-229 1420 23.0	16.5 9.3 11.0
130.	1-229 1602 20.5	1% 4 12.0 10.1
131.	1-229 1807 15.0	17.0 13.0 10.1
132.	1-229 2155 3.0	10.0 11.7 9.5
133.	1-229 2245 2.0	8.0 11.5 11.0
134.	1-230 0105 -1.0	1.0 10.0 11.1
135.	1-230 0320 -2.0	3.0 9.4 12.0
136.	1-230 0611 -7.2	1.0 6.0 9.2
137.	1-230 0909 9.7	3.7 6.5 11.5
138.	1-230 1101 23.2	11.3 7.3 11.3
139.	1-230 1320 20.0	15.2 9.9 10.1
140.	1-230 1427 21.5	21.2 11.5 10.1
141.	C LAVIC LAKE 1-2	PROBE
142.	1-329 0458 -1.5	2.1 8.1 11.0
143.	1-329 0725 -1.0	2.0 7.3 11.0
144.	1-329 1006 10.5	6.0 7.2 10.5
145.	1-329 1425 24.0	17.1 10.0 10.1
146.	1-329 1606 21.0	18.2 11.6 10.1
147.	1-329 1810 16.0	16.6 13.5 10.9
148.	1-329 2100 6.0	10.5 12.5 11.0
149.	1-329 2250 3.2	8.4 12.0 13.5
150.	1-330 0110 -0.5	5.0 10.0 11.1
151.	1-330 0330 -2.0	3.2 9.8 11.5
152.	1-330 0616 -4.9	1.0 7.9 11.0
153.	1-330 0907 10.2	4.8 7.5 11.3
154.	1-330 1102 14.2	12.5 8.2 11.0
155.	1-330 1305 31.0	20.0 10.1 10.1
156.	1-330 1432 32.4	22.0 11.1 10.0
157.	C LAVIC LAKE ALLUVIUM	2-1 PROBE
158.	2-129 0515 1.0	4.5 8.3 10.0
159.	2-129 0655 0.0	2.1 7.1 10.8
160.	2-129 1015 10.2	6.1 7.0 11.0
161.	2-129 1240 22.9	13.1 8.9 11.0
162.	2-129 1435 25.5	17.5 11.0 11.0
163.	2-129 1615 22.0	18.0 12.5 10.9
164.	2-129 1820 16.5	17.0 14.0 11.5
165.	2-129 2030 8.0	13.5 13.5 12.0
166.	2-129 2300 3.7	8.4 11.2 11.9
167.	2-130 0120 1.0	6.6 11.0 12.0
168.	2-130 0345 -1.0	4.2 9.7 12.0
169.	2-130 0600 -2.0	2.8 7.7 11.9
170.	2-130 0900 6.2	5.0 7.9 12.3
171.	2-130 1105 24.6	17.8 8.6 12.0
172.	2-130 1340 33.4	20.1 11.1 11.0
173.	2-130 1500 34.4	22.5 13.1 11.0
174.	C LAVIC LAKE 2-2	PROBE
175.	2-229 0502 -1.5	2.0 8.1 11.9
176.	2-229 0715 -1.2	1.8 7.4 11.5
177.	2-229 1005 12.7	6.8 10.9 11.3
178.	2-229 1222 23.5	13.5 8.8 11.3
179.	2-229 1430 25.5	18.0 10.1 11.0
180.	2-229 1610 22.0	18.9 11.6 10.4
181.	2-229 1815 15.0	17.0 13.0 11.0
182.	2-229 2105 4.2	10.8 13.0 11.5

13.6

9.2

12.9

183.	2-229	2251	1.3	7.8	12.1	11.9	12.7
184.	2-230	0115	-1.7	4.5	10.5	11.7	12.7
185.	2-230	0235	-2.0	1.5	6.0	11.4	11.6
186.	2-230	0620	-6.0	6.0	7.5	11.1	12.5
187.	2-230	0918	10.5	5.2	7.3	11.9	13.3
188.	2-230	1-152	22.9	12.2	7.8	11.8	13.2
189.	2-230	1330	22.5	20.1	10.0	10.8	13.5
190.	2-230	1435	32.5	22.1	11.1	10.5	13.1
191.	C LAVIC LAKE	2-3			PROBE		
192.	2-329	0504	-2.0	3.1	8.2	11.9	
193.	2-329	0720	-3.0	1.5	7.0	10.4	
194.	2-329	1012	16.0	6.0	6.9	11.8	
195.	2-329	1225	24.0	12.1	8.4	11.0	
196.	2-329	1433	25.5	16.4	9.9	10.7	
197.	2-329	1613	21.2	17.5	11.2	9.1	
198.	2-329	1818	13.2	16.1	12.1	10.2	
199.	2-329	2106	2.0	10.5	12.0	11.0	
200.	2-329	2255	-1.0	8.0	11.8	11.2	
201.	2-330	0116	-4.3	5.0	10.2	11.0	
202.	2-330	0336	-5.5	4.5	9.0	11.0	
203.	2-330	0621	-8.0	1.0	7.8	11.0	
204.	2-330	0917	15.8	4.8	7.5	11.6	
205.	2-330	1055	21.4	11.0	8.0	11.4	
206.	2-330	1231	23.2	16.0	10.1	10.8	
207.	2-330	1436	25.0	20.5	11.0	10.1	
208.	C LAVIC LAKE	1-4			PROBE		
209.	1-429	0623	-4.0	0.0	6.0	11.4	
210.	1-429	0737	2.0	3.0	11.9	12.0	
211.	1-429	1025	15.5	8.5	8.1	12.1	
212.	1-429	1253	24.0	15.1	6.5	11.0	
213.	1-429	1445	25.8	19.0	12.0	11.0	
214.	1-429	1625	25.0	21.5	14.5	12.0	
215.	1-429	1823	16.9	17.7	14.0	11.1	
216.	1-429	2113	6.1	10.7	13.5	11.6	
217.	1-429	2314	3.0	8.0	12.0	12.0	
218.	1-430	0125	-0.1	5.0	10.4	11.9	
219.	1-430	0351	-2.3	2.7	9.2	11.8	
220.	1-430	0627	-4.0	1.2	8.0	11.9	
221.	1-430	0920	13.4	6.0	7.4	12.0	
222.	1-430	1113	27.4	14.1	9.0	11.8	
223.	1-430	1346	23.0	21.5	12.0	11.0	
224.	1-430	1446	24.2	22.1	13.7	11.0	
225.	C LAVIC LAKE	1-5			PROBE		
226.	1-529	0620	0.0	2.0	6.0	10.0	11.5
227.	1-529	0740	0.5	2.1	5.0	8.5	10.1
228.	1-529	1020	11.0	6.0	5.2	7.6	
229.	1-529	1250	24.5	15.0	9.5	6.2	9.1
230.	1-529	1440	29.0	20.5	13.0	9.5	9.5
231.	1-529	1620	30.0	23.5	15.0	11.0	9.8
232.	1-529	1822	22.2	21.2	18.2	12.7	10.2
233.	1-529	2112	9.0	12.0	15.0	13.5	12.5
234.	1-529	2303	4.5	5.5	13.4	13.9	12.2
235.	1-530	0121	2.2	6.5	10.5	12.2	12.0
236.	1-530	0350	1.0	4.0	8.5	11.7	11.8
237.	1-530	0626	-1.5	2.0	7.7	11.2	12.4
238.	1-530	0923	0.3	6.0	6.0	9.8	11.6
239.	1-530	1111	23.0	14.5	8.8	9.6	11.3
240.	1-530	1345	25.0	23.0	14.0	10.0	10.0
241.	1-530	1445	28.0	25.0	11.1	11.0	10.1
242.	C LAVIC LAKE	1-6			PROBE		
243.	1-629	0625	0.0	2.1	7.5	13.0	0.0

244. 1-629 0743 -1.0 0.0 4.6 10.0 0.0  
 245. 1-629 1027 12.6 5.4 8.9 13.1 5.0  
 246. 1-629 1252 21.2 16.0 11.0 12.0 8.3  
 247. 1-629 1443 22.2 19.5 13.5 12.4 11.1  
 248. 1-629 1630 22.0 20.8 15.8 12.9 13.3  
 249. 1-629 1825 18.1 19.0 16.2 13.1 12.6  
 250. 1-629 2114 11.5 14.0 13.2 12.5 10.4  
 251. 1-629 2305 7.0 10.1 13.4 13.5 1.7  
 252. 1-630 0127 4.8 6.2 13.0 10.0 -1.1  
 253. 1-630 0352 1.8 5.4 10.2 14.0 -3.3  
 254. 1-630 0628 0.0 3.5 9.0 13.8 -6.7  
 255. 1-630 0925 10.8 7.5 8.9 14.0 8.3  
 256. 1-630 1112 21.1 15.0 10.7 13.7 17.6  
 257. 1-630 1348 29.0 22.0 14.0 12.5 20.0  
 258. 1-630 1450 21.0 24.1 15.6 12.5 21.7  
 259. C LAVIC LAKE 1-1  
 260. 1-129 0442L.360 .287 .388 .384 .329 -5.8 -4.7 -4.7 -5.0 -6.8  
 261. 1-129 0610L.372 .335 .387 .390 .355 -2.4 -0.5 -5.7 -4.5 -7.5 33.0 29.5 L-5  
 262. 1-129 0728 29.0 29.0 31.0 28.0 30.0  
 263. 1-129 0955M.471 .413 .385 .406 .490 15.5 13.8 12.8 13.4 16.4  
 264. 1-129 1207M.775 .801 .759 .810 .798 24.3 25.2 25.2 25.7 25.3  
 265. 1-129 1415M.872 .542 .892 .913 .924 27.2 28.7 28.8 28.8 28.4  
 266. 1-129 1557M.723 .736 .693 .694 .705 22.9 23.4 22.1 22.2 20.6  
 267. 1-129 1805M.421 .416 .480 .400 .410 14.2 13.8 14.2 13.4 13.8  
 268. 1-129 2050L.726 .782 .757 .806 .759 4.5 2.0 1.5 3.4 1.6  
 269. 1-129 2236L.732 .728 .736 .706 .692 0.4 0.2 0.5 -0.7 -1.5 S-5  
 270. 1-130 0100L.675 .670 .680 .690 .662 -2.4 -2.3 -2.0 -1.5 -2.7 S-5  
 271. 1-130 0315L.678 .636 .637 .617 .658 1.5 -3.3 -3.8 -4.8 -3.0 S-5  
 272. 1-130 0610L.592 .614 .625 .598 .563 -5.5 -4.3 -4.2 -5.5 -7.2 S-5  
 273. 1-130 1316F.279 .291 .309 .299 .274 57.6 38.1 38.9 39.1 37.4 S-5  
 274. 1-130 1425F.290 .265 .271 .274 .251 39.3 38.0 37.4 37.4 36.6 S-5  
 275. C LAVIC LAKE 1-2  
 276. 1-229 0451L.362 .357 .360 .357 .343 -5.5 -2.7 -0.5 -6.5 -5.5  
 277. 1-229 0615L.372 .391 .303 .367 .350 -5.0 -4.5 -5.0 -5.4 -5.5  
 278. 1-229 0730 34.0 34.0 33.0 32.0 33.0  
 279. 1-229 1000M.475 .452 .420 .462 .487 15.0 14.8 14.2 15.6 16.2  
 280. 1-229 1215M.774 .742 .860 .722 .838 24.3 23.7 20.8 23.0 26.4  
 281. 1-229 1220M.626 .635 .630 .686 .890 25.8 20.6 26.3 27.6 27.4  
 282. 1-229 1430M.905 .567 .670 .870 .882 27.8 29.5 27.2 26.8 27.3  
 283. 1-229 1602M.685 .762 .670 .725 .635 22.0 24.0 21.6 24.2 20.6  
 284. 1-229 1807M.421 .385 .353 .390 .430 14.1 15.0 13.0 13.1 13.6  
 285. 1-229 2055L.751 .776 .784 .768 .763 2.0 2.2 2.6 1.9 1.8  
 286. 1-229 2245L.734 .725 .721 .712 .694 0.0 -0.2 -0.2 -0.2 -0.4 S-5  
 287. 1-230 0105L.707 .661 .680 .678 .652 -1.0 -2.5 -1.7 -2.0 -3.1 S-5  
 288. 1-230 0320L.655 .652 .646 .652 .655 -2.6 -3.0 -3.3 -3.0 -3.0 S-5  
 289. 1-230 0611L.611 .605 .558 .604 .569 -5.0 -5.2 -5.6 -5.3 -6.0 S-5  
 290. 1-230 1320F.272 .243 .247 .244 .244 57.6 55.2 34.8 36.4 S-5  
 291. 1-230 1427F.247 .232 .269 .258 .235 36.1 35.6 37.5 37.0 35.6 S-5  
 292. C LAVIC LAKE RC4E  
 293. PC29 0455L.370 .380 .366 .355 .378 -5.5 -5.0 -5.0 -6.0 -5.2  
 294. PC29 0610L.394 .390 .363 .377 .394 -4.2 -4.1 -4.0 -4.5 -5.0  
 295. RD29 0735 33.0 34.0 34.0 36.0 35.0  
 296. PC29 1004M.417 .445 .526 .456 .508 13.6 14.8 17.4 15.2 15.8  
 297. RD29 1217M.345 .766 .840 .804 .920 20.6 24.2 20.4 25.4 28.5  
 298. RD29 1422M.870 .502H.152 .062 .052 27.4 28.2H.2 28.0 27.2  
 299. RD29 1604M.682 .741 .728 .712 .652 22.0 23.0 23.2 23.0 24.2  
 300. RD29 1800M.456 .439 .409 .414 .402 15.2 14.0 14.1 13.6 13.4  
 301. C LAVIC LAKE 1-3  
 302. 1-329 0458L.390 .337 .372 .379 .366 -5.1 -4.8 -5.5 -5.0 -4.9  
 303. 1-329 0725 34.0 34.0 34.0 34.0 34.0  
 304. 1-329 1006M.422 .471 .447 .480 .410 13.6 15.3 14.7 15.8 13.6

305. 1-325 1425M.053 .085 .038 .044 .073 26.5 28.8 26.5 26.7 28.3  
 306. 1-325 1604M.748 .728 .727 .674 .715 24.0 23.2 23.2 21.8 22.8  
 307. 1-325 1810M.394 .410 .397 .399 .074 19.2 19.8 19.2 13.4 12.7  
 308. 1-325 2100L.812 .615 .924 .619 .815 .606 3.7 4.0 4.0 3.9 S-5  
 309. 1-325 2250L.752 .755 .750 .755 .734 1.5 1.4 1.0 1.3 0.7 S-5  
 310. 1-329 0110L.713 .699 .697 .074 .682 -0.5 -1.0 -1.2 -2.2 -1.7 S-5  
 311. 1-329 0331L.680 .672 .674 .050 .643 -2.0 -2.2 -2.3 -3.2 -3.2 S-5  
 312. 1-329 0616L.622 .631 .614 .009 .625 -4.5 -4.4 -4.4 -5.1 -4.4 S-5  
 313. 1-329 1335H.181 .225 .215 .139 .170 39.6 55.2 34.9 31.4 33.2 S-5  
 314. 1-329 1432H.235 .273 .281 .235 .281 .506 37.4 37.7 35.5 37.7 S-5  
 315. C LAVIC LAKE ALLUVIUM 2-1 S-5  
 316. 2-129 0515L.416 .398 .390 .411 .381 -3.8 -4.2 -4.8 -3.0 -4.6 Q-4  
 317. 2-129 0655 42.0  
 318. 2-129 1015M.580 .530 .530 .560 .580 18.6 17.2 17.4 18.2 18.7  
 319. 2-129 1240M.581 .898 .912 .878 .836 29.7 26.2 27.5 28.2 26.3  
 320. 2-129 1435H.161 .135 .140 .128 .139 56.2 51.2 31.4 30.6 31.3  
 321. 2-129 1615M.754 .722 .721 .739 .710 24.2 23.2 23.1 23.6 23.0  
 322. 2-129 1820M.425 .432 .455 .402 .434 14.2 14.4 15.2 15.4 14.4  
 323. 2-129 2045H.174 .157 .161 .142 .129 5.6 5.4 5.4 4.0 4.3 2\$ S-5  
 324. 2-129 2300L.780 .775 .755 .782 .754 2.5 2.0 1.6 1.8 2.4 S-5  
 325. 2-130 0120L.717 .713 .703 .692 .695 -0.3 -0.5 -0.6 -1.5 -1.2 S-5  
 326. 2-130 0345L.691 .682 .664 .659 .687 -1.4 -2.0 -2.2 -2.6 -1.8 S-5  
 327. 2-130 0618L.663 .654 .640 .670 .656 -2.5 -3.0 -2.5 -2.1 -2.5 S-5  
 328. 2-130 1340H.303 .324 .328 .314 .294 39.0 39.6 39.6 39.2 38.2 S-5  
 329. 2-130 1500H.329 .284 .247 .314 .256 39.3 37.8 36.2 39.2 36.6 S-5  
 330. C LAVIC LAKE 2-2  
 331. 2-229 0502L.417 .367 .385 .391 .353 -3.8 -5.2 -5.9 -4.8 -5.6 S-5  
 332. 2-229 0715 27.0 32.0 30.0 32.0 30.0  
 333. 2-229 1005M.451 .4CE .500 .390 .414 19.2 19.8 16.4 13.1 13.7  
 334. 2-229 1222M.793 .777 .753 .864 .770 24.8 24.7 24.8 26.3 24.4  
 335. 2-229 1427M.047 .032 .010 M.819 .875 27.0 25.2 25.2 25.7 27.4  
 336. 2-229 1610M.707 .638 .643 .650 .649 22.7 20.7 20.8 21.0 21.0  
 337. 2-229 1915M.211 .324 .256 .380 .291 10.3 11.0 9.8 10.7 8.8 S-5  
 338. 2-229 2105L.804 .744 .804 .742 .705 3.3 3.0 3.5 0.7 1.6 S-5  
 339. 2-229 2251L.711 .744 .723 .768 .756 -1.5 0.0 0.2 1.7 1.4 S-5  
 340. 2-230 0115L.645 .630 .672 .680 .641 -3.3 -2.2 -2.1 -2.0 -3.6 S-5  
 341. 2-230 0335L.637 .652 .631 .636 .608 -3.7 -3.0 -4.0 -4.0 -5.2 S-5  
 342. 2-230 0626L.568 .608 .626 .610 .580 -5.6 -5.2 -4.3 -4.9 -6.0 S-5  
 343. 2-230 1320H.238 .226 .191 .244 .216 35.8 35.4 33.7 36.1 35.0 S-5  
 344. 2-230 1425M.260 .245 .197 .232 .246 36.8 36.2 34.2 35.2 35.8 S-5  
 345. C LAVIC LAKE 2-2  
 346. 2-329 0504L.420 .38E .350 .322 .362 -3.5 -4.0 -5.4 -6.5 -4.5 S-5  
 347. 2-329 0720 34.0 32.0 35.0 33.0 33.0  
 348. 2-329 1012M.404 .461 .460 .485 .478 15.2 15.2 15.2 16.0 15.8  
 349. 2-329 1225M.545 .831 .842 .803 .816 28.2 25.8 26.2 25.4 25.4  
 350. 2-329 1430H.050 .075 .097 H.125 .112 27.1 27.8 28.0 30.5 30.2  
 351. 2-329 1612M.695 .725 .641 .666 .573 22.5 23.7 21.0 21.4 21.5  
 352. 2-329 1812M.358 .305 .275 .370 .392 12.0 10.2 9.2 10.4 13.0 S-5  
 353. 2-329 2106L.794 .165 .756 .754 .758 3.0 1.3 1.7 2.0 1.8 S-5  
 354. 2-329 2255L.736 .731 .732 .094 .715 0.6 0.3 0.4 -1.2 -0.3 S-5  
 355. 2-330 0116L.679 .678 .665 .626 .652 -2.0 -2.2 -2.5 -4.2 -3.2 S-5  
 356. 2-330 0336L.631 .614 .612 .275 .612 -4.0 -4.6 -4.6 -6.7 -5.2 S-5  
 357. 2-330 0621L.604 .605 .574 .608 .619 -5.2 -5.3 -6.8 -5.2 -4.5 S-5  
 358. 2-330 1331H.225 .255 .195 .277 .276 34.9 36.7 34.0 37.4 37.3 S-5  
 359. 2-330 1436H.221 .245 .236 .197 .200 34.8 36.0 35.2 34.2 34.2 S-5  
 360. C LAVIC LAKE 1-4  
 361. 1-429 0623L.400 .414 .415 .410 .422 -4.0 -3.8 -3.2 -4.0 -3.6 S-5  
 362. 1-429 0737 36.0 36.0 37.0 37.0 36.0  
 363. 1-429 1025M.502 .602 .554 .574 .563 16.4 19.0 18.2 18.4 18.4  
 364. 1-429 1253H.069 .091 .062 .086 .058 27.6 28.6 27.6 28.6 27.3  
 365. 1-429 1445M.120 .121 .113 .070 .085 30.2 30.6 30.2 28.4 28.7

362.														
267.	1-429	1621L	.675	.675	.664	.663	.663	.663	.663	.663	.663	.663	.663	.663
304.	1-429	149254L	.377	.402	.377	.385	.385	.385	.385	.385	.385	.385	.385	.385
363.	1-429	2113L	.652	.571	.826	.046	.046	.046	.046	.046	.046	.046	.046	.046
271.	1-429	2204L	.068	.786	.787	.775	.781	.785	.785	.785	.785	.785	.785	.785
371.	1-429	1125L	.730	.744	.729	.739	.722	.722	.722	.722	.722	.722	.722	.722
372.	1-430	0351L	.713	.690	.692	.704	.634	.634	.634	.634	.634	.634	.634	.634
373.	1-429	0627L	.657	.675	.669	.669	.655	.655	.655	.655	.655	.655	.655	.655
374.	1-429	1346H	.145	.126	.154	.043	.160	.264	.264	.264	.264	.264	.264	.264
375.														
375.	1-429	0820L	.475	.452	.462	.480	.504	.504	.504	.504	.504	.504	.504	.504
377.	1-525	0140L												
378.	1-525	1020W	.295	.366	.242	.275	.286	.314	.314	.314	.314	.314	.314	.314
379.	1-525	1250N	.777	.745	.716	.633	.773	.247	.247	.247	.247	.247	.247	.247
360.	1-529	1427H	.142	.127	.103	.060	.045	.314	.306	.306	.306	.306	.306	.306
381.	1-529	1622H	.177	.181	.144	.097	.053	.330	.332	.332	.332	.332	.332	.332
382.	1-525	1A22W	.950	.805	.812	.037	.820	.449	.252	.252	.252	.252	.252	.252
383.	1-525	2112W	.328	.300	.296	.296	.296	.110	.110	.110	.110	.110	.110	.110
384.	1-526	2303L	.909	.841	.880	.834	.902	.755	.690	.690	.690	.690	.690	.690
385.	1-520	0121L	.907	.912	.832	.844	.825	.806	.806	.806	.806	.806	.806	.806
386.	1-520	035CL	.606	.150	.772	.794	.788	.555	.555	.555	.555	.555	.555	.555
387.	1-520	0625L	.713	.724	.729	.719	.745	.255	.255	.255	.255	.255	.255	.255
388.	1-520	1345H	.286	.211	.154	.165	.185	.376	.340	.340	.340	.340	.340	.340
389.	1-520	1445H	.335	.312	.260	.275	.308	.401	.391	.391	.391	.391	.391	.391
390.														
391.	1-629	0625L	.445	.480	.455	.441	.450	.450	.450	.450	.450	.450	.450	.450
392.	1-629	0743												
393.	1-529	1274	.572	.670	.603	.027	.069	.217	.245	.245	.245	.245	.245	.245
394.	1-629	1251H	.159	.162	.130	.060	.047	.326	.347	.347	.347	.347	.347	.347
395.	1-629	1445H	.102	.072	.124	.124	.129	.135	.345	.345	.345	.345	.345	.345
396.	1-625	1632W	.326	.780	.302	.966	.815	.259	.248	.248	.248	.248	.248	.248
397.	1-629	2114H	.153	.145	.139	.148	.142	.152	.51	.47	.47	.47	.47	.47
398.	1-625	2305L	.930	.733	.781	.794	.768	.349	.24	.24	.24	.24	.24	.24
399.	1-630	0127L	.752	.716	.743	.742	.745	.153	.07	.07	.07	.07	.07	.07
400.	1-630	0352L	.710	.705	.704	.699	.715	.055	.055	.055	.055	.055	.055	.055
401.	1-620	0628L	.594	.686	.664	.670	.672	.401	.16	.16	.16	.16	.16	.16
402.	1-620	1349H	.265	.250	.305	.281	.352	.414	.380	.380	.380	.380	.380	.380
403.	1-630	1450H	.337	.322	.275	.250	.355	.598	.394	.394	.394	.394	.394	.394
404.														

PK1-5 SPECIAL (Spectral Passband, 8 - 14 $\mu$ )S-5

LO RANGE		MED RANGE		HI RANGE	
Meter (°C)	Recorder (MV D-C)	Meter (°C)	Recorder (MV D-C)	Meter (°C)	Recorder (MV D-C)
-40.0	0.0	0.0	0.0	25.0	0.0
-39.0	14.0	1.0	28.6	26.0	21.3
-38.0	28.3	2.0	57.6	27.0	42.7
-37.0	42.8	3.0	86.9	28.0	64.3
-36.0	57.5	4.0	116.5	29.0	86.2
-35.0	72.4	5.0	146.4	30.0	108.2
-34.0	87.6	6.0	176.6	31.0	130.4
-33.0	103.0	7.0	207.2	32.0	152.8
-32.0	118.7	8.0	238.1	33.0	175.4
-31.0	134.5	9.0	269.3	34.0	198.2
-30.0	150.6	10.0	300.8	35.0	221.2
-29.0	167.0	11.0	332.7	36.0	244.3
-28.0	183.6	12.0	364.8	37.0	267.7
-27.0	200.4	13.0	397.3	38.0	291.2
-26.0	217.5	14.0	430.2	39.0	315.0
-25.0	234.8	15.0	463.3	40.0	338.9
-24.0	252.3	16.0	496.8	41.0	363.1
-23.0	270.1	17.0	530.6	42.0	387.4
-22.0	288.1	18.0	564.7	43.0	411.9
-21.0	306.4	19.0	599.2	44.0	436.6
-20.0	324.9	20.0	634.0	45.0	461.5
-19.0	343.7	21.0	669.1	46.0	486.6
-18.0	362.7	22.0	704.6	47.0	511.9
-17.0	382.0	23.0	740.3	48.0	537.4
-16.0	401.5	24.0	776.4	49.0	563.1
-15.0	421.3	25.0	812.9	50.0	588.9
-14.0	441.3	26.0	849.6	51.0	615.0
-13.0	461.6	27.0	886.7	52.0	641.2
-12.0	482.2	28.0	924.2	53.0	667.7
-11.0	503.0	29.0	961.9	54.0	694.3
-10.0	524.0	30.0	1000.0	55.0	721.2
-9.0	545.3			56.0	748.2
-8.0	566.9			57.0	775.4
-7.0	588.7			58.0	802.8
-6.0	610.8			59.0	830.4
-5.0	633.1			60.0	858.2
-4.0	655.7			61.0	886.2
-3.0	678.6			62.0	914.3
-2.0	701.7			63.0	942.7
-1.0	725.1			64.0	971.3
0.0	748.8			65.0	1000.0
1.0	772.7				
2.0	796.9				
3.0	821.3				
4.0	846.1				
5.0	871.0				
6.0	896.3				
7.0	921.8				
8.0	947.6				
9.0	973.7				
10.0	1000.0				

INTEGRITY OF THE  
PAGE IS POOR.

\* High-level output. Low level output is 1/20th of listed value.

Figure 2-2 RECORDER-OUTPUT CALIBRATION\*  
 (Standard Spectral Passband, 8 to 14 $\mu$ )

LOW RANGE		MEDIUM RANGE		HIGH RANGE	
Meter (°C)	Recorder (mv d-c)	Meter (°C)	Recorder (mv d-c)	Meter (°C)	Recorder (mv d-c)
-20	0.0	10	0.0	40	0.0
-19	24.0	11	24.5	41	25.3
-18	48.4	12	49.4	42	51.1
-17	73.1	13	74.9	43	77.3
-16	98.2	14	100.9	44	104.0
-15	123.5	15	127.3	45	131.2
-14	149.1	16	154.3	46	158.8
-13	175.0	17	181.7	47	186.9
-12	201.4	18	209.8	48	215.5
-11	228.0	19	237.1	49	243.4
-10	255.0	20	264.8	50	271.4
-9	282.3	21	292.7	51	299.7
-8	319.9	22	320.8	52	328.2
-7	337.9	23	352.0	53	356.9
-6	366.1	24	377.8	54	385.7
-5	394.7	25	406.8	55	414.8
-4	423.5	26	436.0	56	441.1
-3	452.9	27	465.5	57	473.7
-2	482.4	28	495.1	58	503.5
-1	512.4	29	525.0	59	535.3
0	542.6	30	554.8	60	562.4
+1	573.1	31	584.7	61	592.1
2	604.1	32	614.2	62	622.0
3	643.7	33	644.5	63	651.3
4	665.3	34	674.2	64	680.8
5	695.2	35	704.8	65	711.0
6	727.1	36	735.0	66	742.1
7	758.7	37	765.2	67	771.1
8	790.5	38	795.7	68	801.0
9	822.6	39	829.0	69	830.0
10	841.7	40	855.0	70	857.6
11	880.3	41	883.5	71	885.7
12	909.8	42	912.2	72	914.9
13	939.8	43	941.1	73	943.0
14	969.2	44	970.1	74	971.0
15	1000.0	45	1000.0	75	1000.0

Note: High-level output is listed. Low-level output is 5% of value listed for each temperature.

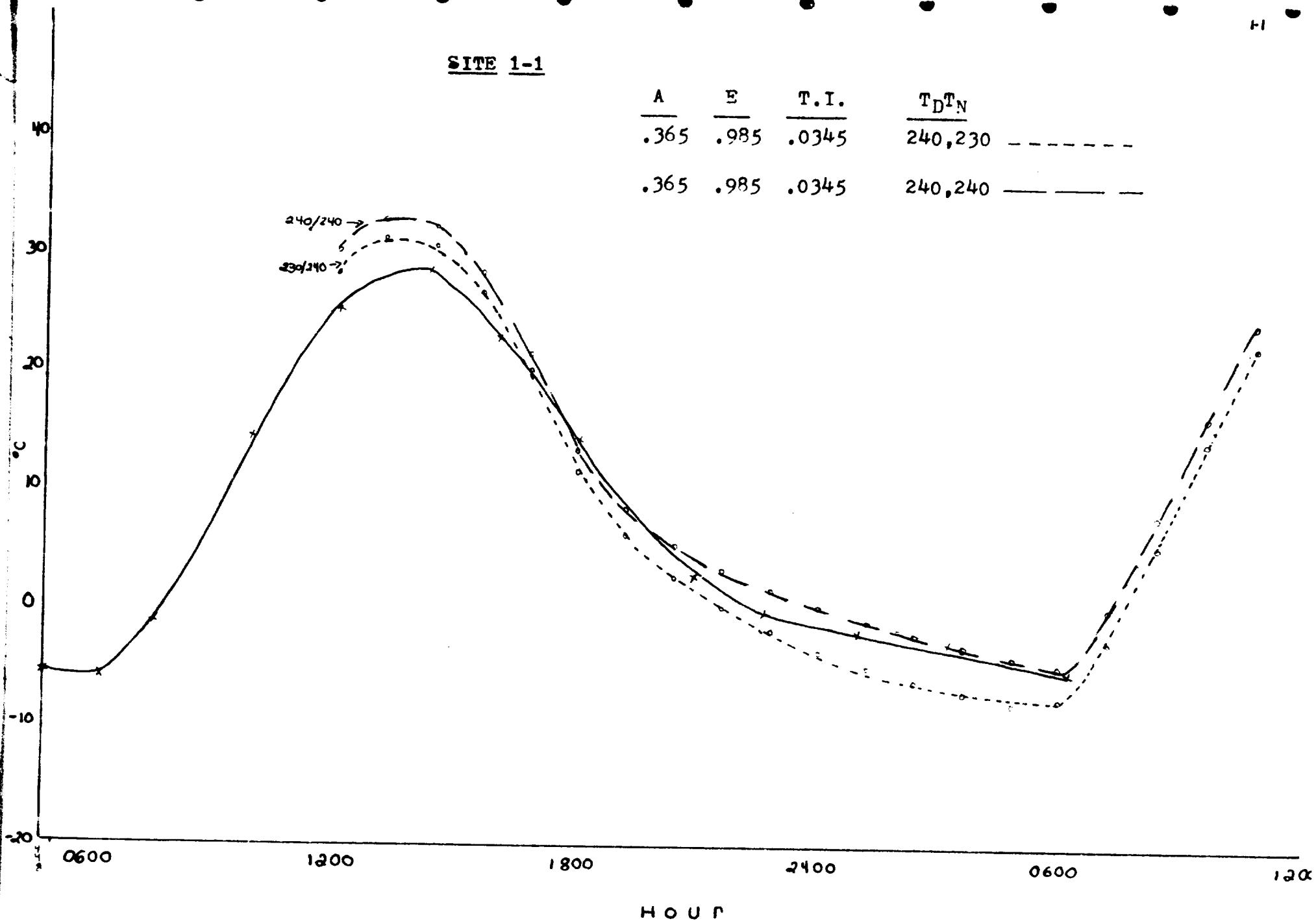
APPENDIX 4

GRAPHICAL REPRESENTATION OF MEASURED DIURNAL SURFACE

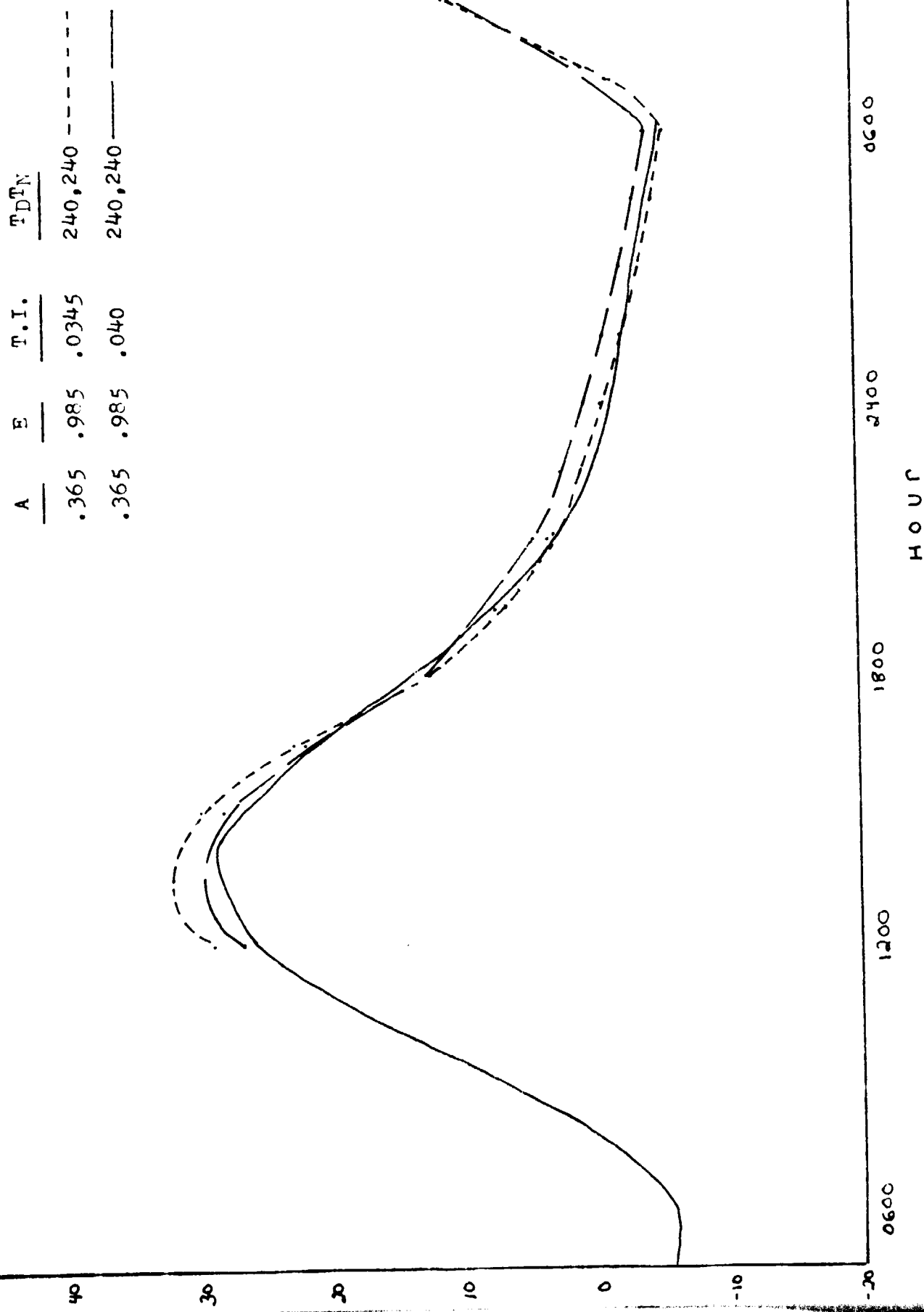
TEMPERATURES v. THERMAL MODEL RUNS

SITE 1-1

A	E	T.I.	$\frac{T_D T_N}{240,230}$
.365	.985	.0345	-----
.365	.985	.0345	240,240 -----

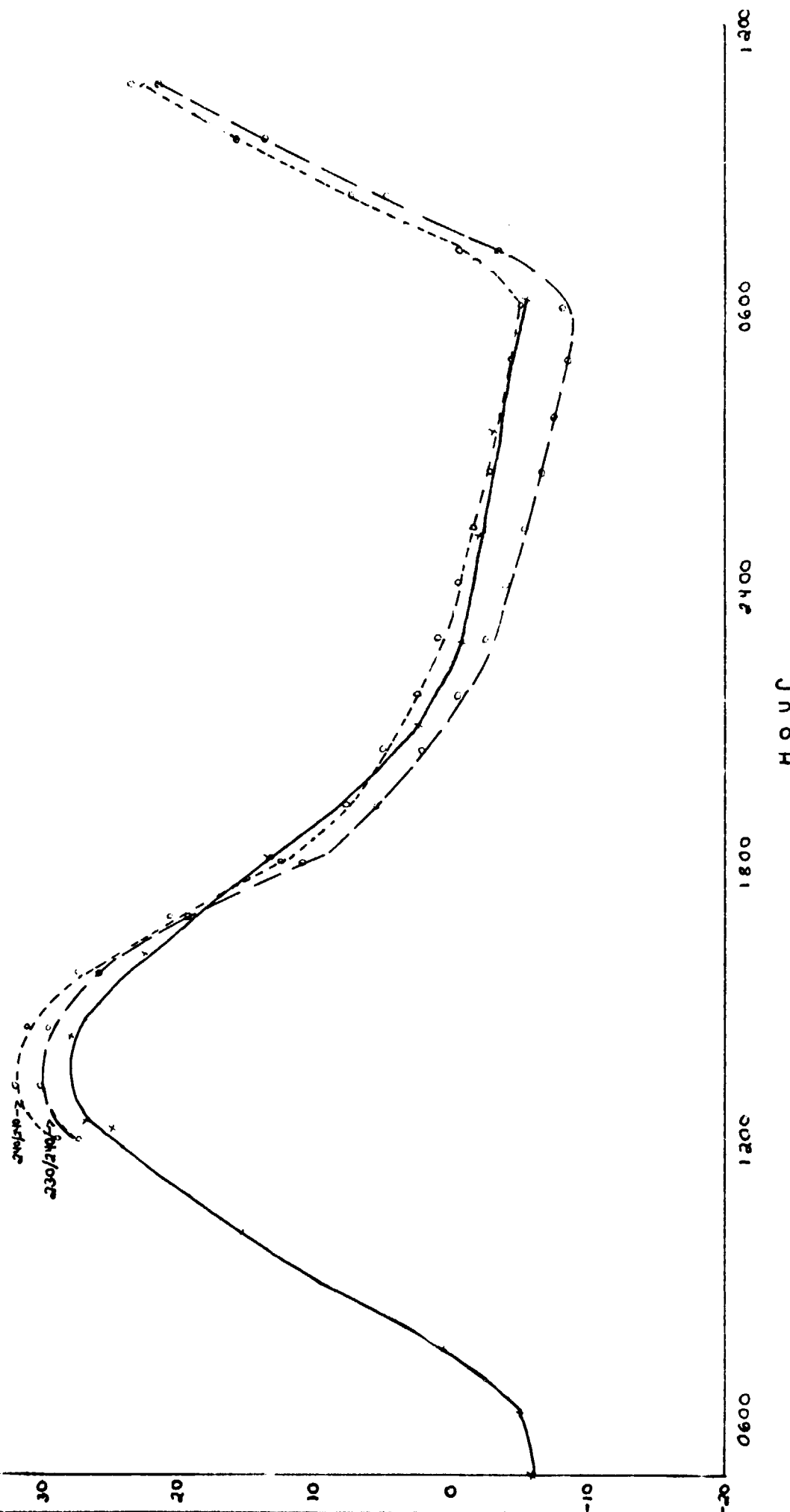


Site 1-1 WATEMP Program



SITE 1-2

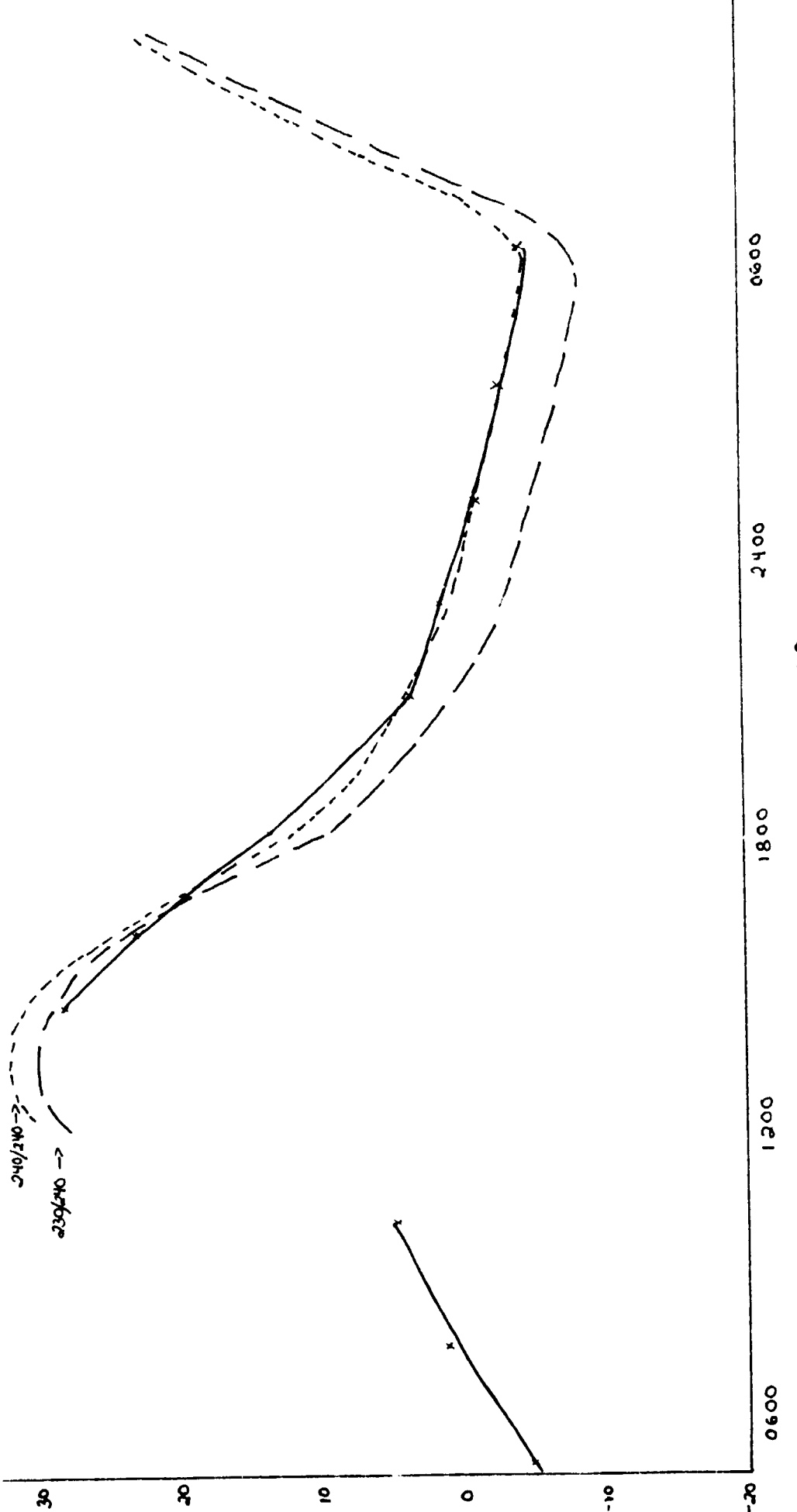
	<u>A</u>	<u>E</u>	<u>T.I.</u>	<u>T<sub>D</sub>T<sub>N</sub></u>
	.378	.985	.034	240,230 - - -
	.378	.985	.034	240,240 - - -



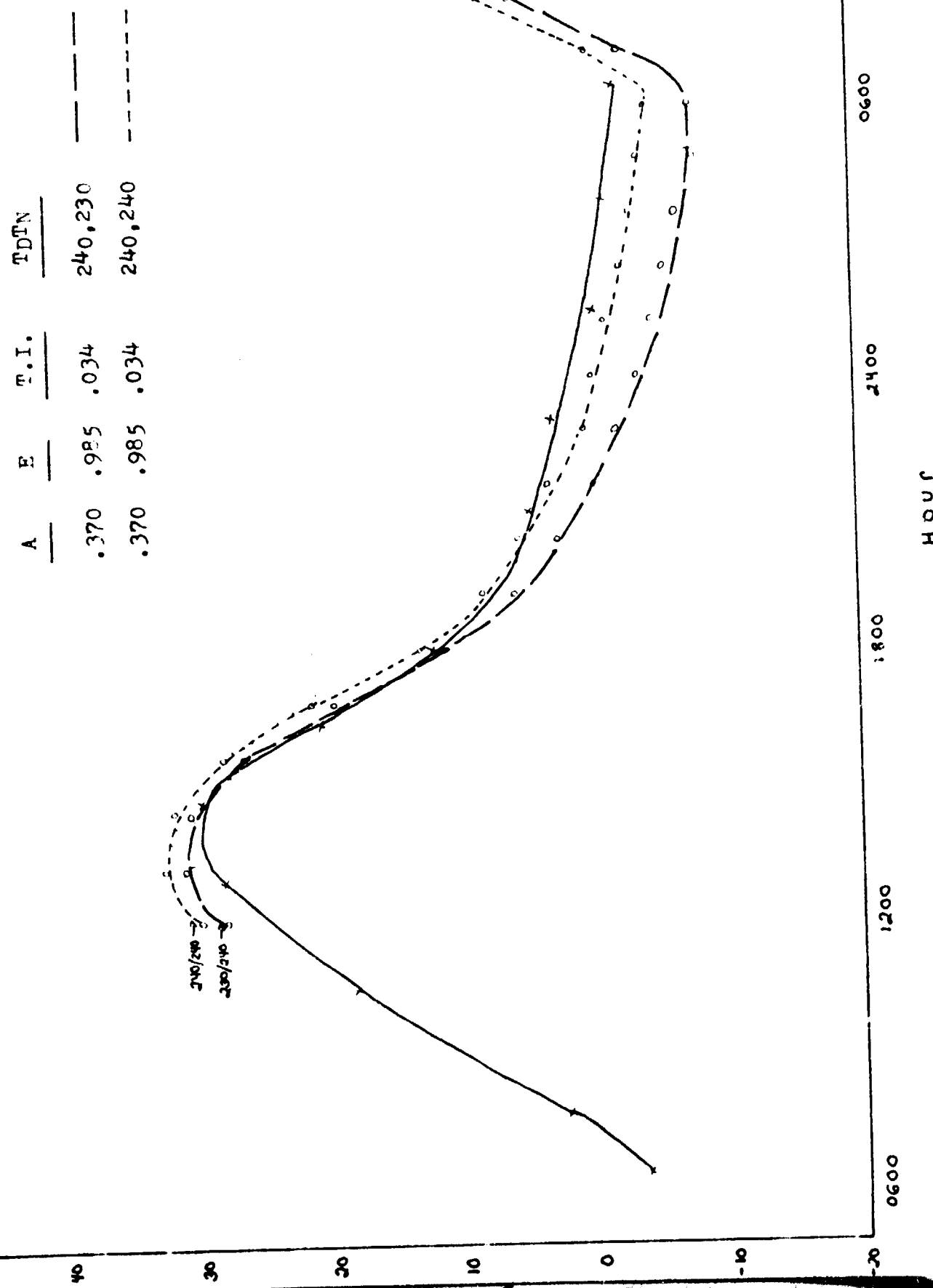
SITE 1-3

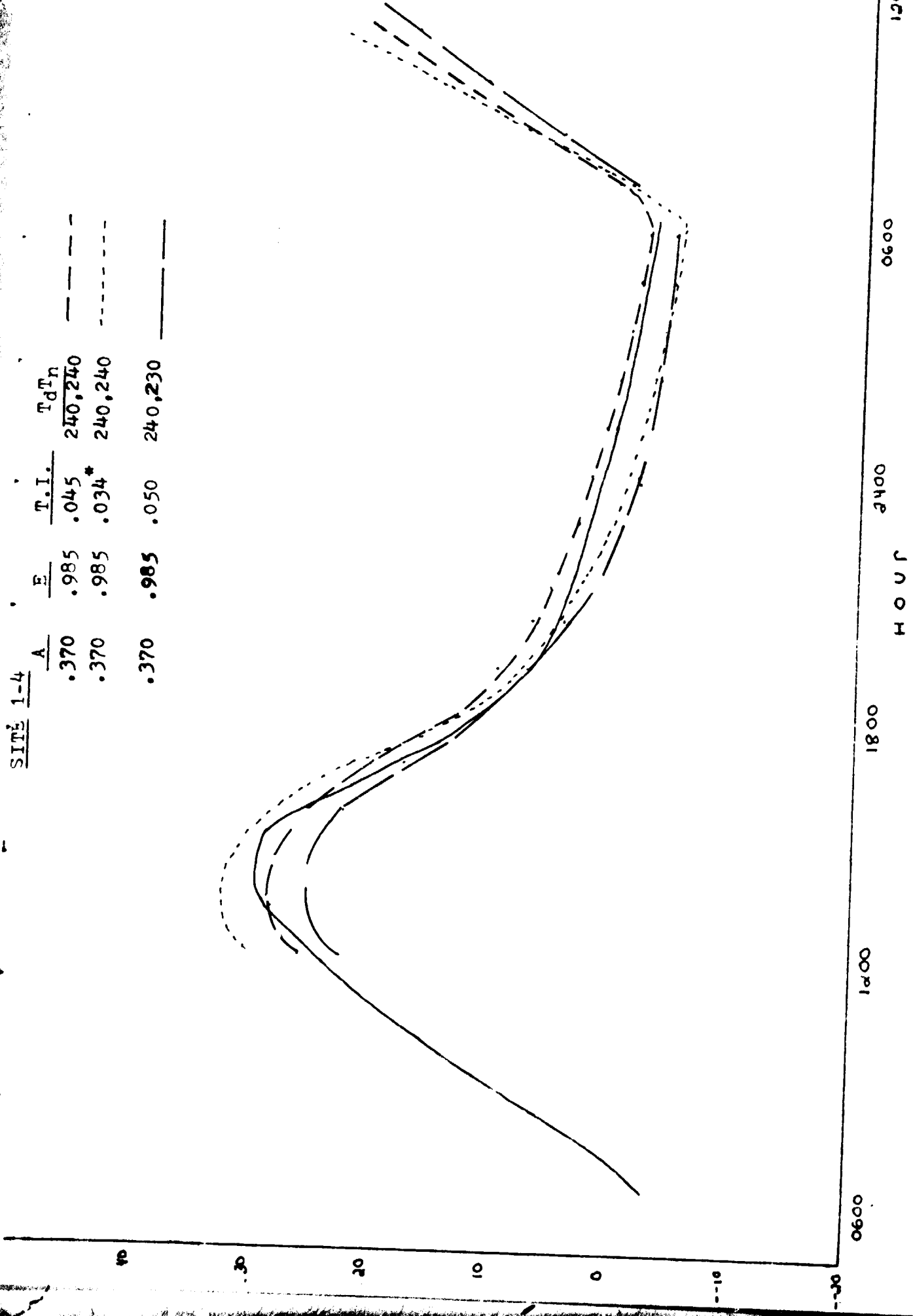
A      E      T.I.      T<sub>D<sup>IN</sup></sub>

.378	.985	.034	240,230
.378	.985	.034	240,240



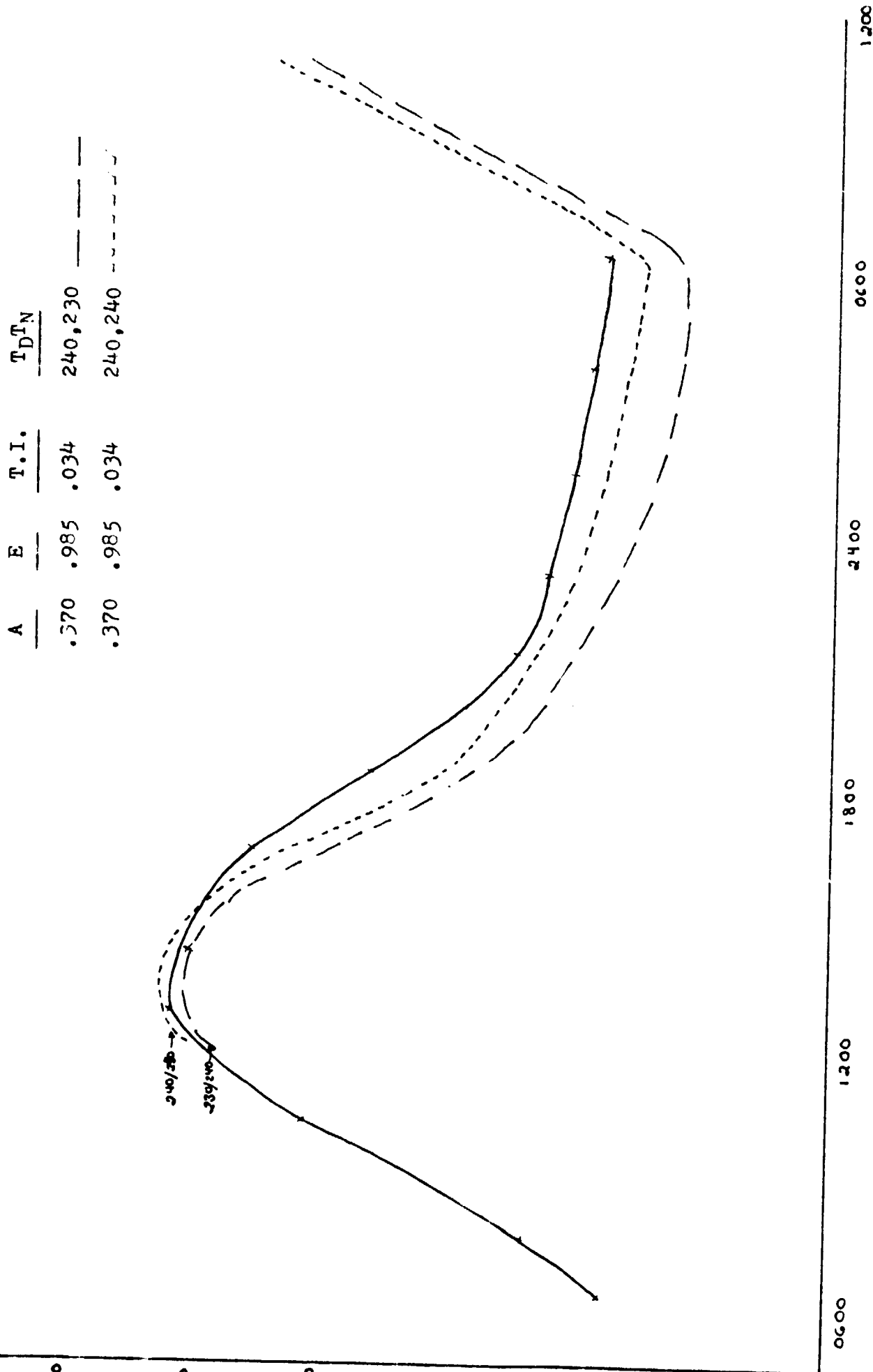
SITE 1-4





1-6

SITE 1-6



HOUR

0000 1800 2400 3000 3600

1200 1000 800 600 400 200

1200

600

2400

HOUR

1200

600

0

2000

1000

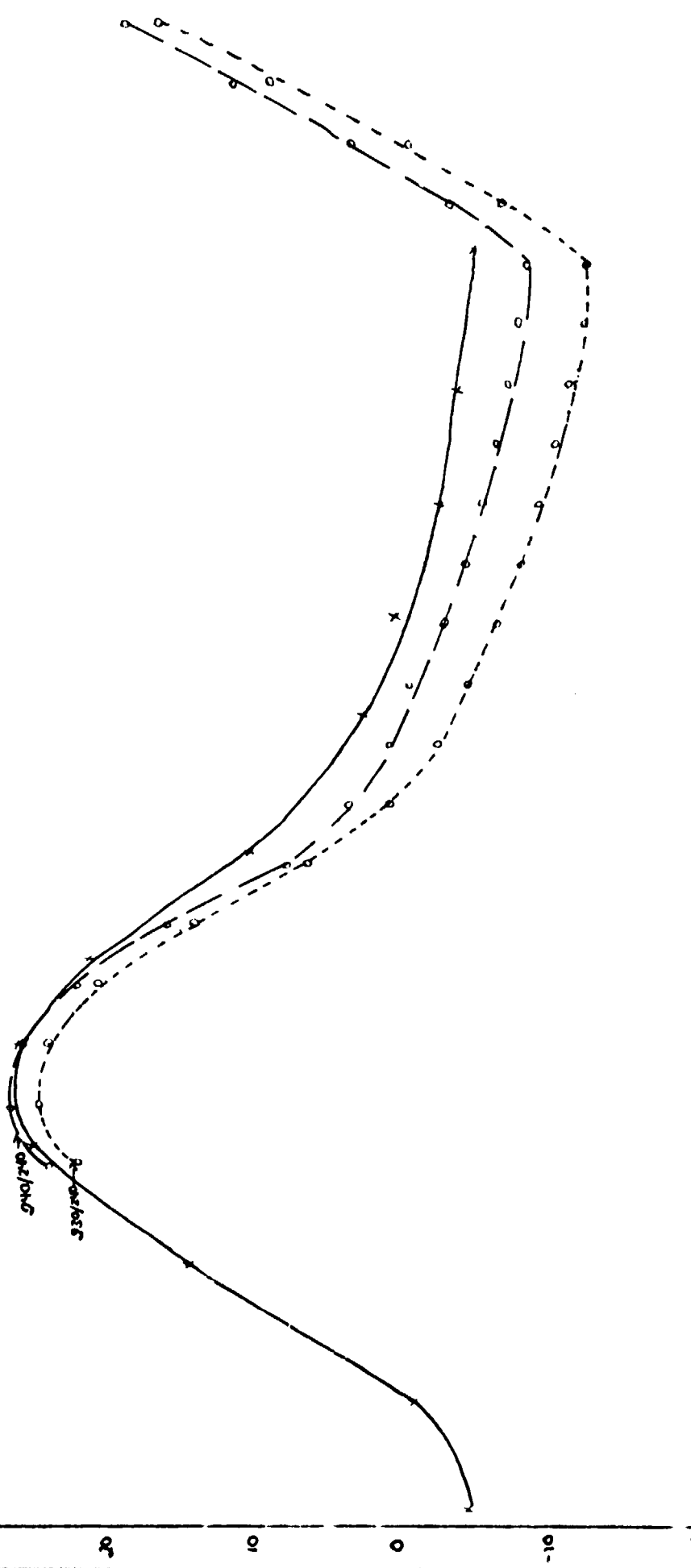
1800

1000

0

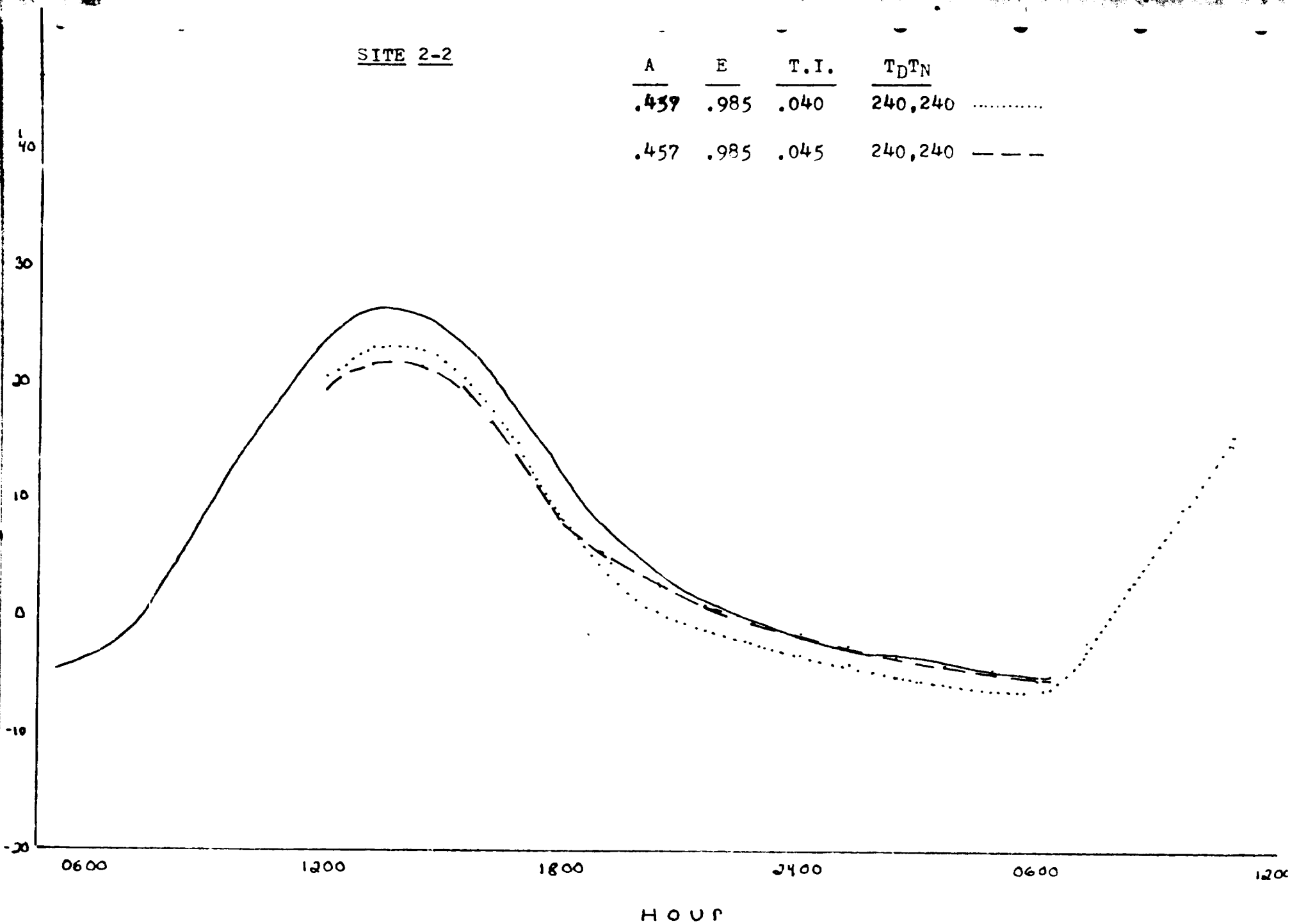
SITE 2-2

<u>A</u>	<u>E</u>	<u>T.I.</u>	<u>TDTN</u>
.457	.985	.031	240,230
.457	.985	.031	240,240



SITE 2-2

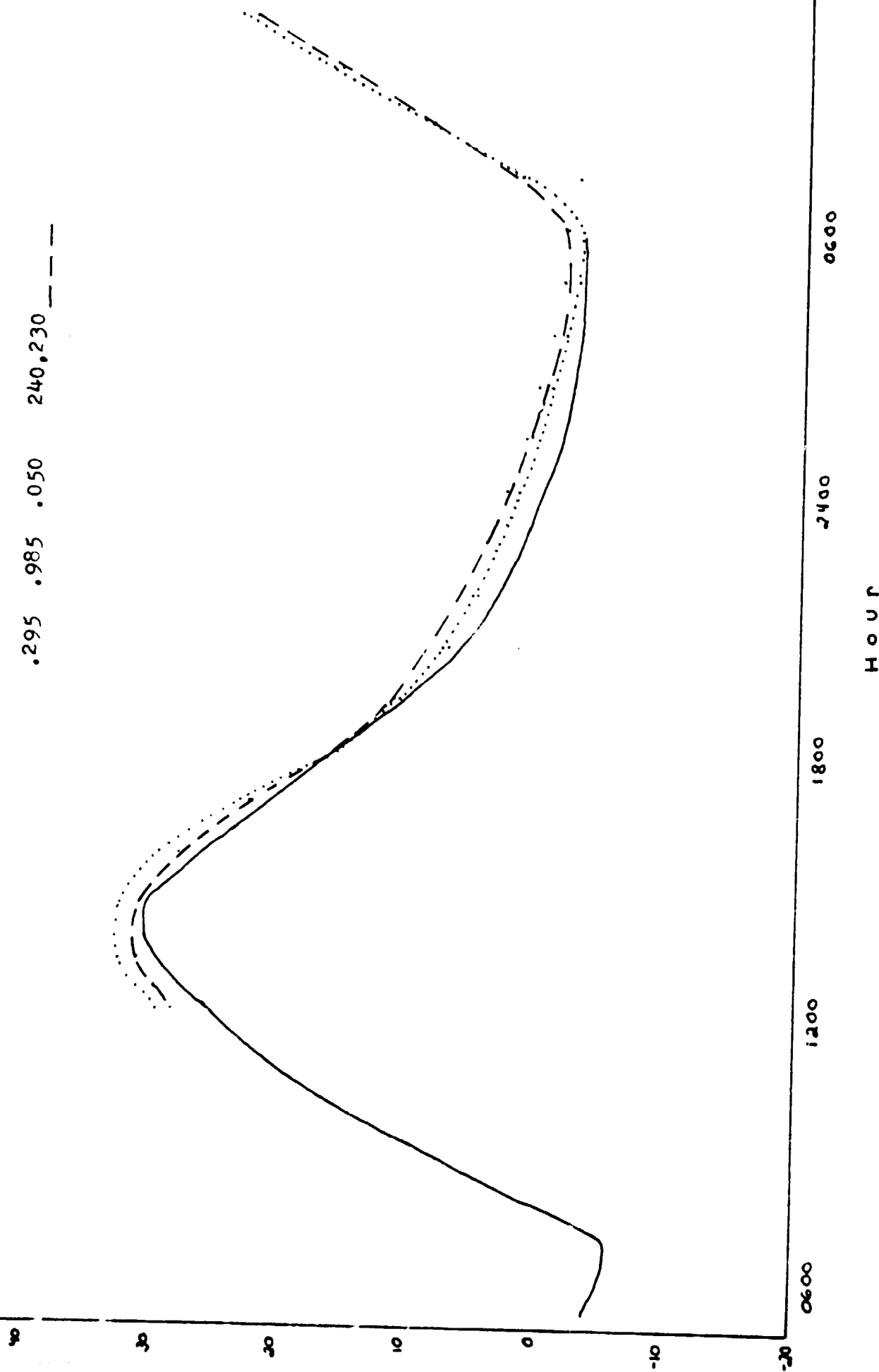
A	E	T.I.	T <sub>D</sub> T <sub>N</sub>
.439	.985	.040	240,240 .....
.457	.985	.045	240,240 ---



SITE 2-1

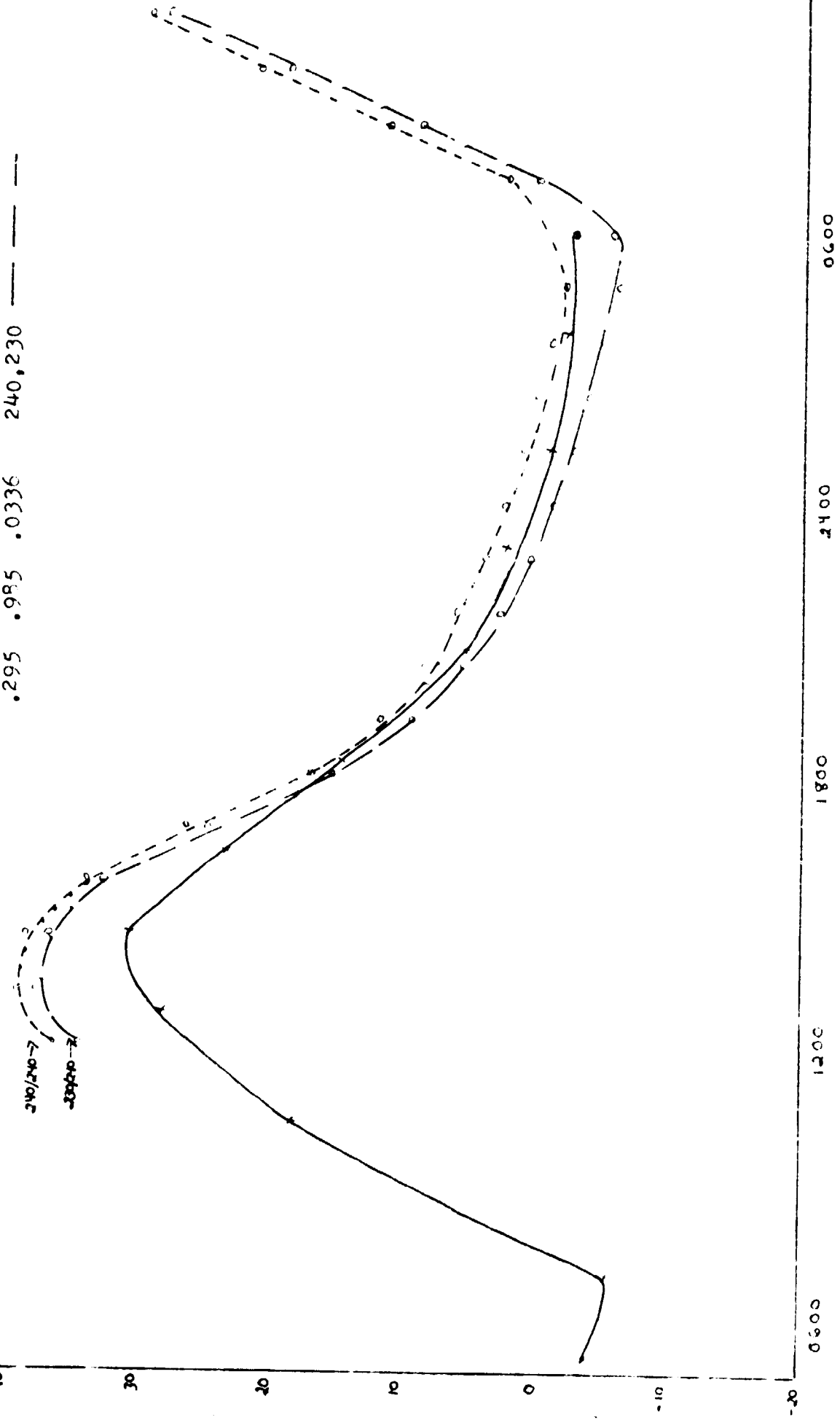
$$\frac{A}{.295} \quad \frac{E}{.985} \quad \frac{T.I.}{.045} \quad \frac{TDTN}{240,230}$$

$$.295 \quad .985 \quad .050 \quad 240,230$$



SITE 21

<u>A</u>	<u>E</u>	<u>T.I.</u>	<u>TDTN</u>
.295	.985	.0336	240,240
.295	.985	.0336	240,230



APPENDIX 5

DETAILED ANALYSIS OF STATION 1-1 EMPLOYING SURTEMP

THERMAL MODEL - "INPUT TEMP" MEASURED AT SITE

MARCH 29-30, 1975

16128 FRI 29 MAY 75

Page 3

GEWBUDI>SEM.,1

0000000000

TIMES, FINAL SURFACE TEMPERATURES, AND INPUT TEMPERATURES

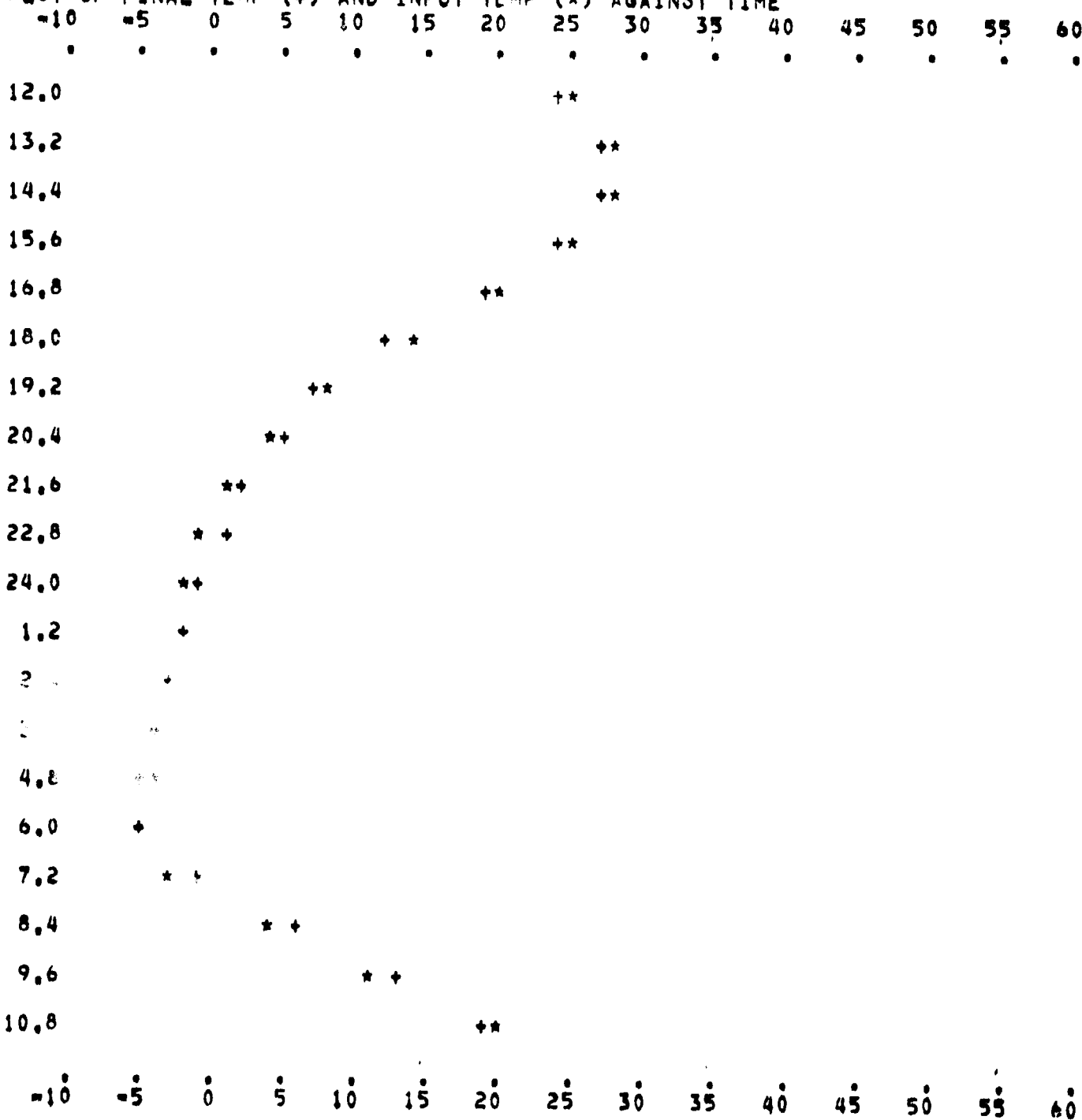
12.0	24.5	25.1	13.2	27.1	28.1	14.4	27.0	27.7	15.6	24.1	24.5	16.8	18.7	20.1
18.0	12.0	14.3	19.2	7.5	8.0	20.4	4.6	3.7	21.6	2.4	1.3	22.8	0.7	-1.0
24.0	-0.8	-2.0	1.2	-2.0	-2.3	2.4	-3.0	-2.6	3.6	-4.0	-3.7	4.8	-4.8	-4.4
6.0	-4.8	-5.4	7.2	-0.8	-2.8	8.4	5.7	4.0	9.6	12.9	11.4	10.8	19.5	20.3

T MAX 27.1 T MIN -4.8 AVERAGE TEMP 8.32

PROGRAM PARAMETERS CURRENT VALUES

(5) CLOUD 0.0 (6) ALB 0.365 (7) EMS 0.9850 (8) T IN 0.045 (9) LAT 34.7  
(10) DEC 3.0 (11) DIP 0.0 (12) STR 0.0 (13) TN 230.0 (14) TD 240.0

PLOT OF FINAL TEMP (+) AND INPUT TEMP (\*) AGAINST TIME



16120 THU 29 MAY 75

Page 5

NEWBUDI STU. 31

□□□□□□□□

## **TIMES, FINAL SURFACE TEMPERATURES, AND INPUT TEMPERATURES**

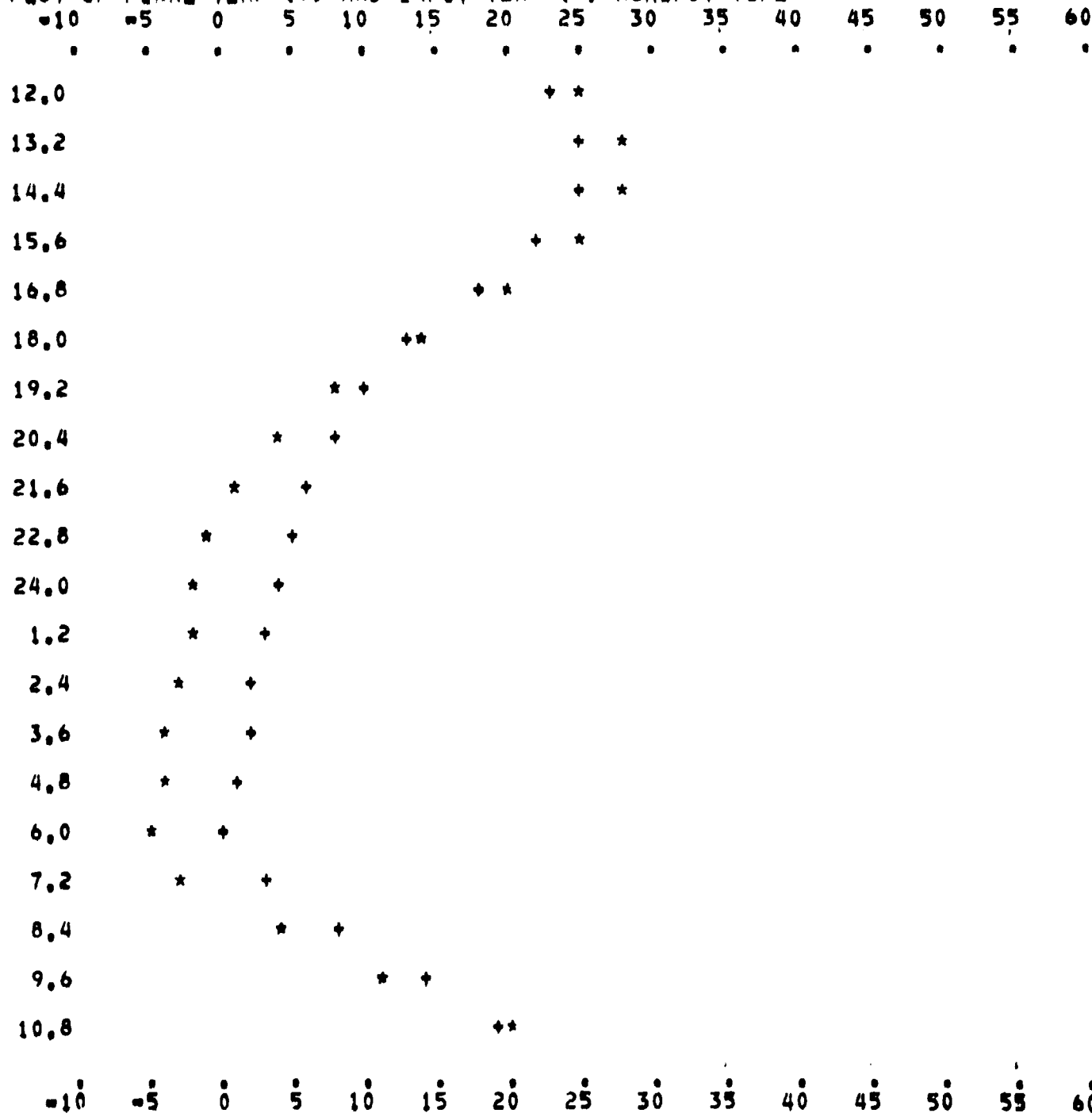
12.0	22.9	25.1	13.2	25.0	28.1	14.4	24.8	27.7	15.6	22.4	24.5	16.8	18.1	20.1
18.0	12.6	14.3	19.2	9.6	8.0	20.4	7.6	3.7	21.6	6.0	1.3	22.8	4.8	-1.0
24.0	3.8	-2.0	1.2	2.9	-2.3	2.4	2.2	-2.6	3.6	1.5	-3.7	4.8	0.9	-4.4
6.0	0.4	-5.4	7.2	3.3	-2.8	8.4	8.2	4.0	9.6	13.8	11.4	10.8	19.0	20.3

T MAX 25.0 T MIN 0.4 AVERAGE TEMP 10.50

**PROGRAM PARAMETERS CURRENT VALUES**

(5) CLOUD 0.2 (6) ALB 0.365 (7) EMS 0.9850 (8) T IN 0.045 (9) LAT 34.7  
(10) DEC 3.0 (11) DIP 0.0 (12) STR 0.0 (13) TN 250.0 (14) TD 250.0

PLOT OF FINAL TEMP (+) AND INPUT TEMP (\*) AGAINST TIME



16:20 THU 29 MAY 75

Page 13

<EWBUDI>STU,11

oooooooooooo

TIMES, FINAL SURFACE TEMPERATURES, AND INPUT TEMPERATURES

12.0	30.8	25.1	13.2	32.8	28.1	14.4	31.1	27.7	15.6	25.7	24.5	16.8	17.0	20.1
18.0	6.8	14.3	19.2	5.3	8.0	20.4	3.7	3.7	21.6	2.4	1.3	22.8	1.3	-1.0
24.0	0.5	-2.0	1.2	-0.3	-2.3	2.4	-0.9	-2.6	3.6	-1.4	-3.7	4.8	-1.9	-4.4
6.0	-6.1	-5.4	7.2	-1.4	-2.8	8.4	7.4	4.0	9.6	16.9	11.4	10.8	25.2	20.3

T MAX 32.8 T MIN -6.1 AVERAGE TEMP 9.75

PROGRAM PARAMETERS CURRENT VALUES

(5) CLOUD 0.2 (6) ALB 0.365 (7) EMS 0.9850 (8) T IN 0.020 (9) LAT 34.7  
(10) DEC 3.0 (11) DIP 0.0 (12) STR 0.0 (13) TN 260.0 (14) TD 240.0

PLOT OF FINAL TEMP (+) AND INPUT TEMP (\*) AGAINST TIME

-10 -5 0 5 10 15 20 25 30 35 40 45 50 55 60

12.0

\* \*

13.2

\* \*

14.4

\* \*

15.6

\*\*

16.8

+ \*

18.0

+ \*

19.2

+ \*

20.4

+

21.6

\*\*

22.8

\* \*

24.0

\* \*

1.2

\* \*

2.4

\* \*

3.6

\* \*

4.8

\* \*

6.0

\*\*

7.2

\* \*

8.4

\* \*

9.6

\* \*

10.8

\* \*

-10 -5 0 5 10 15 20 25 30 35 40 45 50 55 60

10126 THU 29 MAY 75

Page 5

<EWBUDI>SEM.,1

oooooooooooo

TIMES, FINAL SURFACE TEMPERATURES, AND INPUT TEMPERATURES

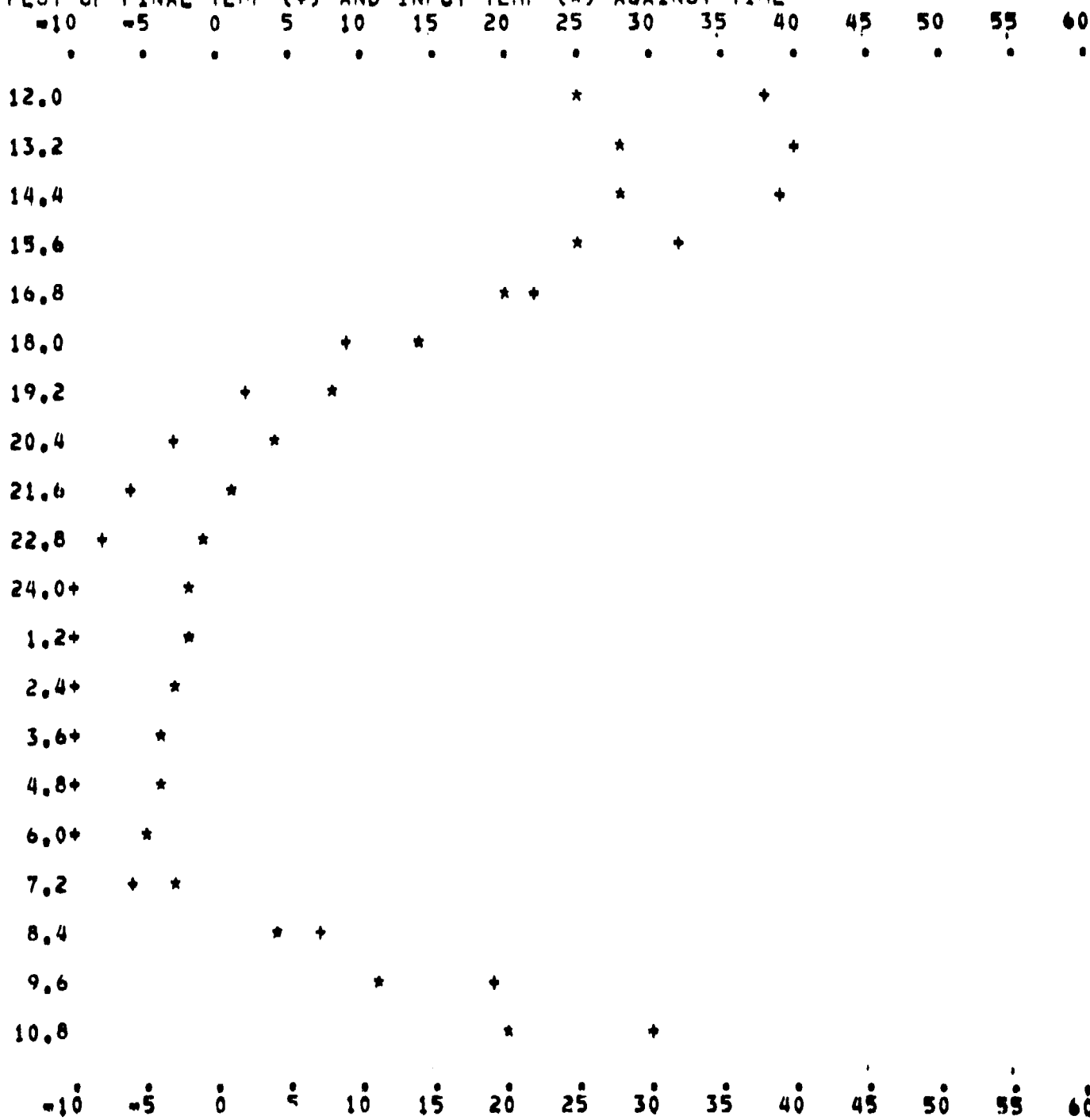
12.0	37.6	25.1	13.2	40.5	28.1	14.4	38.6	27.7	15.6	32.2	24.5	16.8	21.8	20.1
18.0	9.4	14.3	19.2	1.8	8.0	20.4	-2.7	3.7	21.6	-5.8	1.3	22.8	-8.2	-4.0
24.0	=10.1	-2.0	1.2=11.7	-2.3	2.4=13.0	-2.6	3.6=14.2	-3.7	4.8=15.2	-4.4				
6.0	=14.5	-5.4	7.2	-6.0	-2.8	8.4	6.5	4.0	9.6	19.5	11.4	10.8	30.4	20.3

T MAX 40.5 T MIN -15.2 AVERAGE TEMP 6.84

PROGRAM PARAMETERS CURRENT VALUES

(5) CLOUD 0.0 (6) ALB 0.365 (7) EMS 0.9850 (8) T IN 0.020 (9) LAT 34.7  
(10) DEC 3.0 (11) DIP 0.0 (12) STR 0.0 (13) TN 230.0 (14) TD 240.0

PLOT OF FINAL TEMP (+) AND INPUT TEMP (\*) AGAINST TIME



16:20 THU 29 MAY 75

Page 7

<EWBUDI>STU,11

oooooooooooo

TIME8, FINAL SURFACE TEMPERATURES, AND INPUT TEMPERATURES

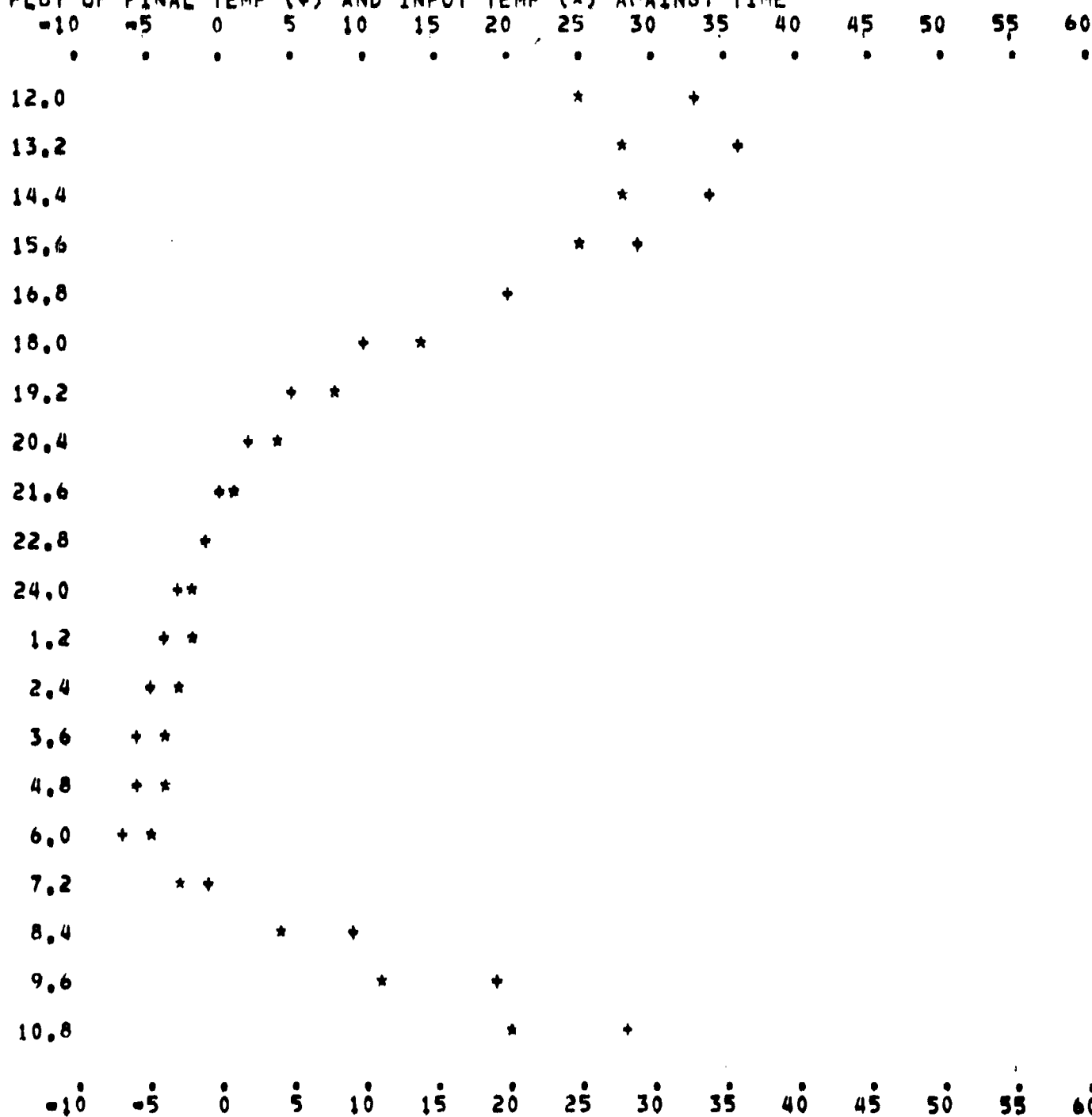
12.0	33.4	25.1	13.2	35.6	28.1	14.4	34.1	27.7	15.6	28.8	24.5	16.8	20.3	20.1
18.0	10.3	14.3	19.2	5.5	8.0	20.4	2.4	3.7	21.6	0.2	1.3	22.8	-1.4	-1.0
24.0	-2.8	-2.0	1.2	-3.9	-2.3	2.4	-4.8	-2.6	3.6	-5.6	-3.7	4.8	-6.3	-4.4
6.0	-6.9	-5.4	7.2	-0.7	-2.8	8.4	8.9	4.0	9.6	19.0	11.4	10.8	27.6	20.3

T MAX 35.6 T MIN -6.9 AVERAGE TEMP 9.69

PROGRAM PARAMETERS CURRENT VALUES

(5) CLOUD 0.2 (6) ALB 0.365 (7) EMS 0.9850 (8) T IN 0.020 (9) LAT 34.7  
(10) DEC 3.0 (11) DIP 0.0 (12) STR 0.0 (13) TN 250.0 (14) TD 250.0

PLOT OF FINAL TEMP (+) AND INPUT TEMP (\*) AGAINST TIME



16:20 THU 29 MAY 75

Page 11

EWBUDI>STU,11

000000000

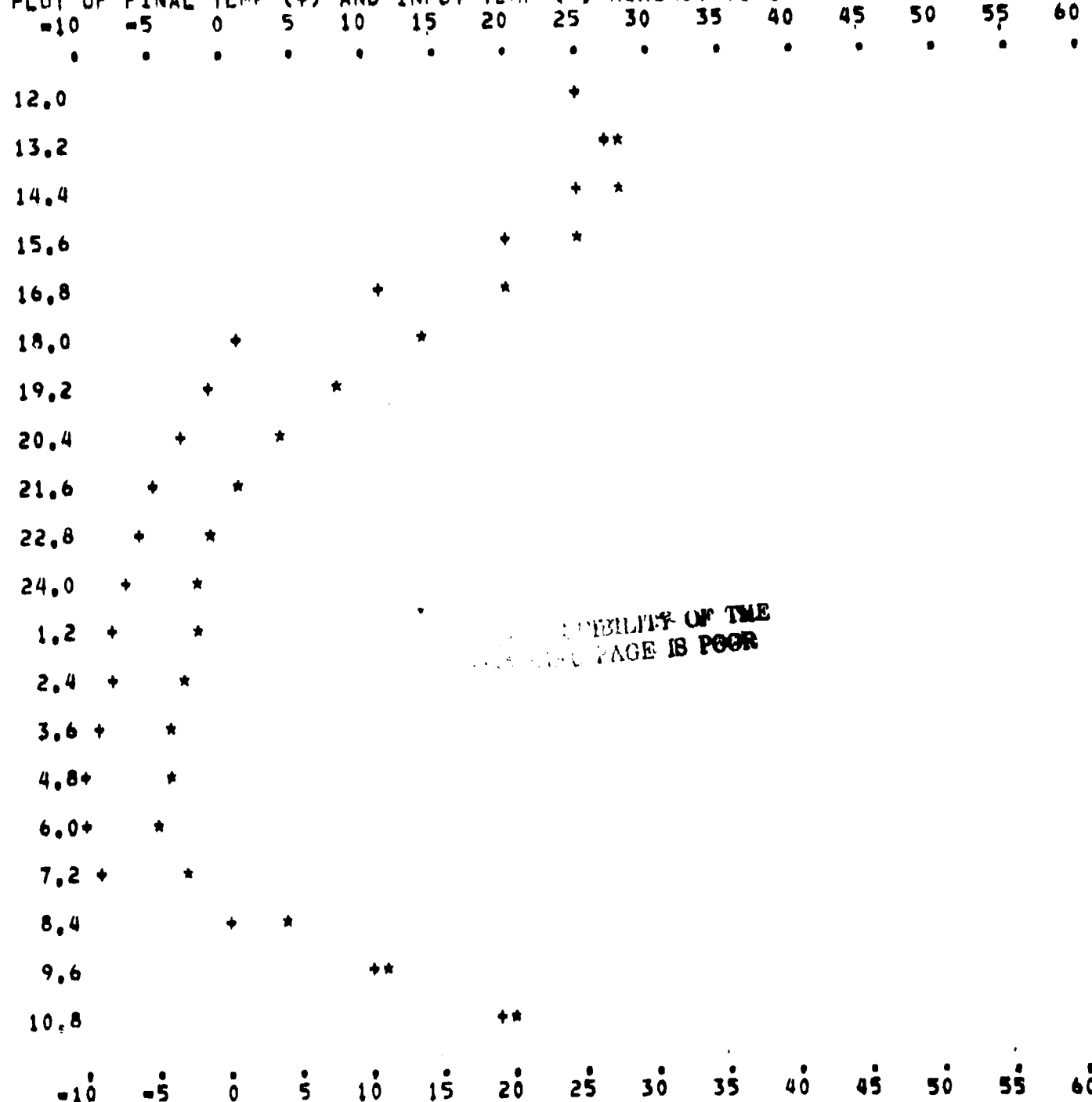
TIMES, FINAL SURFACE TEMPERATURES, AND INPUT TEMPERATURES  
12.0 24.8 25.1 13.2 27.0 28.1 14.4 25.4 27.7 15.6 19.9 24.5 16.8 11.1 20.1  
18.0 0.7 14.3 19.2 -1.3 8.0 20.4 -3.1 3.7 21.6 -4.7 1.3 22.8 -5.9 -1.0  
24.0 -6.9 -2.0 1.2 -7.7 -2.3 2.4 -8.4 -2.6 3.6 -9.0 -3.7 4.8 -9.6 -4.4  
6.0 -13.4 -5.4 7.2 -8.6 -2.8 8.4 0.5 4.0 9.6 10.4 11.4 10.8 18.9 20.3

T MAX 27.0 T MIN -13.4 AVERAGE TEMP 3.01

PROGRAM PARAMETERS CURRENT VALUES

(5) CLOUD 0.2 (6) ALB 0.365 (7) EMS 0.9850 (8) T IN 0.020 (9) LAT 34.7  
(10) DEC 3.0 (11) DIP 0.0 (12) STR 0.0 (13) TN 250.0 (14) TD 230.0

PLOT OF FINAL TEMP (+) AND INPUT TEMP (\*) AGAINST TIME



16:20 THU 29 MAY 75

Page 9

**NEWBUDI STU. 1**

□□□□□□□□□

## **TIMES, FINAL SURFACE TEMPERATURES, AND INPUT TEMPERATURES**

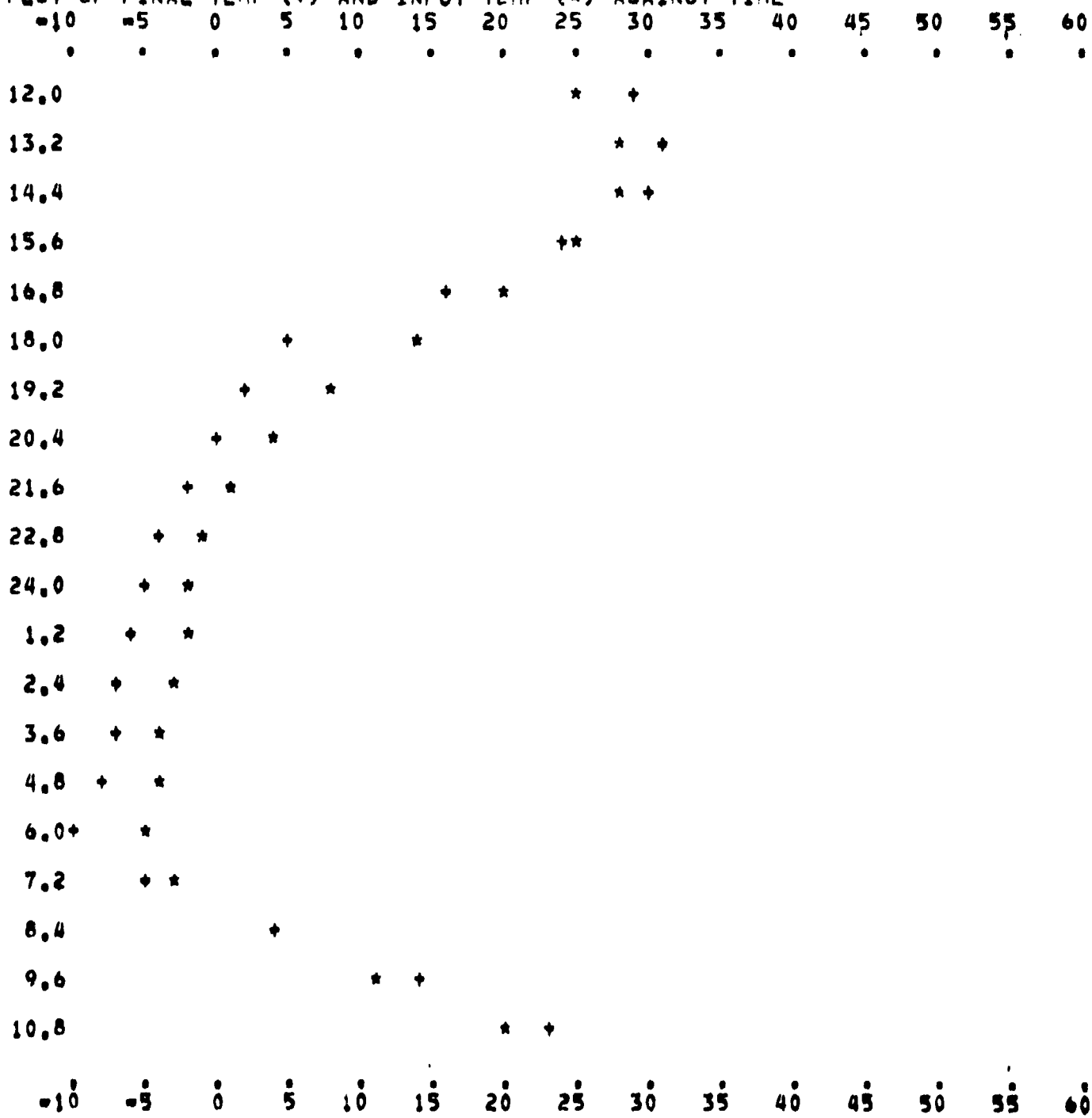
12.0 28.9 25.1 13.2 31.1 28.1 14.4 29.5 27.7 15.6 24.2 24.5 16.8 15.5 20.1  
 18.0 5.3 14.3 19.2 2.0 8.0 20.4 -0.5 3.7 21.6 -2.3 1.3 22.8 -3.7 -1.0  
 24.0 -4.9 -2.0 1.2 -5.8 -2.3 2.4 -6.7 -2.6 3.6 -7.4 -3.7 4.8 -8.0 -4.4  
 6.0 =10.3 -5.4 7.2 -4.8 -2.8 8.4 4.5 4.0 9.6 14.5 11.4 10.8 23.1 20.3

T MAX 31.1 T MIN -10.3 AVERAGE TEMP 6.21

**PROGRAM PARAMETERS CURRENT VALUES**

(5) CLOUD 0.2 (6) ALB 0.365 (7) EMS 0.9850 (8) T IN 0.020 (9) LAT 34.7  
(10) DEC 3.0 (11) DIP 0.0 (12) STR 0.0 (13) TN 250.0 (14) TD 240.0

PLOT OF FINAL TEMP (+) AND INPUT TEMP (\*) AGAINST TIME



16:29 THU 29 MAY 75

Page 7

<EWBUDI>SEM, 11

0000000000

TIMES, FINAL SURFACE TEMPERATURES, AND INPUT TEMPERATURES

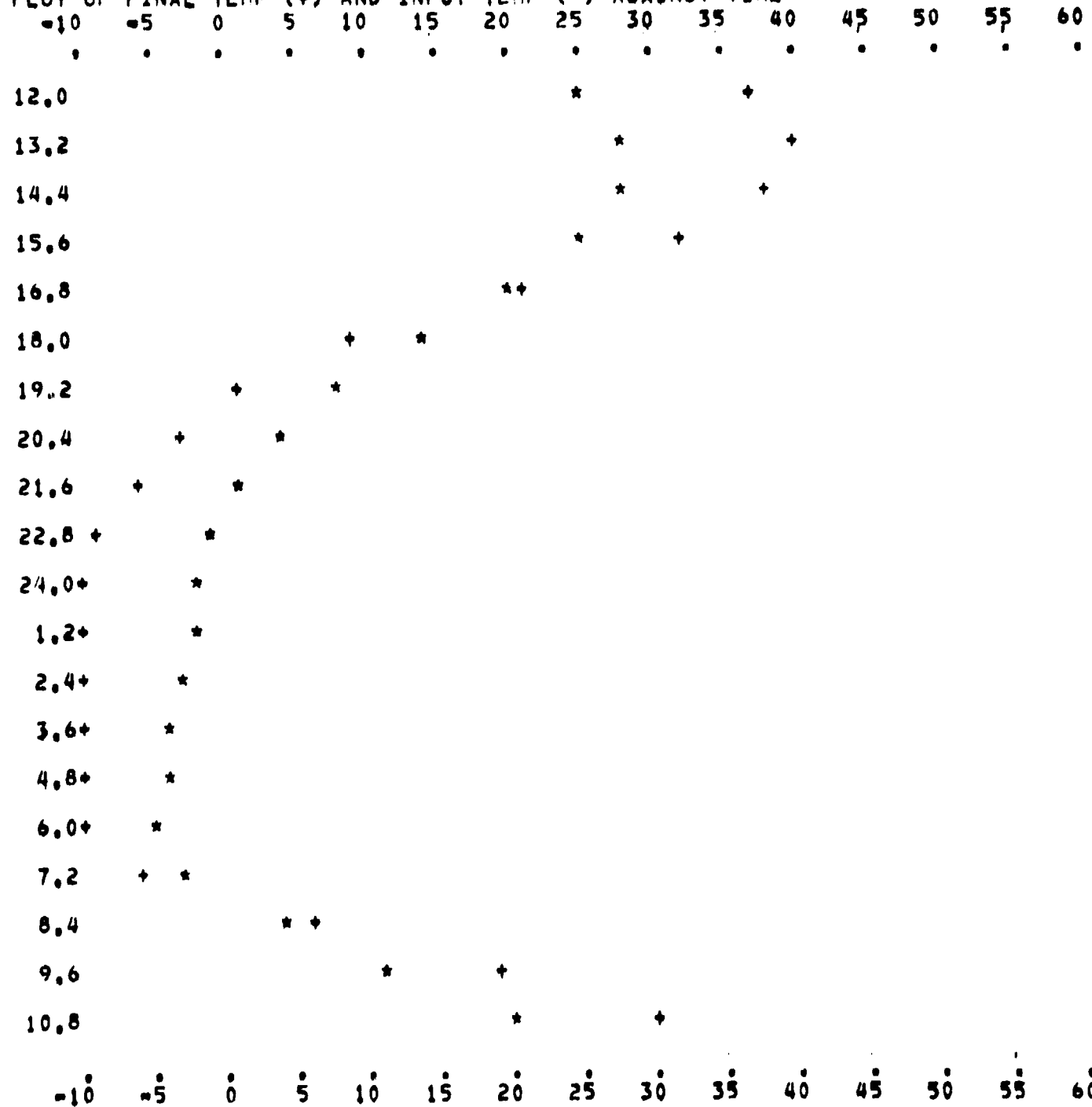
12.0 37.0 25.1 13.2 39.9 28.1 14.4 38.0 27.7 15.6 31.6 24.5 16.8 21.2 20.1  
18.0 8.8 14.3 19.2 1.3 8.0 20.4 -3.2 3.7 21.6 -6.3 1.3 22.8 -8.7 -1.0  
24.0 =10.6 =2.0 1.2 =12.2 =2.3 2.4 =13.5 =2.6 3.6 =14.7 =3.7 4.8 =15.7 =4.4  
6.0 =14.9 =5.4 7.2 =6.5 =2.8 8.4 6.1 4.0 9.6 19.0 11.4 10.8 29.0 20.3

T MAX 39.9 T MIN -15.7 AVERAGE TEMP 6.31

PROGRAM PARAMETERS CURRENT VALUES

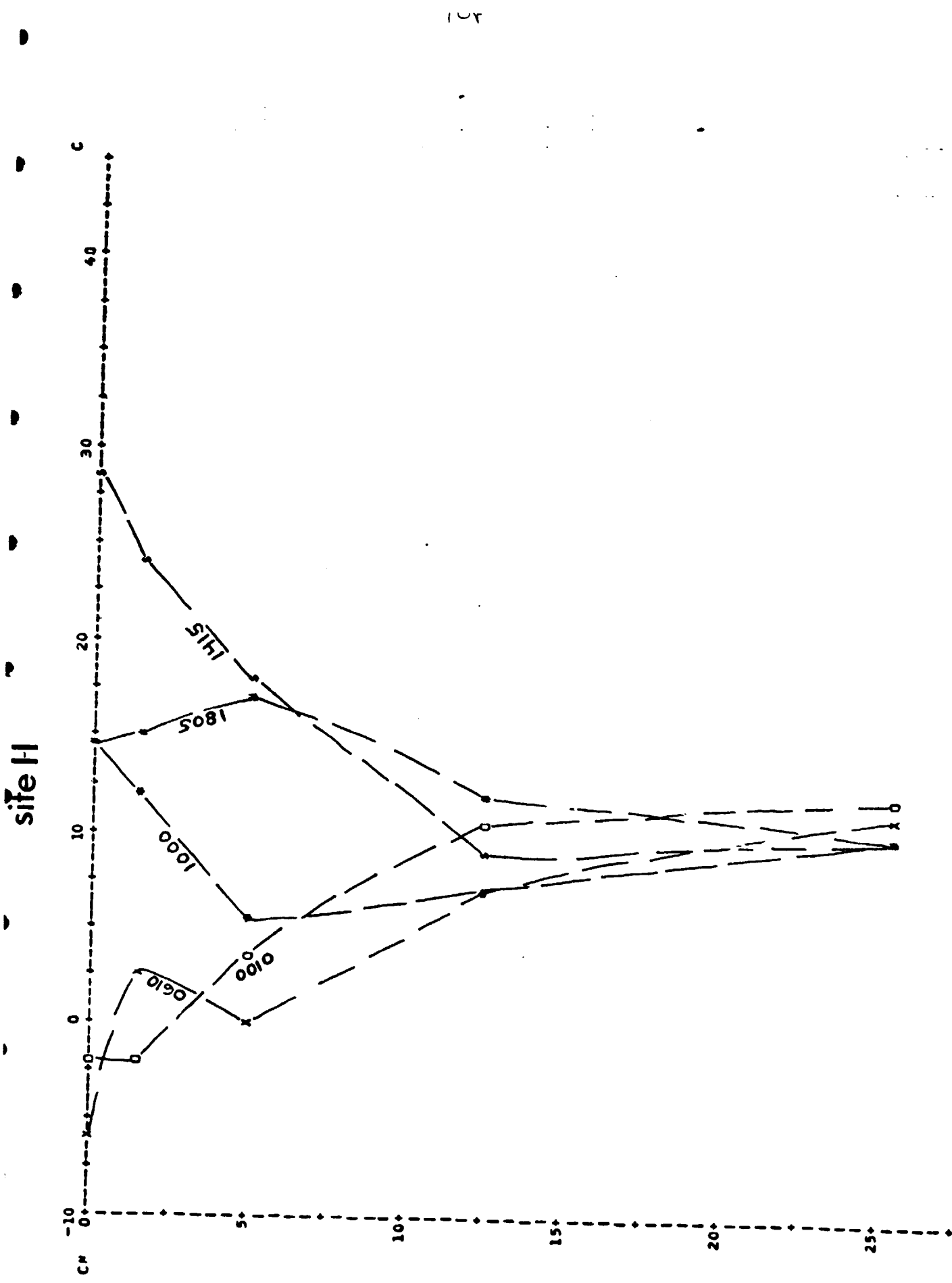
(5) CLOUD 0.0 (6) ALB 0.365 (7) EMS 1.0000 (8) T IN 0.020 (9) LAT 34.7  
(10) DEC 3.0 (11) DIP 0.0 (12) STR 0.0 (13) TN 230.0 (14) TD 240.0

PLOT OF FINAL TEMP (+) AND INPUT TEMP (\*) AGAINST TIME

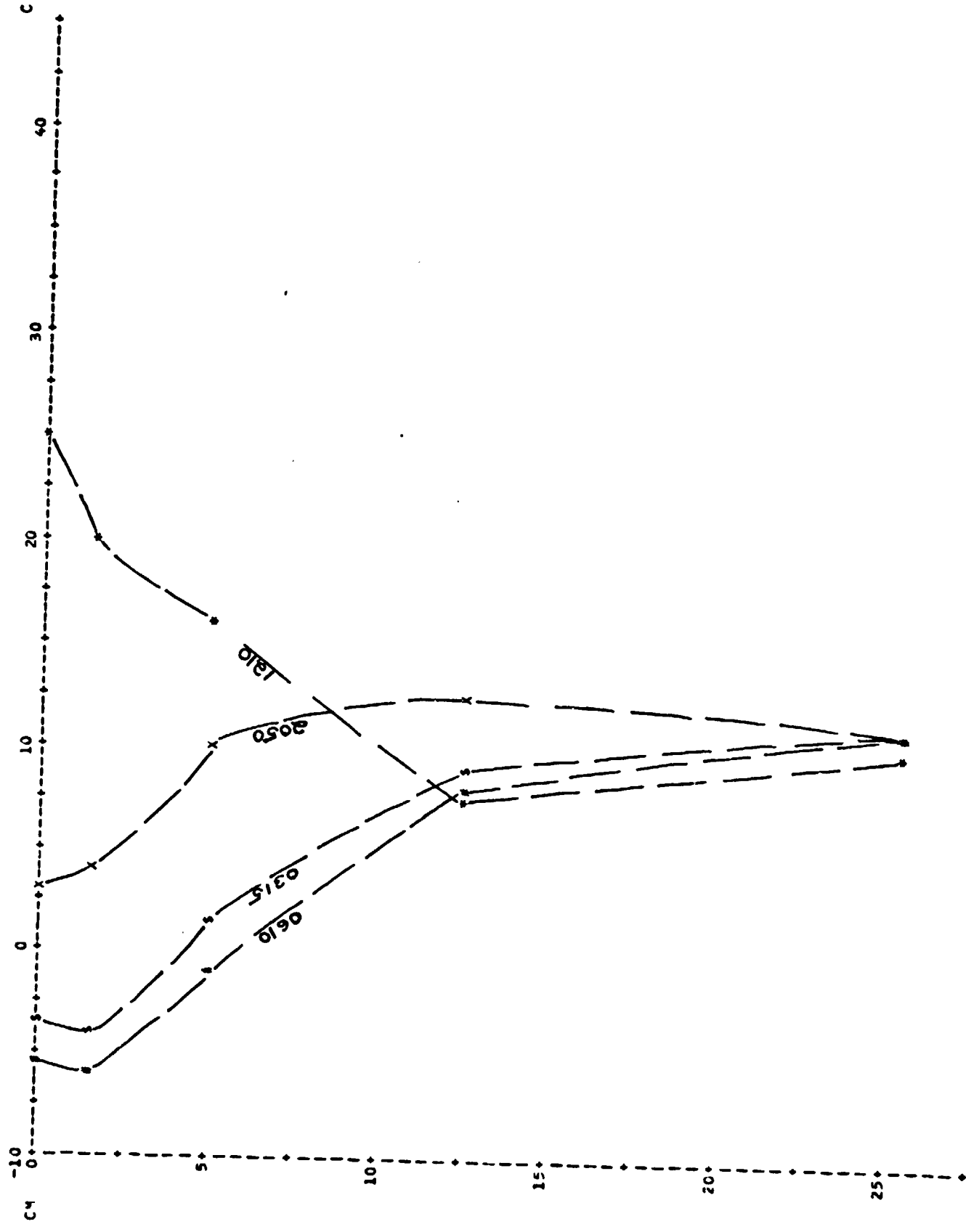


**APPENDIX 6**

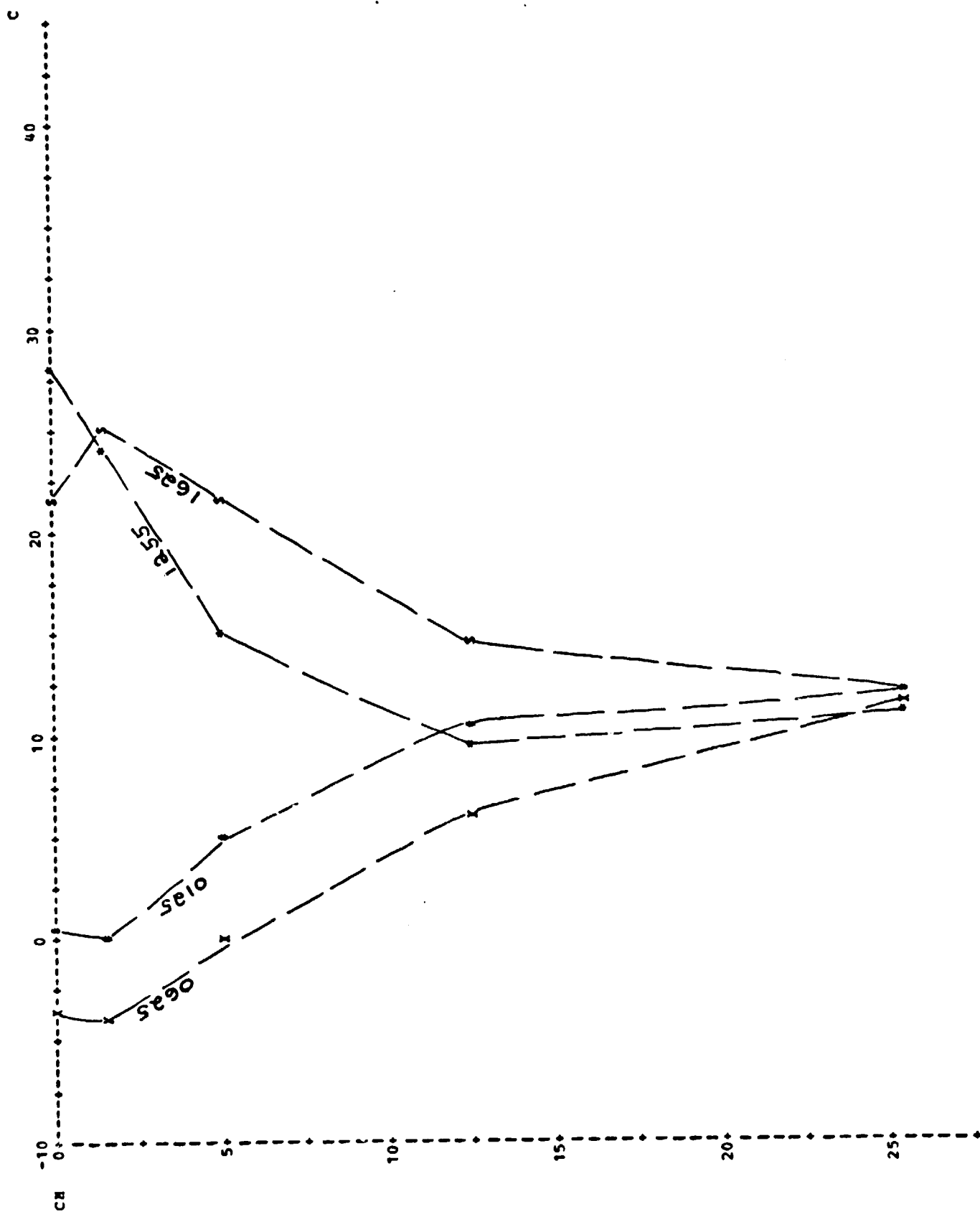
**TAUTOCHRONES FROM PLAYA PROBE MEASUREMENTS**



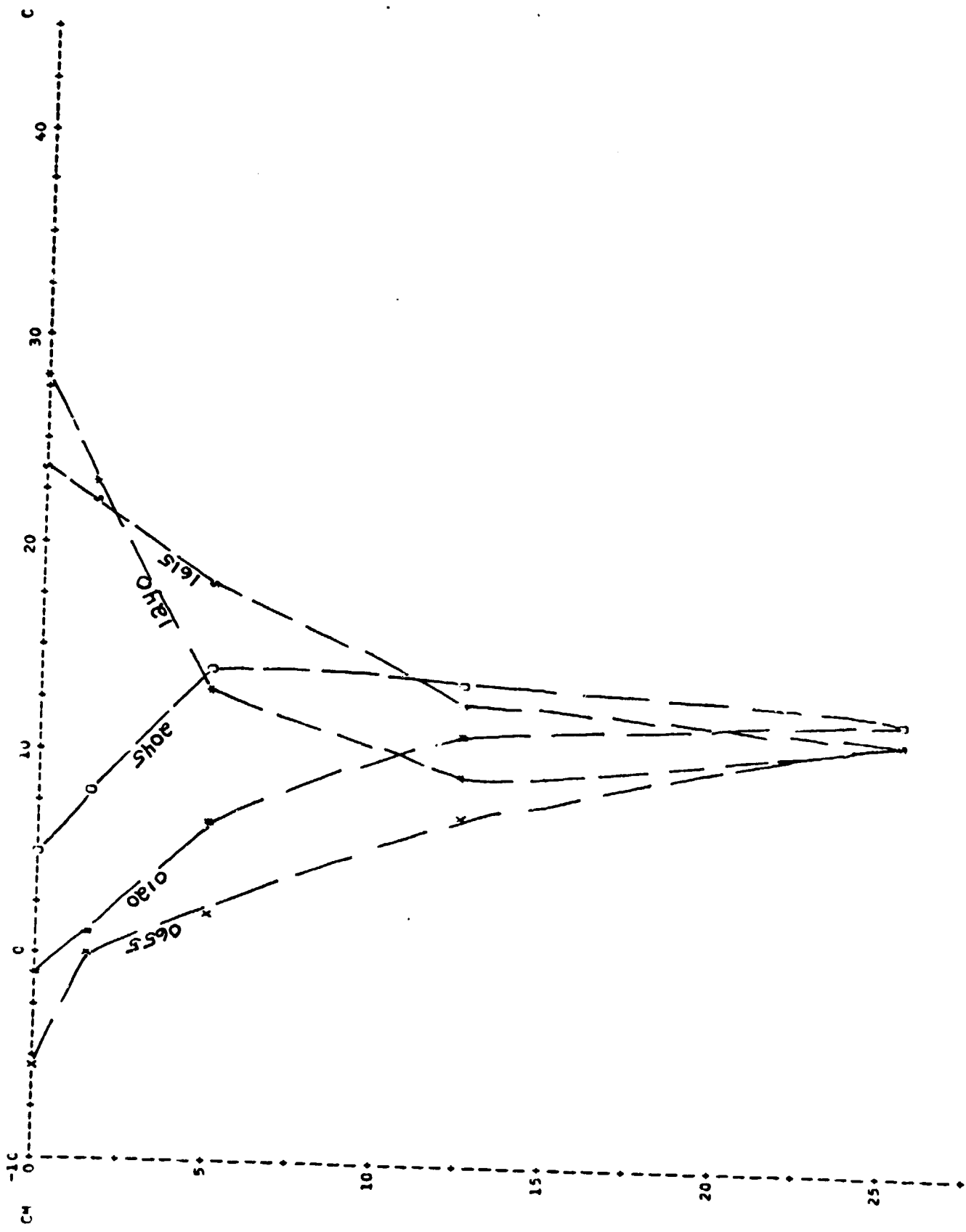
**Site H**



Site I-4



site 2



Site 2~2

